QUASI-STATIC SYSTEM-GENERATED ELECTRO-MAGNETIC PULSE CODE FOR SATELLITE ANALYSIS

Volume II

Appendixes 1 through 3

Daniel F. Higgins
R. Marks
Michael A. Messier

Mission Research Corporation
735 State Street
Santa Barbara, CA 87115

May 1976

Final Report

AIR FORCE WEAPONS LABORATORY
Air Force Systems Command
Kirtland Air Force Base, NM 87117

UNCLASSIFIED

SECURITY CLASSIFICATION OF THIS PAGE *(When Data Entered)*

REPORT DOCUMENTATION PAGE		READ INSTRUCTIONS BEFORE COMPLETING FORM
1. REPORT NUMBER AFWL-TR-75-141, Vol. II	2. GOVT ACCESSION NO.	3. RECIPIENT'S CATALOG NUMBER
4. TITLE *(and Subtitle)* QUASI-STATIC SYSTEM-GENERATED EMP ELECTROMAGNETIC PULSE CODE FOR SATELLITE Volume II--Appendixes 1 through 3		5. TYPE OF REPORT & PERIOD COVERED Final Report 6. PERFORMING ORG. REPORT NUMBER 8111-070
7. AUTHOR(s) Daniel F. Higgins R. Marks Michael A. Messier		8. CONTRACT OR GRANT NUMBER(s) F29601-74-C-0039
9. PERFORMING ORGANIZATION NAME AND ADDRESS Mission Research Corporation 735 State Street Santa Barbara, California 93102		10. PROGRAM ELEMENT, PROJECT, TASK AREA & WORK UNIT NUMBERS 64711F 46950310
11. CONTROLLING OFFICE NAME AND ADDRESS Air Force Weapons Laboratory Kirtland Air Force Base, NM 87117		12. REPORT DATE May 1976 13. NUMBER OF PAGES 180
14. MONITORING AGENCY NAME & ADDRESS*(if different from Controlling Office)*		15. SECURITY CLASS. *(of this report)* UNCLASSIFIED 15a. DECLASSIFICATION/DOWNGRADING SCHEDULE

16. DISTRIBUTION STATEMENT *(of this Report)*

Approved for public release; distribution unlimited.

17. DISTRIBUTION STATEMENT *(of the abstract entered in Block 20, if different from Report)*

18. SUPPLEMENTARY NOTES This report consists of two volumes: Vol. I--Lumped-Element Satellite Modeling in SGEMP, Including Space-Charge-Limited Currents; and Vol. II--Appendixes 1 through 3.

19. KEY WORDS *(Continue on reverse side if necessary and identify by block number)*

Lumped-Element Modeling
System-Generated Electromagnetic Pulse
Quasi-static
Equivalent Circuit
Computer Codes
Satellite Systems
Structural Return Currents

20. ABSTRACT *(Continue on reverse side if necessary and identify by block number)*

Investigations of lumped-element modeling techniques are performed for application to system-generated electromagnetic pulse (SGEMP) analyses of satellite systems. The thrust of the effort is twofold: (1) a quantification of errors introduced by the quasi-static approximation and other modeling approximations, and (2) the addition of a particle-pusher routine to the lumped-element model to obtain a self-consistent solution applicable to space-charge-limited problems.

DD FORM 1 JAN 73 1473 EDITION OF 1 NOV 65 IS OBSOLETE

UNCLASSIFIED

SECURITY CLASSIFICATION OF THIS PAGE *(When Data Entered)*

APPENDIX 1

THE QUASI-STATIC METHOD APPLIED TO SATELLITE STRUCTURAL RETURN CURRENT ANALYSIS: SURFACE NODE ANALYSIS

NOTE: This appendix is self-contained and all mention of sections, figures, tables, equations, and references refers only to items contained herein. This appendix has not been published as a separate document.

TABLE OF CONTENTS

LIST OF ILLUSTRATIONS

FIGURE

SECTION 1

INTRODUCTION

This report is the first in a series designed to educate the reader in the techniques used in the computer code QUASI, which calculates the currents running on various portions of a satellite structure. We will outline the general method first and then concentrate on how one would construct the node/branch model of the satellite that is required by the code. In order to perform the latter task in a manner which brings out all of the problems clearly, we proceed from very simple models to more complicated structures, each of which emphasizes a particular aspect of the problem. At the end of all this, the reader (and, indeed, the author) will still have a great deal of difficulty in constructing a reasonable node model of a real structure, but we should all have a better understanding of why we are having so much trouble. It would be possible, as has been done in the past with transmission line models, to start off with a very complicated realistic satellite system and claim that we have modeled it well in our code. Until tests have been performed, no one could prove otherwise. As in the transmission line models, the quasi-static model can be manipulated to ring with the proper period (it uses inductors also). However, we will start by modeling spheres and cylinders, where the amount of fudging required to make them work will be immediately obvious. Hopefully, the amount of insight obtained in this way will more than compensate for the embarassment and can be considered a deposit in the bank of intuition from which we will all have to withdraw when the time comes to predict the currents running on an actual satellite.

SECTION 2

THE QUASI-STATIC APPROXIMATION

The quasi-static approximation can be thought of as a static version of the method of moments with self-inductive terms and radiation losses approximated by the inclusion of lumped parameters. It would be possible, of course, to include mutual inductance terms. The important point is that inductive terms are not inherent in the solution, but must be added as corrections to the static solution. Experience with finite difference solutions to two-dimensional (azimuthally symmetric) geometries indicates that the oscillation modes are not excited to an important degree in realistic SGEMP problems and that the quasi-static approximation should suffice. However, one is still left with the problem of determining values of inductance and resistance by other means. In the future, it would be wise to use method of moments (MOM) and integral equation techniques to determine the coupling coefficients in terms of lumped parameters (Reference 1, 2, 3). With those methods, the impedance (coupling) parameters can be found by solving the free-field scattering problem and fed into the quasi-static code as the satellite model. The quasi-static code then would calculate spatial and return currents in a self-consistent manner. The moment method solutions can be made in a rather-crude manner compared to what is normally required in an antenna calculation, since the parameters will be used in a problem in which higher modes are not excited. There is no sense in dividing the surface of the body into more area increments for the MOM calculation than is going to be used in the quasi-static model. The only change required would be that elastance coefficients would be computed instead of capacitance coefficients. The decreased accuracy requirements would

allow three-dimensional objects (objects without azimuthal symmetry) to be analyzed with minimal computer storage and time requirements. Other approximations might also be allowed, which normally would not be considered in a MOM code.

In the quasi-static approximation, both space and the satellite body are divided into nodes, where charge is allowed to accumulate. The electrostatic potential at a particular node is given by the sum of the charges at all the nodes, each times an elastance coefficient, i.e., the potential at the i^{th} node is

$$V_i = \sum_{j=1}^{J} E_{ij} Q_j + \sum_{k=1}^{K} e_{ik} q_k \quad . \tag{2-1}$$

Here, for later convenience, we have summed separately over the structural node charges, Q_j, and the spatial node charges q_k. The structural and spatial elastances are E_{ij} and e_{ik} respectively.

At the moment, we calculate the internode elastances by assuming that the nodes consist of point charges, i.e.,

$$E_{ij} = \frac{1}{4\pi\varepsilon_0 R_{ij}} \quad , \quad i \neq j \ , \tag{2-2}$$

$$e_{ik} = \frac{1}{4\pi\varepsilon_0 r_{ik}} \quad , \quad i \neq k \ , \tag{2-3}$$

where MKS units are used ($\varepsilon_0 = 8.854 \times 10^{-12}$ farad/m), R_{ij} is the distance between a surface node and the node at which the potential is desired, and r_{ik} is the distance between a spatial node and the one in question. The self-elastance of a structural node is usually calculated by (1) taking the area of the satellite structure that is represented by the node, A_i, (2) determining the radius of a sphere with the same area*, a_i, where

---

* The procedure for calculating a_i is different for long thin objects. This will be discussed in Section 5.

$$a_i = \sqrt{\frac{A_i}{4\pi}} \quad , \tag{2-4}$$

and, (3) using the self-elastance of a charged sphere,

$$E_{ii} = \frac{1}{4\pi\varepsilon_0 a_i} \quad . \tag{2-5}$$

Figure 1 shows the example of a cylinder which we will transform into a nodal model. In this case, we choose to break up the surface of the cylinder into 14 segments, each of which will be represented by a node. The surface nodes will eventually be connected by impedances to allow current to flow between them. Figure 2 shows the nodal representation of the cylinder, where those nodes which will have impedance branches between them are connected by lines. The nodes are represented by spheres in the diagram, but it must be remembered that they are treated as such only in the calculation of the self-elastance; otherwise, they are treated as point charges. Figure 3 shows a cross-section of the node model. Here the spheres representing the nodes are drawn to scale. Nodes 1 and 14 are chosen to represent half the area of the end caps. Nodes 6 through 9 each represent $1/8^{th}$ the area of the cylinder wall. The remainder of the nodes, situated at the corners, each represent $1/8^{th}$ the area of an end cap plus $1/16^{th}$ the area of the side.

The self-elastance of a spatial node is calculated by assuming that the charge contained in the incremental volume of space represented by the node is evenly distributed throughout a sphere of the same volume. Since cartesian coordinates are used in QUASI, the incremental volume is

$$\tau = \Delta x \cdot \Delta y \cdot \Delta z \quad , \tag{2-6}$$

and the radius of the sphere is

$$a_i = [3\tau/(4\pi)]^{1/3} \quad . \tag{2-7}$$

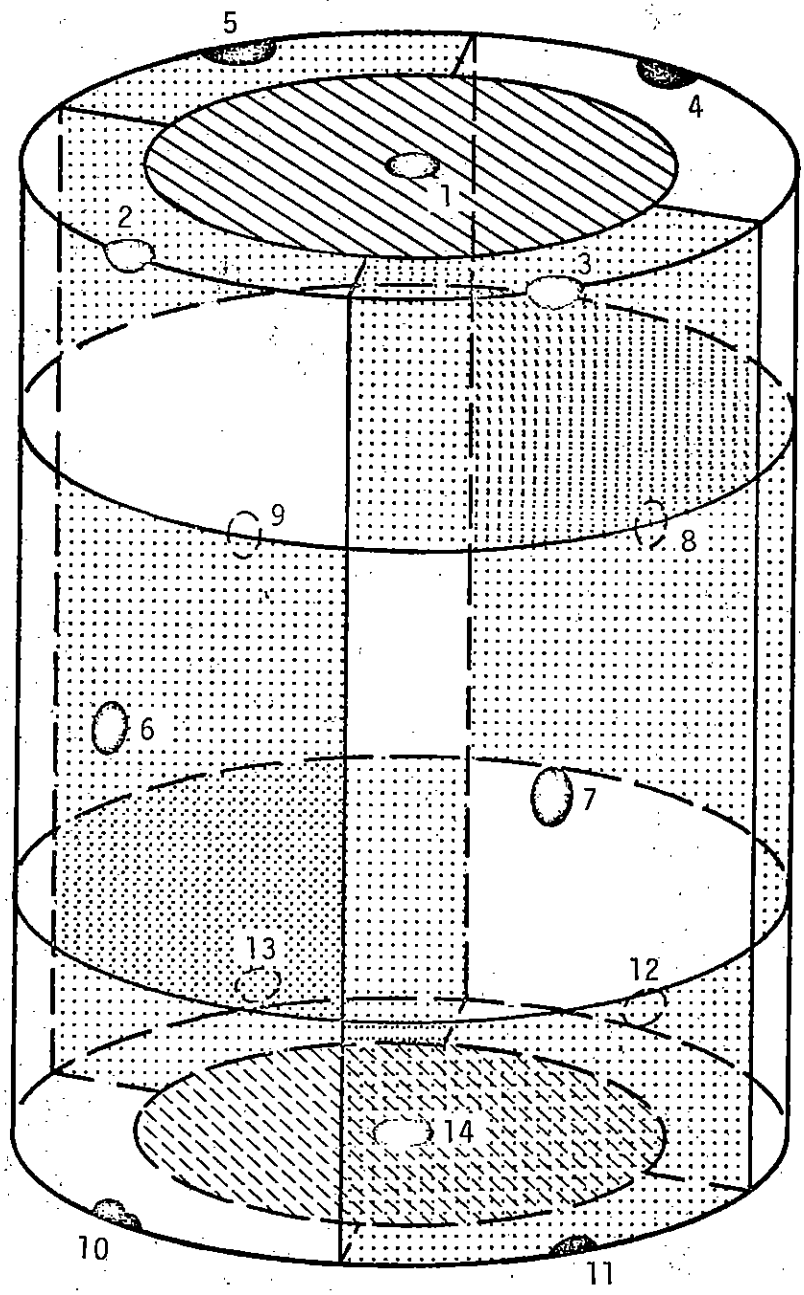

Figure 1. Example showing how the surface of a cylinder would be divided in order to prepare a node model.

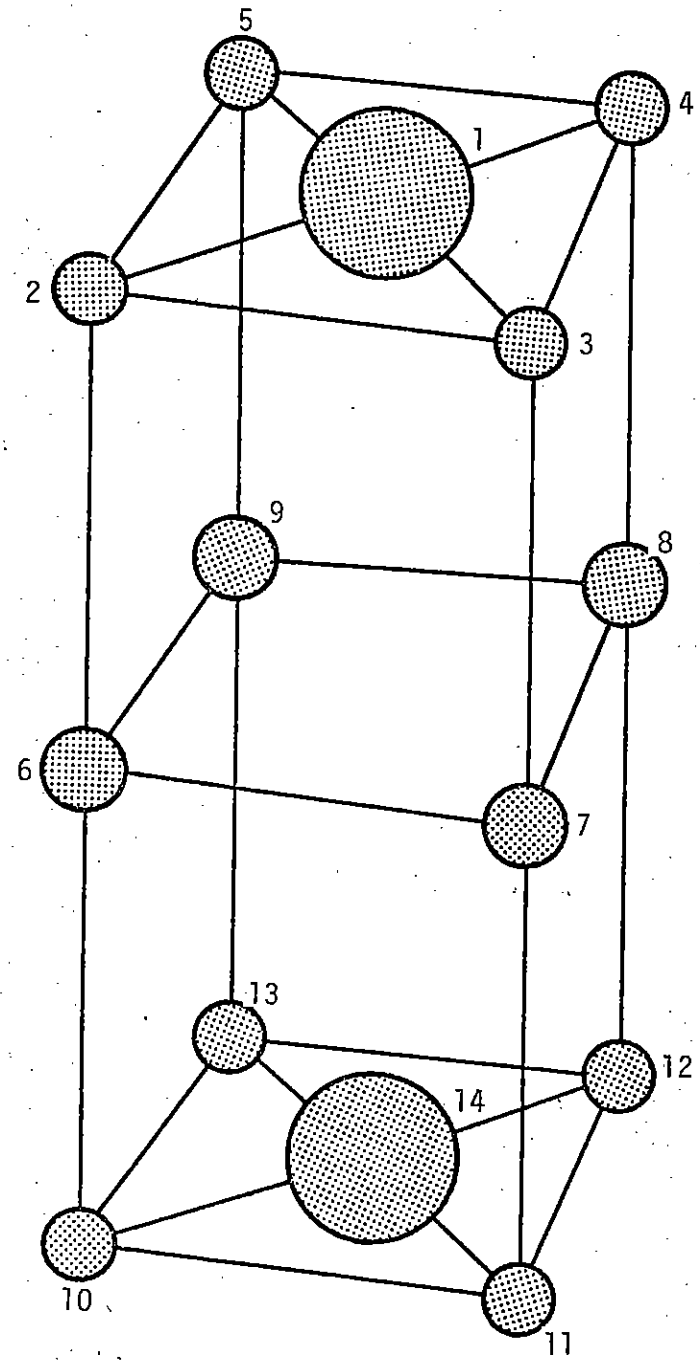

Figure 2. Placement of the nodes used to represent the cylinder shown in Figure 1. Lines show which nodes will be connected by current carrying branches.

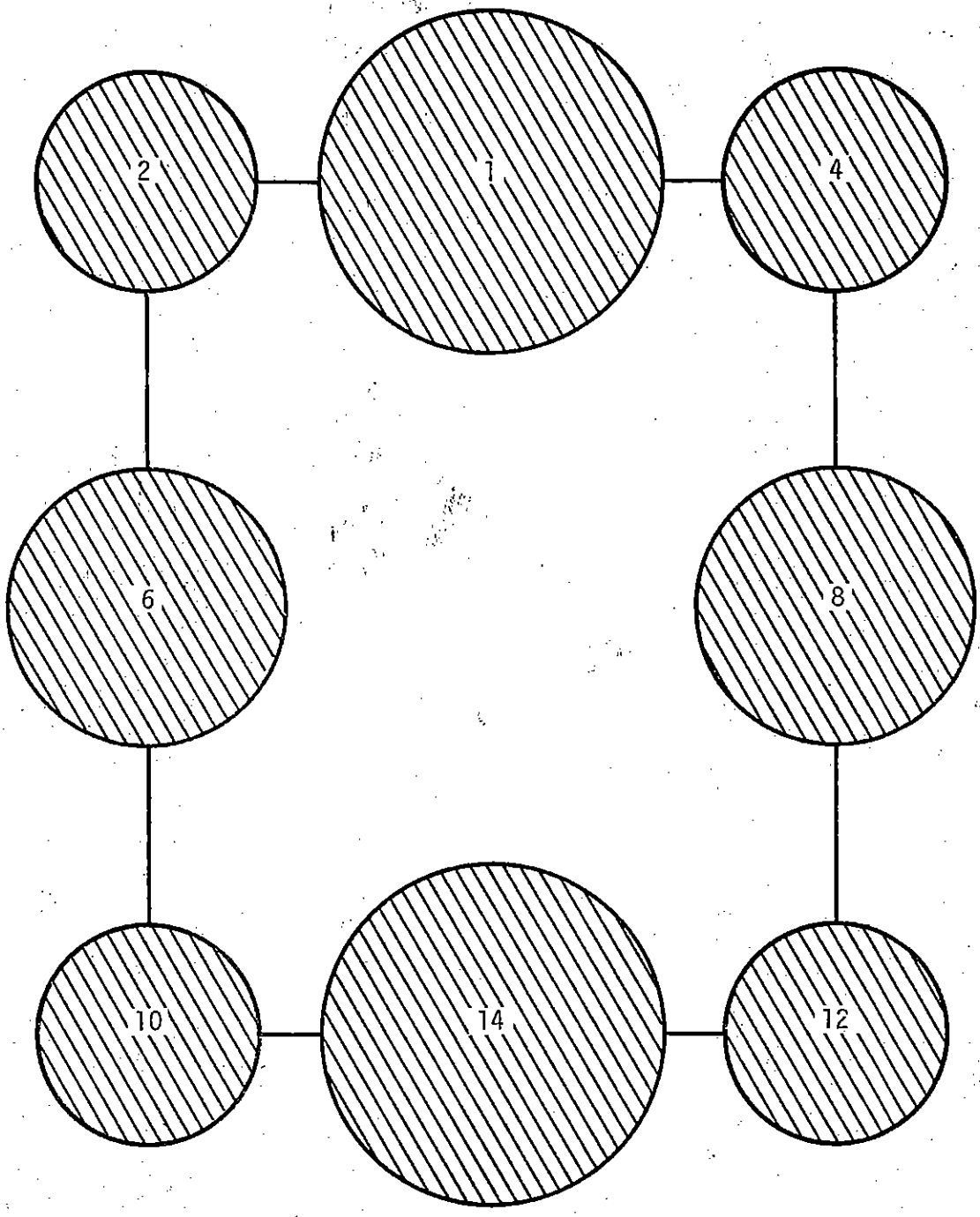

Figure 3. Cross section of the node model shown in Figure 2 indicating the relative radii used in the calculation of self-elastance.

The potential at the surface of the sphere due to the charge contained within it is

$$V_i = \frac{Q_i}{8\pi\epsilon_0 a_i} , \qquad (2\text{-}8)$$

or

$$e_{ii} = \frac{1}{8\pi\epsilon_0 a_i} . \qquad (2\text{-}9)$$

This elastance is half of that which would be present if the charge was distributed over the surface of the sphere, as in the case of the surface nodes.

Electrons moving through space have their trajectories altered by the presence of electric fields (magnetic field terms are ignored in the quasi-static approximation). These fields are generated by charge distributions in space and on the satellite body. They are calculated by finding the gradient of the potential in the vicinity of the particle.

In order to calculate the current running on satellites, i.e, on the branches connecting the nodes we must specify the impedance which is assumed to connect the nodes. This will usually consist of inductive and resistive elements, the capacitance being determined by the nodes. Consider the current running between the m^{th} and n^{th} surface node. In the absence of a connecting branch, the potential difference between them would be

$$\Delta_{mn} = V_m - V_n , \qquad (2\text{-}10)$$

where V_m and V_n are calculated using Equation 1 with i being replaced by m and n. When a connnecting impedance is present, there is also the condition that

$$\Delta_{mn} = \hat{Z}_{mn} I_{mn} \ , \tag{2-11}$$

where $\hat{Z}_{mn}$ is a time domain operator representing the branch impedance and I_{mn} is the current flowing on the branch. For example, if a pure inductance connects the two nodes, then

$$\Delta_{mn} = L_{mn} \frac{\partial}{\partial t} I_{mn} \ , \tag{2-12}$$

where L_{mn} is the inductance. Mutual inductances could be used to couple branches, just as the nodes are through E_{mn}.

There are several methods for solving the set of equations defined by 2-9 and 2-10, where the currents flowing in all the branches must be considered, as well as electrons returning to the nodes from space and leaving them through photoemission, and the spatial charge distribution in space. A time stepping procedure was chosen for use in program QUASI. This is outlined by the flow chart shown in Figure 4. From the circuit solution viewpoint, the important aspect of this method is that a two-step time iteration scheme is involved and that it amounts to a large impedance approximation. It was chosen for its simplicity. In the future, after the entire code has been shown to operate correctly, more accurate techniques could be used.

In the remainder of this report, we will apply the quasi-static approximation to simple geometries in order to examine some of the factors which must be considered when determining the branch impedances. The meaning of such quantities as capacitance, in the node model context, will be made clear. The same is true with the concept of ringing modes. At this point, we must specify the complex frequency with which the object will ring. Then, from a knowledge of the self and internode elastances of the surface nodes, we can find the required inductances and resistances. Thus,

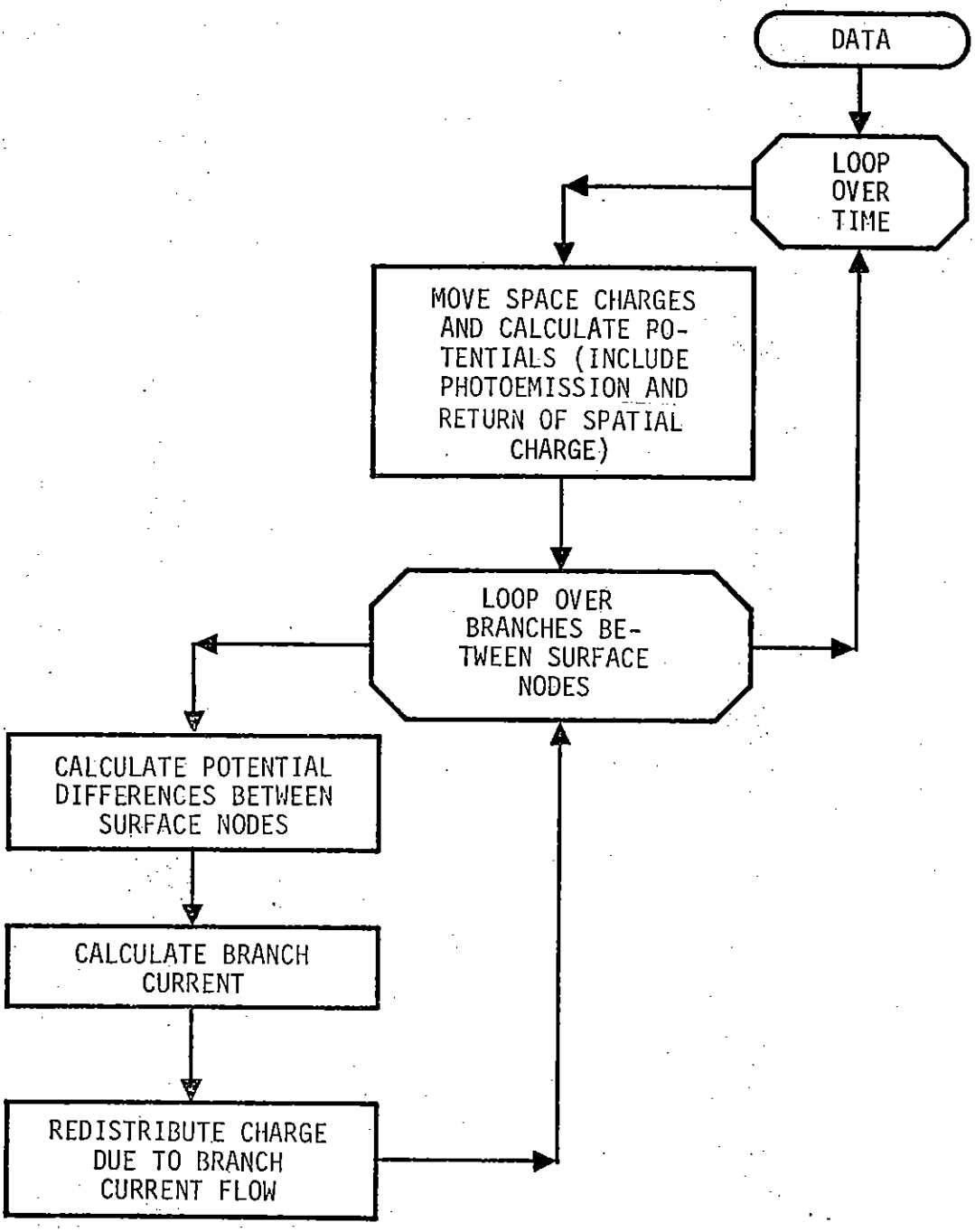

Figure 4. Outline of the structural current calculation used in program QUASI.

for this part of the problem, the interaction with spatial charges can be ignored and Equation 1 reduces to

$$V_i = \sum_{j=1}^{J} E_{ij} Q_j \quad . \tag{2-13}$$

As mentioned previously, moment methods might be used in the future to generate the proper coupling impedances, thus eliminating the guesswork. This is still a good exercise from the aspect of understanding the coupling processes involved.

SECTION 3

SOME CIRCUIT RELATIONS

In the studies of the node models which follow, we will need to derive equivalent circuit networks which give the same results as the node model. In order to standardize the notation, certain elementary concepts are displayed here.

In Figure 5a, a series RLC impedance is shown, connected in series with a voltage source. A parallel RLC impedance is in parallel with a current source in Figure 5b. Considering the underdamped cases only, the ringing frequency in each case is given by

$$\omega_r^2 = \omega_0^2 - \nu^2 \ , \tag{3-1}$$

where ν is the damping rate ($\nu = 1/\tau$, where τ is the e-fold decay time) and ω_0 is the undamped ringing frequency. In both the series and parallel impedances,

$$\omega_0 = \frac{1}{\sqrt{LC}} \ (\text{sec}^{-1}) \ . \tag{3-2}$$

The damping rate is given in each case by

$$\nu = \begin{cases} \frac{1}{2RC} \ (\text{sec}^{-1}), \text{ parallel} \\ \\ \frac{R}{2L} \ (\text{sec}^{-1}), \text{ series} \ . \end{cases} \tag{3-3}$$

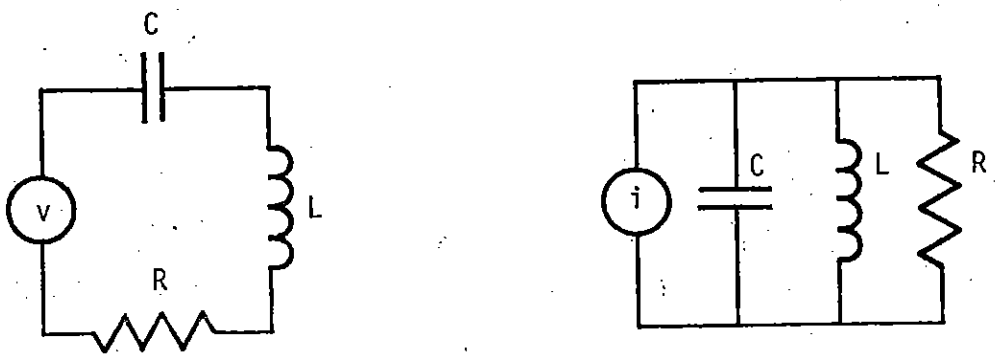

(a) Series (b) Parallel

Figure 5. RLC resonant circuits.

In order to determine R, L, and C from the behavior of a circuit, we require one more parameter in addition to ω_0 and ν. For this parameter we chose the characteristic impedance

$$\eta = \sqrt{\frac{L}{C}} \text{ (ohms)} . \tag{3-4}$$

Then, in both cases,

$$L = \eta/\omega_0 \text{ (henries)} , \tag{3-5}$$

$$C = 1/(\omega_0\eta) \text{ (farads)} , \tag{3-6}$$

while

$$R = \begin{cases} \frac{\omega_0\eta}{2\nu} \text{ (ohms), parallel} \\ 2\nu\eta/\omega_0 \text{ (ohms), series} . \end{cases} \tag{3-7}$$

Obviously, more information about a circuit is required in order to choose between the series and parallel forms. This can come from the required behavior at low frequencies, for example.

Note that the same complex ringing frequency is exhibited by a second circuit with parameters L', C', and R' when the individual impedances are related by a multiplicative constant, i.e.,

$$\omega' = \omega$$
$$\nu' = \nu \qquad (3\text{-}8)$$

if

$$L' = kL$$
$$C' = C/k$$
$$R' = kR$$

where k is any constant. The circuit's characteristic impedance changes, however

$$\eta' = k\eta \ . \qquad (3\text{-}9)$$

In the following sections, we will attempt to formulate equivalent circuits which predict the behavior of simple geometric shapes. The node models will give us an effective capacitance, C. It will then be necessary to estimate the values of L and R which will make the circuit ring at the frequency of the primary resonance. It will also be necessary to choose the arrangement of circuit elements to give the proper low-frequency behavior. Higher frequency behavior depends on the excitation of higher modes, which will not be simulated. With the simple shapes to be considered, it will be relatively easy to estimate the undamped ringing frequency, ω_0. This is done by making the wavelength of the oscillation equal to the perimeter length of the object in the direction that the oscillation is assumed to occur. For example, using this formulation, the wavelength at which a cylinder of length ℓ and diameter d would oscillate, if it did not radiate, would be $2(d + \ell)$. Of course, the complex frequency of such simple objects is already known to high accuracy, but the purpose of this exercise is to investigate techniques which might be used in more

realistic problems. Given ω_0 and C, the inductance, L, can be calculated. A radiation resistance must also be estimated to give the damping rate and true ringing frequency. The damping rate will usually be small compared to the undamped frequency. The worst case is the sphere.

In order to see how the procedure might work, without actually using the node model to calculate C, we apply it to the problem of an oscillating sphere. Let the sphere have the radius a. The undamped oscillation frequency for the primary resonance would then be estimated as

$$\omega_0 = 2\pi c/(2\pi a) = c/a \ , \tag{3-10}$$

where c is the speed of light and the wavelength is

$$\lambda_0 = 2\pi a \ . \tag{3-11}$$

The wave number is then

$$k_0 = \frac{\omega_0}{c} = 1/a \ , \tag{3-12}$$

so that

$$k_0 a = 1 \ . \tag{3-13}$$

An estimate of C is now required in the absence of a node model calculation. The static capacitance (capacitance to infinity) of a sphere is

$$C_\infty = 4\pi\varepsilon_0 a \ , \tag{3-14}$$

where ε_0 is the permittivity of free space (8.854×10^{-12} farad/m). This is not the capacitance required for our problem, however. We are concerned with the problem of the oscillation of charge from one side of the sphere to the other, with the total charge being zero. Therefore the capacitance of interest is the capacitance between the two sides of the sphere rather than the capacitance of the sphere relative to infinity. The capacitance between two hemispherical shells separated by an infinitesimal gap is

$$C = \frac{3\pi}{2} \varepsilon_0 a \ . \qquad (3\text{-}15)$$

The inductance which will make the circuit ring at ω_0 is given by Equation 3-2 as

$$L = \frac{2}{3\pi} \mu_0 a \ , \qquad (3\text{-}16)$$

where μ_0 is the permeability of free space ($\mu_0 = 4\pi \times 10^{-7}$ henry/m) and where

$$c^2 = 1/(\mu_0 \varepsilon_0) \ . \qquad (3\text{-}17)$$

The characteristic impedance is then

$$\eta = \frac{2\eta_0}{3\pi} \ , \qquad (3\text{-}18)$$

where η_0 is the impedance of free space ($\simeq 120\ \pi$ ohms).

Finally, we need an estimate for the resistance R. In a real problem, it would be estimated from the damping rate of a simple, but geometrically similar, object (probably with equal surface area). In this case, we started with a simple object so that we have gone as far as is practical. Note, however, that the equivalent parallel and series circuit resistances are related by

$$R_s R_p = \eta^2 \ . \qquad (3\text{-}19)$$

The complex wave number corresponding to the first resonance of a sphere is given by (Reference 4)

$$ka = \pm \frac{\sqrt{3}}{2} + i \frac{1}{2} = \frac{\omega a}{c} \ , \qquad (3\text{-}20)$$

so that

$$\frac{\nu a}{c} = \frac{1}{2} \ . \qquad (3\text{-}21)$$

The ringing frequency is given by

$$\frac{\omega_r a}{c} = \frac{\sqrt{3}}{2} \quad , \tag{3-22}$$

so that

$$\left(\frac{\omega_0 a}{c}\right)^2 = \left(\frac{\omega_r a}{c}\right)^2 + \left(\frac{\nu a}{c}\right)^2 = 1 \quad , \tag{3-23}$$

which is identical to Equation 3-13. Using Equation 3-7, the parallel resistance is

$$R_p = \frac{(\frac{c}{a})\eta}{(2)(\frac{1}{2})(\frac{c}{a})} = \eta \quad . \tag{3-24}$$

The series resistance is the same in this case, so that we can consider a single resistance in both circuits, i.e.,

$$R = R_s = R_p = \eta \quad . \tag{3-25}$$

Therefore all of the elements in both the series and parallel resonant circuits are equal.

Instead of trying to use the hemispherical capacitance, we might have tried using half the static capacitance,

$$C = \frac{1}{2} C_\infty = 2\pi\varepsilon_0 a \quad , \tag{3-26}$$

and, in this case at least, the error would not be large (25 percent). No general statement can be made at this time about the error involved in using this procedure for other shapes. It would be useful because the static capacitance is known for many geometries, including cylinders, spheroids, and the limiting forms of spheroids, e.g., discs (References 5 and 6). The modal frequencies are also known for many such shapes, which helps in estimating the radiation resistance (References 7 through 9).

In order to decide whether a series or parallel impedance is more appropriate, we must look at the low-frequency behavior. The radiation

resistance of an electrically small dipole is (Reference 4)

$$R_{RAD} = \frac{2\mu_0}{3\pi c} (\omega h)^2 , \qquad (3\text{-}27)$$

where h is half the dipole length. This is valid for the spherical antenna with h = a. The important aspect is the ω^2 dependence. The real part of the impedance of a parallel RL circuit is

$$Z_R = \frac{L^2}{R} \omega^2 , \qquad (3\text{-}28)$$

which has the same ω^2 dependence. Now, if a voltage source is inserted in the parallel circuit, where it would be in series with the capacitor which stores electrical energy, the impedance is described by a parallel RL in series with C. Therefore, the parallel circuit provides the proper low-frequency response (see Figure 6). Substituting the formulas for R and L into Equation 3-28 yields 3-27 (with h = a) and hence the proper limit.

The parallel circuit cannot be used directly with a current driver required to simulate SGEMP because the capacitance C must be broken up to represent the proper capacitances to infinity, as well as between the two halves of the object. This will be done in Section 4, during the analysis of the two-node model. Figure 7 shows a possible configuration suitable for current driver calculations. The capacitance C must be equal to

$$C = \frac{1}{\frac{1}{C_A} + \frac{1}{C_B}} + C_{AB} , \qquad (3\text{-}29)$$

The current driver is across only one of the capacitances to infinity, since it is intended to represent electron emission from one side. In a symmetrical problem, such as the sphere, $C_A = C_B$.

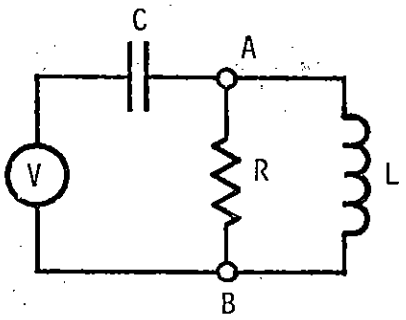

For Sphere:

$$C = \frac{3\pi}{2}\varepsilon_0 a$$

$$L = \frac{2\mu_0}{3\pi} a$$

$$R = \frac{2\eta_0}{3\pi}$$

Figure 6. Parallel RLC circuit driven by a voltage source.

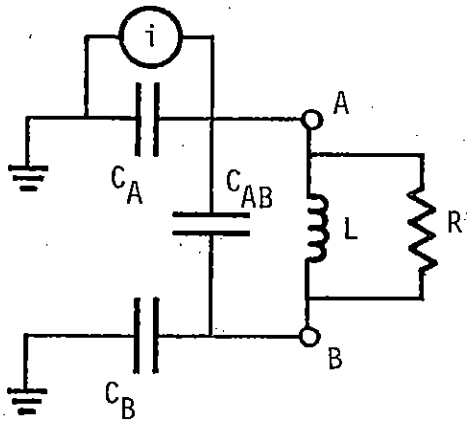

Figure 7. Parallel RLC circuit modified to simulate electron emission from one side of the satellite.

The sphere has the property that its characteristic impedance, η, is equal to the resistance term, R. In transmission line terminology, it is terminated in its characteristic impedance. Therefore reflections are eliminated and it radiates immediately. This is not true with other simple shapes, in general, i.e., they are not matched well to the impedance representing space. It is this mismatch that is responsible for the relatively poor radiation rate of other geometries relative to the sphere. Standing waves are set up.

The behavior of a system, as far as the influence of the radiation term is concerned, can be bracketed by first making a calculation with $R = 0$ and then repeating the calculation with $R = \eta$. In the latter case, the radiation rate at resonance will be $\nu = \omega_0/2$. Since the resonance of a satellite is not usually excited in a typical SGEMP problem, the actual radiation loss should be a small correction, even with $R = \eta$.

SECTION 4

THE TWO-NODE (DUMBBELL) MODEL

The basic model for studying structural currents is the two-node or "dumbbell" model. The current flowing across the equator of a sphere, for example, could be calculated with a dumbbell model in which the two nodes represent the two hemispheres and the impedance connecting them is given the proper inductance and resistance to allow a current flow equal to the actual current on a sphere.* Dividing the object into more segments improves the accuracy of the model and allows a more detailed description of the current flow, but does not improve the basic ability to resolve higher model responses. Each time another node is added, another undetermined branch impedance is also added. Its value is determined by the additional current continuity requirement (along with the modal frequency requirement). Therefore, another parameter other than self-inductance and resistance must be added for each higher mode than needs simulation. The natural parameters are mutual inductance terms, first between adjacent branches and then between branches which are farther apart. This subject will be touched upon in later sections, but we are not interested in higher resonances at this time. The subject is also mentioned in Reference 10.

---

* Actually, fat objects, such as cylinders with diameters which are not small compared to their length require more than two nodes for a proper model. This is because there is a restriction on the ratio of node radius to node separation arising from the 1/r elastance approximation.

The dumbbell model, because of its basic simplicity, illustrates many aspects of the basic node model approach which might be hidden in a more complicated one. One of the concepts emphasized by it is the difference in the types of capacitance one can encounter in a single problem. Confusion in the use of the term "capacitance" can lead to poor application of the model. The dumbbell model is a realistic representation of a structure consisting of two large, fat segments connected by a thin rod. The inductance of the system is determined by the rod and the system capacitance is determined by the end objects. Figure 8a shows the two-node model, with the nodes being represented by spheres of radius a_1 and a_2. The impedance is represented by an inductance, but would normally include a parallel or series resistance. The capacitance between nodes completes the resonant circuit. Figure 8b shows the LC network sufficient to describe the ringing properties of the model. Our initial goal will be to calculate C, so that L can be determined from the desired undamped ringing frequency. The inductance, plus a resistance to give the proper damping rate, are sufficient data for the circuit calculation in QUASI. We will proceed farther, however, and develop a capacitive network which can be used in a complete circuit representation (Figure 7). This will not only be instructive, but will set up a comparison with the transmission line model in the next section.

The potentials at the two nodes are

$$V_1 = E_{11}Q_1 + E_{12}Q_2 \ , \qquad (4\text{-}1)$$

$$V_2 = E_{12}Q_1 + E_{22}Q_2 \ , \qquad (4\text{-}2)$$

where $E_{21} = E_{12}$ (the variables are defined in Section 1). The potential difference between the two nodes is

$$\Delta V = V_1 - V_2 = (E_{11} - E_{12})Q_1 - (E_{22} - E_{12})Q_2 \ . \qquad (4\text{-}3)$$

If the two nodes are thought of as the plates of a capacitor, the capacitance would be

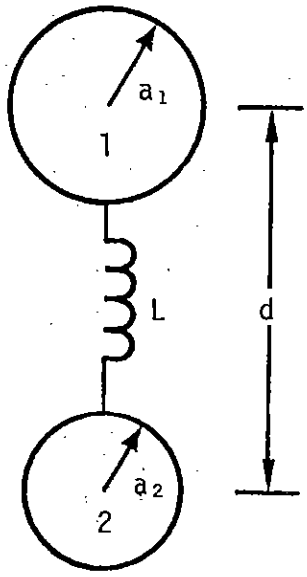

(a) Schematic representation

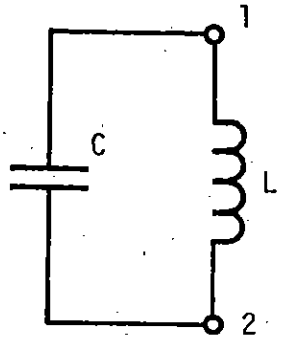

(b) Equivalent circuit suitable for impedance calculation

Figure 8. Two-node (dumbbell) model.

$$C = \frac{Q}{\Delta V} = \frac{1}{E_{11} + E_{22} - 2E_{12}} , \qquad (4\text{-}4)$$

where ΔV is the potential difference induced when a + Q charge is placed on one node and - Q is placed on another. This capacitance will be called the "dynamic" capacitance because it will be used to determine L.

If the node system has been charged and allowed to reach equalibrium, the charge will arrange itself on the two nodes in such a way that ΔV will be zero. The relation between Q_1 and Q_2 will be

$$\frac{Q_1}{Q_2} = \frac{E_{22} - E_{12}}{E_{11} - E_{12}} \equiv F . \qquad (4\text{-}5)$$

The difference between the charges Q_1 and Q_2 is given by

$$\Delta Q = \frac{F - 1}{F + 1} , \qquad (4\text{-}6)$$

where

$$Q_1 + Q_2 = Q \ , \tag{4-7}$$

$$Q_1 - Q_2 = \Delta Q \ . \tag{4-8}$$

A two-capacitor system is required to form an equivalent network which allows a charge separation to occur. Figure 9 shows such a network where the single capacitance, C, has been replaced by the series capacitors C_1 and C_2. The ratio of the capacitances is given by

$$\frac{C_1}{C_2} = \frac{Q_1}{Q_2} = F \ . \tag{4-9}$$

Also,

$$C = \frac{C_1 C_2}{C_1 + C_2} \ , \tag{4-10}$$

so that

$$\begin{aligned} C_1 &= (1 + F)C \\ C_2 &= FC_1 \end{aligned} \tag{4-11}$$

where F is given by Equation 4-5.

We digress at this point to show how a purely static approximation would work, in the case of a two-node model. Assume that a single electron of charge - q has been emitted from the system. The potentials at the two nodes are

$$V_1 = E_{11}Q_1 + E_{12}Q_2 - e_1 q \ , \tag{4-12}$$

$$V_2 = E_{12}Q_1 + E_{22}Q_2 - e_2 q \ , \tag{4-13}$$

where the spatial elastances are a function of time, i.e., the distances between the electron and the two nodes is a function of time. The static approximation assumes that, as a first approximation, the nodes are connected by a short circuit so that $\Delta V = 0$ and

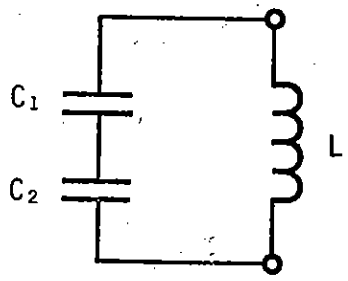

Figure 9. Two-node model equivalent circuit modified to give proper charge distribution between nodes.

$$Q_1 = FQ_2 + \frac{e_1 - e_2}{E_{11} - E_{12}} q \ . \tag{4-14}$$

Now,

$$Q_1 + Q_2 = q \ , \tag{4-15}$$

$$Q_1 - Q_2 = \Delta Q \ , \tag{4-16}$$

so that

$$Q_1 = \frac{1}{2} (q + \Delta Q) \ , \tag{4-17}$$

and

$$\Delta Q = \left(\frac{F - 1}{F + 1} + \frac{2}{F + 1} \frac{e_1 - e_2}{E_{11} - E_{12}} \right) q \ . \tag{4-18}$$

The current running between the two nodes is then

$$I_{sc} = \frac{d}{dt} (\Delta Q) = \frac{2}{F + 1} \frac{q}{E_{11} - E_{12}} \frac{d}{dt} (e_1 - e_2) \ , \tag{4-19}$$

where it has been assumed that q is constant and the only time variation is in the spatial elastance coefficients. A first order estimate of the potential difference developed between the two nodes, in the presence of a connecting impedance is obtained by computing the voltage drop across the load when I_{sc} is flowing through it. The exact solutions for the current

and voltage across a load impedance can be obtained from the Thevinen and Norton equivalent circuits shown in Figure 10.

Maxwell's capacitance coefficients are defined by

$$Q_i = \sum_j C_{ij} V_{ij} \ . \tag{4-20}$$

For the two-node model,

$$Q_1 = C_{11}V_1 + C_{12}V_2 \ , \tag{4-21}$$

$$Q_2 = C_{12}V_1 + C_{22}V_2 \ , \tag{4-22}$$

where $C_{21} = C_{12}$. Inverting the equations yields the relationship between the elastance coefficients and the capacitance coefficients:

$$\begin{aligned} C_{11} &= E_{22}/D \\ C_{22} &= E_{11}/D \\ C_{12} &= - E_{12}/D \ , \end{aligned} \tag{4-23}$$

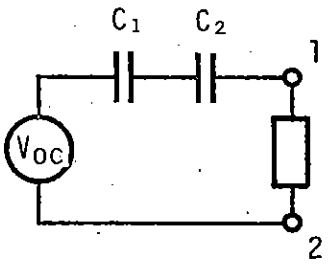

$V_{oc} = 2q(e_1-e_2)$

(a) Thevinen

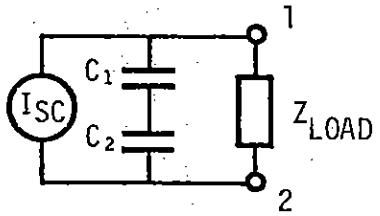

$I_{SC} = \frac{2}{F+1} \frac{q}{E_{11}-E_{12}} \frac{d}{dt} (e_1 - e_2)$

(b) Norton

Figure 10. Thevinen and Norton equivalent circuits providing the current and voltage across the branch in a two-node model when a single electron of charge -q is emitted. The model is based on static solution approximation. Two capacitors are used to give proper charge distribution between nodes.

where

$$D = E_{11}E_{22} - E_{12}^2 .$$

When the nodes are widely spaced, so that $d >> a_{1,2}$,

$$C_{11} \simeq 1/E_{11}$$

$$C_{22} \simeq 1/E_{22} \qquad (4\text{-}24)$$

$$C_{12} \simeq -E_{12}/(E_{11}E_{22}) .$$

The capacitance C_{12} is negative, meaning that a positive potential at one node induces a negative charge at the second, grounded, node. For future use, we define the positive quantity

$$C'_{12} = |C_{12}| . \qquad (4\text{-}25)$$

The dynamic capacitance, C, is given in terms of the modified Maxwell coefficients as

$$C = \frac{C_{11}C_{22} - C'^2_{12}}{C_{11} + C_{22} - 2C'_{12}} . \qquad (4\text{-}26)$$

A capacitance network of the form used in Figure 7 can be synthesized which gives the same relation shown above, i.e., with $C_A = C_{11} - C_{12}$, $C_B = C_{22} - C_{12}$, and $C_{AB} = C_{12}$. This is shown in Figure 11.

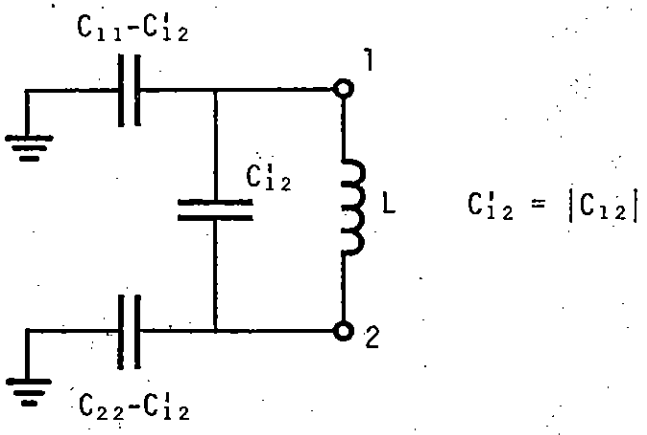

Figure 11. Network formed by capacitors representing Maxwell's capacitance coefficients which equals the dynamic capacitance between nodes 1 and 2.

We now show that the dynamic capacitance, C, is, indeed, the value of capacitance required to calculate the values of L and R needed to make the system oscillate at the required frequency. We do this specifically for L and the undamped frequency, ω_0. The procedure is the same for R and the imaginary frequency, ν.

The current through the inductance, L, connecting the two nodes is given by

$$L \frac{dI}{dt} = \Delta V = (E_{11} - E_{12})Q_1 - (E_{22} - E_{12})Q_2 \ . \qquad (4\text{-}27)$$

Defining positive current as the flow of positive charge from node 1 to node 2, and assuming that each node is initially charged equally, but with opposite polarity, we find, after taking the time derivative of Equation 4-27

$$\begin{aligned} L \frac{d^2I}{dt^2} &= (E_{11} - E_{12})(-I) - (E_{22} - E_{12})I \\ &= -(E_{11} + E_{22} - 2E_{12})I \ . \end{aligned} \qquad (4\text{-}28)$$

Assuming a time dependence of $e^{i\omega_0 t}$,

$$\omega_0^2 = \frac{E_{11} + E_{22} - 2E_{12}}{L} \ . \qquad (4\text{-}29)$$

Comparing with Equation 3-2, yields the dynamic capacitance derived in Equation 4-4 as the static capacitance between nodes.

Referring to Figure 7 again, we wish to show that, with C_A, C_B, and C_{AB} defined as above, in terms of Maxwell's capacitive coefficients, this circuit gives the exact solution for the two node model when i is given by the current leaving one node, but normalized to consider the fact that charge does not immediately become transferred to infinity. This exercise emphasises two errors which have been made in the past using lumped parameter models based on transmission line theory. The first error was referred to above: the charge was effectively transferred instantaneously to infinity. The second error was the assumption that the

driving current was transferred across the node capacitance to infinity (c_{11}) rather than across a smaller capacitance ($C_A = C_{11} - C'_{12}$) with a separate capacitance between nodes ($C_{AB} = C_{12}$). The transmission line model is shown in Figure 12, for comparison with Figure 7. The load impedance, Z_L, represents the parallel RL impedance used in Figure 7.

We begin by redrawing Figure 7 in a form which facilitates analysis. This circuit is shown in Figure 13. Rather than solving for a general load, Z_L, the open circuit voltage ($Z_L = \infty$) is computed. This simplifies the analysis, but allows the basic points to be made. Then the open circuit voltage across two nodes, due to the emission of a single point charge, will be calculated. This will be in terms of the elastance coefficients. After converting to Maxwell's capacitance coefficients, the two solutions will be seen to be identical when the driving current is taken to be the current leaving the node minus a time-dependent quantity which takes into account the distance of the emitted charge and the rate at which it moves away from the node.

Using nodal analysis, the voltage across Z_L, when $Z_L = \infty$ is found to be

$$V_{oc} = \frac{Q}{C_A + C_{AB}\left(1 + \frac{C_A}{C_B}\right)}, \tag{4-30}$$

or

$$V_{oc} = \frac{Q(C_{22} - C'_{12})}{C_{11}C_{22} - C'^2_{12}} \tag{4-31}$$

where

$$Q = \int_0^t i \, dt \, . \tag{4-32}$$

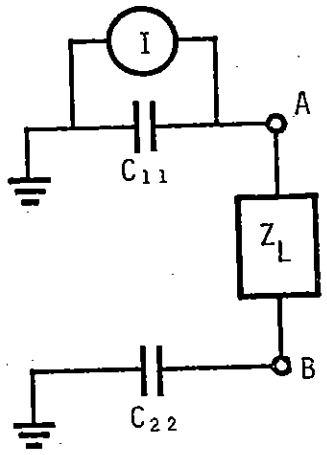

I = current leaving node

Figure 12. Two-node model with electron emission from one node as would be treated using transmission line theory as has been applied in the past. Compare with the correct model shown in Figure 7. Here, the current driver is the current being emitted from the node. The correct current term includes a time-dependent correction term which accounts for the fact that charge, once emitted, moves away from the node with finite velocity, and is not immediately transferred to infinity.

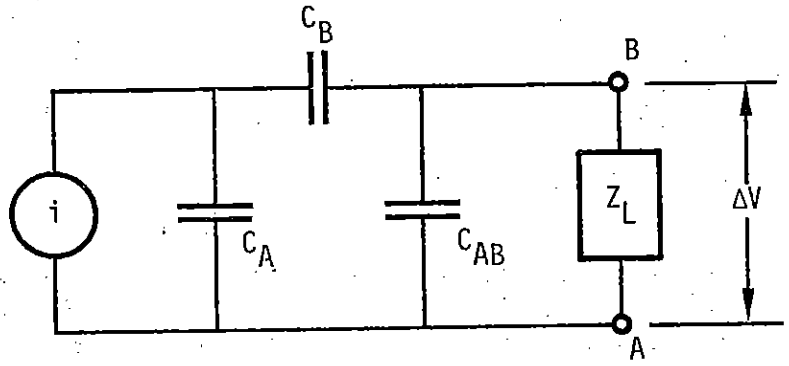

Figure 13. Two-node model for emission from one node. This circuit is the same as shown in Figure 7, rearranged to facilitate analysis. In terms of Maxwell's capacitance coefficients: $C_A = C_{11}-C_{12}$, $C_B = C_{22}-C_{12}$, $C_{AB} = C_{12}$.

The correct expressions for Q and i have yet to be determined.

Consider the open circuit voltage developed across two nodes when a charge of -q is emitted, leaving a charge of +q on node A. The voltage is

$$V = V_{oc} = q[(E_{11} - E_{12}) - (e_1 - e_2)] , \tag{4-33}$$

where the elastance coefficients have previously been defined. This can be rewritten as

$$V_{oc} = Q(E_{11} - E_{12}) , \tag{4-34}$$

where

$$Q = q\left(1 - \frac{e_1 - e_2}{E_{11} - E_{12}}\right) . \tag{4-35}$$

Now, using Equations 4-23 and 4-25,

$$V_{oc} = \frac{Q(C_{22} - C'_{12})}{C_{11}C_{22} - C'^{2}_{12}} , \tag{4-36}$$

which is identical to Equation 4-31. Q is the charge emitted from the node minus a term which is proportional to the difference in spatial elastance coefficients $(e_1 - e_2)$. These elastance coefficients vary inversely with the distance from the nodes, so that when the true charge is many nodal radii away, $Q \simeq q$.

In the case of a single emitted charge, q is a step function in time so that

$$i = I \cdot \left(1 - \frac{e_1 - e_2}{E_{11} - E_{12}}\Big|_{t=0}\right) - q\,\frac{\frac{d}{dt}(e_1 - e_2)}{E_{11} - E_{12}} , \tag{4-37}$$

where

$$I = q\delta(t) . \tag{4-38}$$

and $\delta(t)$ is the impulse function.

In general, when there is a charge distribution in space and the time history of charge build-up on the node is q(t),

$$Q(t) = q(t) - \frac{\int_\tau \rho(\vec{x},t)\Delta e(\vec{x},t)d\tau}{E_{11} - E_{12}}, \qquad (4\text{-}39)$$

and

$$i(t) = I(t) - \frac{\frac{d}{dt}\int_\tau \rho(\vec{x},t)\Delta e(\vec{x},t)d\tau}{E_{11} - E_{12}}, \qquad (4\text{-}40)$$

where the integration is over all space, $\rho(\vec{x},t)$ is the negative charge density, and $\Delta e(\vec{x}, t)$ is the difference in spatial elastances. Relativistic effects are ignored here. A useful example is that in which all charge is emitted in the direction parallel to the line connecting the nodes and with constant velocity, v. There are two ways in which the integral can be interpreted. First, we can look at the time history of the spatial charge density at each fixed point in space, so that $\Delta e = e_1 - e_2$ is independent of time while $\rho(\vec{x})$ is time dependent. This is the approach used in QUASI. The other method is to follow particles of charge $\rho\Delta\tau$ through space, so that $\rho(\vec{x})$ is independent of time, but Δe is time dependent. This is the approach taken so far in this note. The former method is simpler in this case, however.

Figure 14 shows the two nodes with the column of charge that has been emitted at the time t. Let charge leave the node surface at the rate I(t) (coulomb/sec). The charge in a layer of thickness Δz at a distance z is

$$dz = I(t - \frac{z - a_1}{v})\frac{dz}{v}. \qquad (4\text{-}41)$$

The effective charge is then

$$Q(t) = q(t) - \frac{\int_{a_1}^{vt+a_1} I(t - \frac{z - a_1}{v})\,\Delta e(z)\,\frac{dz}{v}}{E_{11} - E_{12}}, \qquad (4\text{-}42)$$

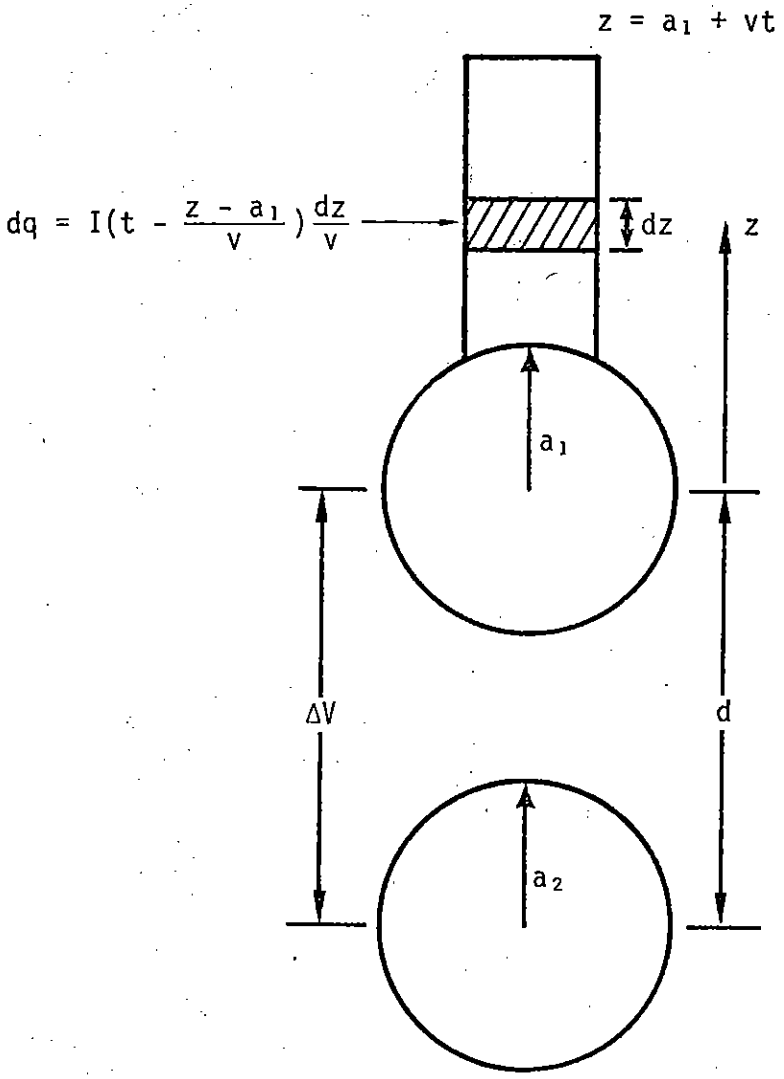

Figure 14. Geometry of open circuit voltage calculation when charge is emitted along z axis with constant velocity v.

and the effective current is

$$i(t) = I(t) - \frac{1}{E_{11} - E_{12}}\left[\int_{a_1}^{vt+a_1} \dot{I}\left(t - \frac{z - a_1}{v}\right)\Delta e(z)\,\frac{dz}{v} + I(0)\Delta e(vt - a_1)\right]. \tag{4-43}$$

As an example, let $I(t) = At$, i.e., a linear rise. Then with

$$\Delta e(z) = \frac{1}{z} - \frac{1}{z + d}. \tag{4-44}$$

$$Q(t) = \frac{A}{2}t^2 - \frac{\frac{1}{v}\int_{a_1}^{vt+a_1} A \cdot (t - \frac{z - a_1}{v})(\frac{1}{z} - \frac{1}{z + d})dz}{E_{11} - E_{12}}$$

or,

$$Q(t) = q(t) - \frac{1}{v(E_{11} - E_{12})}\left[I(t + \frac{a_1}{v})\ell n\left(\frac{1 + \frac{vt}{a_1}}{1 + \frac{vt}{a_1 + d}}\right) - I\left(\frac{d}{v}\right)\ell n\left(1 + \frac{vt}{a_1 + d}\right)\right], \tag{4-45}$$

and

$$i(t) = I(t) - \frac{\dot{I}}{v(E_{11} - E_{12})}\,\ell n\left(\frac{1 + \frac{vt}{a_1}}{1 + \frac{vt}{a_1 + d}}\right), \tag{4-46}$$

where $\dot{I} = A$. In the limit of $t \ll a_1/v$,

$$i(t) \simeq I(t)\left[1 - \frac{\left(\frac{1}{a_1} - \frac{1}{a_1 + d}\right)}{E_{11} - E_{12}}\right]. \tag{4-47}$$

SECTION 5
THE LONG, THIN ROD

In this section, we consider how a long, thin rod would be modeled in the quasi-static approximation. The thin rod represents the next step in the evolution of more complicated objects. It is somewhat unique, however, in that the usual technique of determining the node radius, i.e., the radius of a sphere with area equal to the area of the surface represented, is not valid. The first part of this section will involve a discussion of this point. Then, the values of the inductances required to make the rod ring at the proper frequency will be found using two different methods. The first method assumes, as does the transmission line model, that all inductances are equal. These inductances will not have the same value as predicted for a lumped parameter representation of a transmission line.

When "fat" objects are being modeled, all inductances cannot be presumed equal. The procedure in such cases has been to calculate inductances based on the assumption that no charge accumulates on any nodes except those at the ends of the object. This is not physically realistic, but it does simplify the inductance calculation. The current distribution excited along the object is incorrect, but represents the average of the distribution. This has not been an important consideration in most QUASI calculations, since the first resonance mode has not been strongly excited. This second method will also be applied to the thin rod problem here, in order to compared the results to the equal inductance method.

First, we consider the capacitance to infinity of a cylinder with length 2h and diameter 2a. This static capacitance is known for all ratios of h/a (Reference 5), but we restrict ourselves to the range $h/a \geq 1$. Define an equivalent radius, r_{eq}, such that r_{eq} is the radius of a sphere with the same static capacitance, C_∞. Then

$$C_\infty = 4\pi\varepsilon_0 r_{eq} \ . \tag{5-1}$$

When the object is "fat" (a term that will be defined shortly),

$$r_{eq} \simeq \sqrt{\frac{A}{4\pi}} \ , \tag{5-2}$$

where A is its surface area. When the object is a long, thin cylinder, however,

$$r_{eq} \simeq 2h/(\Omega - 1) \ , \tag{5-3}$$

where the "fatness factor" is

$$\Omega = 2\ell n(2h/a) \ . \tag{5-4}$$

Figure 15 compares the true normalized equivalent radius (r_{eq}/h) with the two approximations, for a range of (h/a) between 1 and 100. The area approximation is best for $h/a < 7$, while the thin rod approximation is best for $(h/a) \geq 7$. Therefore, a "fat" cylinder is one for which $(h/a) < 7$ and a "thin" one has $(h/a) \geq 7$. Table 1 compares the percentage error involved in the two approximations.

As a point of interest, the steady state inductance of a thin rod can be obtained from Equations 5-1 and 5-3 through $\omega_0^2 = 1/LC_\infty$, where $\omega_0 = 2\pi c/(4h)$, i.e.,

$$L_0 \simeq \frac{\mu_0}{4\pi}(2h)(\Omega - 1) \ . \tag{5-5}$$

The capacitance and inductance per unit length are

$$C'_\infty = \frac{1}{4\pi\varepsilon_0(\Omega - 1)} \ , \tag{5-6}$$

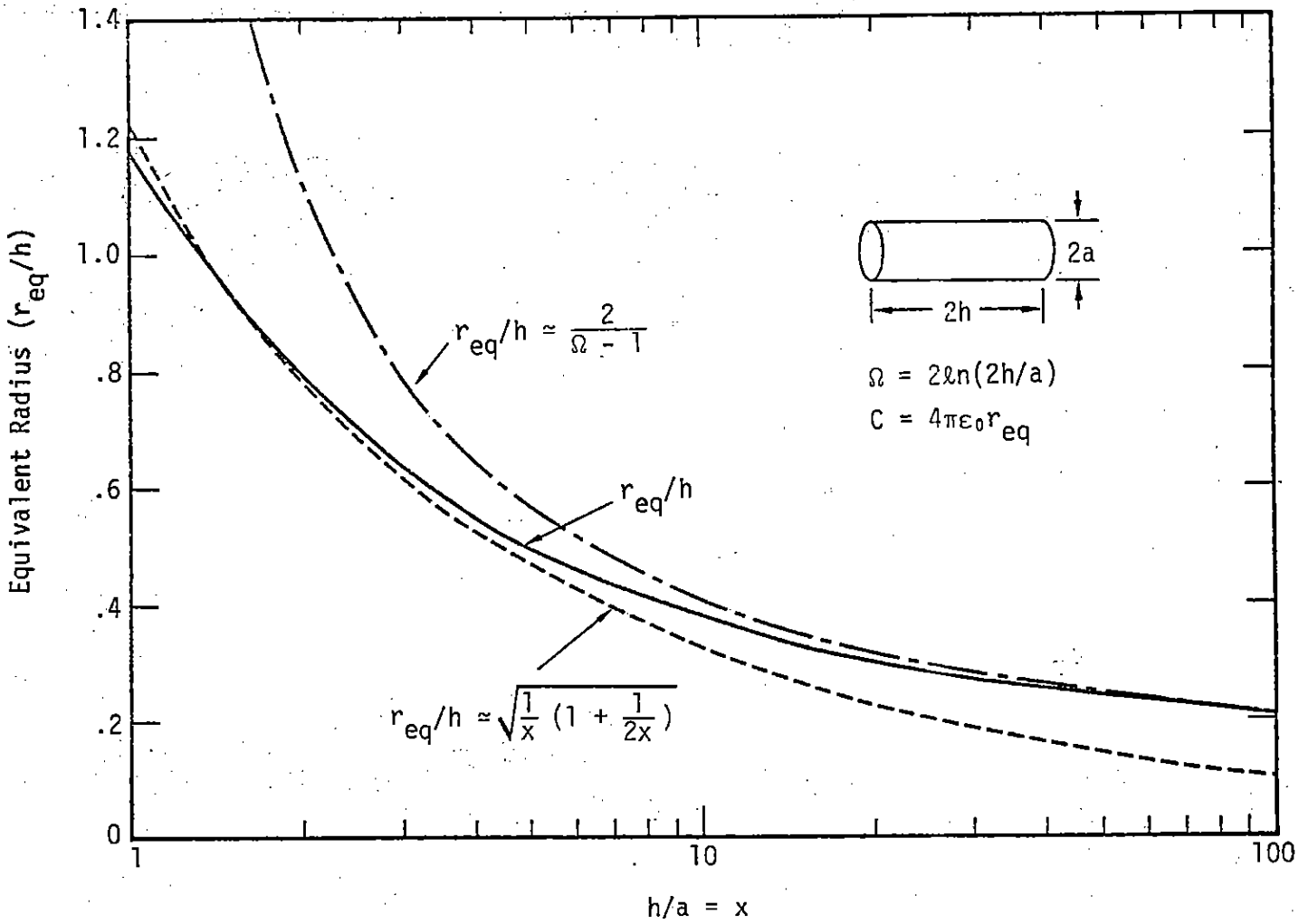

Figure 15. Comparison between approximate capacitive equivalent radii and true equivalent radius for cylinders of various fatness ratios.

$$L_0' = \frac{\mu_0}{4\pi} (\Omega - 1) \ . \qquad (5\text{-}7)$$

Reference 10 shows that the area formula for the radius of a node (Equation 2-4) works well in the case of a sphere, a representative "fat" object. Thus, area conservation is used in determining the node radii (the sum of the node surface areas equals the area of the object). This rule does not work for thin rods. Note that the static capacitances of the individual nodes do not necessarily sum to yield the static capacitance of the object, as in the case of the fat object where the sum of the squares of the individual capacitances equals the square of the total capacitance, i.e., $C_\infty^2 = \sum_i (C_\infty^i)^2$, where C_∞^i is the static capacitance of the i^{th} node in the absence of all others. We need another conservation rule for thin rod problems, and take our clue from the form of the approximation for the thin rod capacitance. A thin rod will be broken into linear segments for a nodal representation, not into surface area segments, as is the procedure for a fat object. Therefore, we are interested in conserving length rather than surface area. Because of the linear relationship, we conserve static capacitance automatically, and $r_{eq} = \sum_i a_i$. For the fat object, the equivalent relation was $r_{eq}^2 = \sum_i a_i^2$.

Table 1. Comparison of approximations for the equivalent radius of a cylinder.

h/a	Ω	r_{eq}/h	$r_{eq}/h = 2/(\Omega - 1)$	Δ%	$r_{eq}/h = \sqrt{\left(\frac{a}{h}\right) + \frac{1}{2}\left(\frac{a}{h}\right)^2}$	Δ%
1	1.39	1.185	5.128		1.225	+ 3.4
1.5	2.20	0.933	1.667	+78.9	.943	+ 1.1
5	4.60	0.502	0.556	+10.8	.469	- 6.6
15	6.80	0.332	0.345	+ 3.9	.262	-21.1
50	9.21	0.238	0.244	+ 2.5	.142	-40.3
100	10.6		0.208			

$\Omega = 2\ell n(2h/a)$

Now consider the values of the inductance required to make the thin rod oscillate in its primary mode when it is divided into N equal segments. Figure 16a shows a rod divided into four segments; Figure 16b shows the schematic diagram of the nodal representation. The radius of each node is

$$a_1 = \frac{r_{eq}}{N} = \frac{\ell}{N} \frac{1}{(\Omega - 1)} , \qquad (5\text{-}8)$$

or

$$a_1 = \frac{\Delta\ell}{\Omega - 1}$$

where

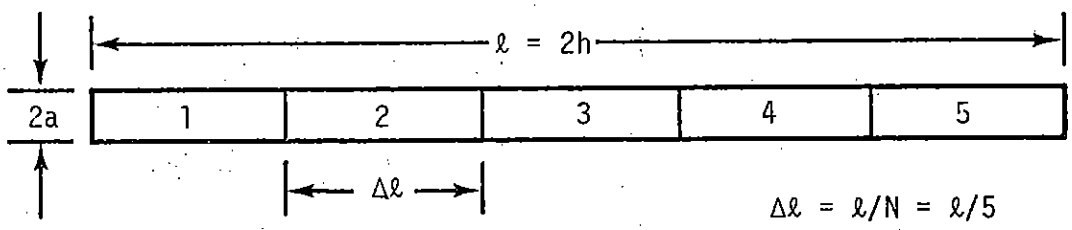

(a) Segmentation of rod

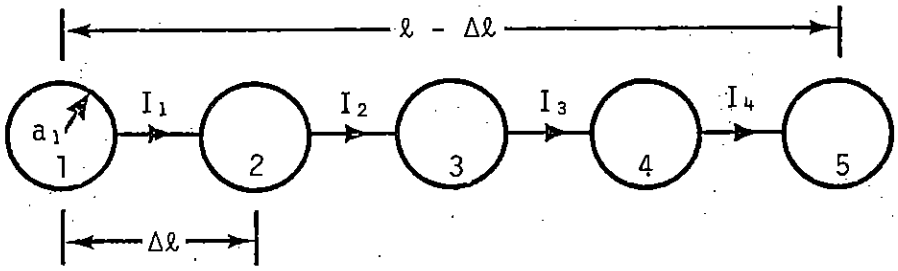

(b) Node representation

Figure 16. Geometry of thin rod approximation (example using five segments).

$$\Omega = 2\ell n(\ell/a)$$

$\ell = 2h$ = rod length

a = rod radius .

When the rod is excited in the dipole mode, symmetry can be used to reduce the number of independent equations. The open circuit potentials at each node are given by

$$V_1 = (E_{11} - E_{15})Q_1 + (E_{12} - E_{14})Q_2 \qquad (5\text{-}9)$$

$$V_2 = (E_{11} - E_{13})Q_2 + (E_{12} - E_{14})Q_1$$

$$V_3 = 0$$

$$V_4 = - V_2$$

$$V_5 = - V_1$$

The relevant open circuit potential differences are

$$\Delta_{12} = V_1 - V_2 = [(E_{11} - E_{15}) - (E_{12} - E_{14})]Q_1 - [(E_{11} - E_{13}) - (E_{12} - E_{14})]Q_2 , \qquad (5\text{-}10)$$

$$\Delta_{23} = V_2 = (E_{11} - E_{13})Q_2 + (E_{12} - E_{14})Q_1. \qquad (5\text{-}11)$$

When the inductances L_1 and L_2 are inserted, the currents through them are governed by the equations

$$L_1 \frac{dI_1}{dt} = \Delta_{12} , \qquad (5\text{-}12)$$

$$L_2 \frac{dI_2}{dt} = \Delta_{23} .$$

Four unknown quantities are involved (L_1, L_2, I_1, I_2) with only two equations. An additional assumption is required. Thus, we are led to the two choices mentioned at the start of this section: equal inductances or equal currents. The first assumption is the more intuitive, in this case,

while the second is the more easily applied.

Applying the equal inductance assumption first, we define

$$L = L_1 = L_2 \ . \tag{5-13}$$

As before, positive current is defined as the flow of positive charge from a lower numbered node to a higher numbered node. Continuity then gives the relation between charge and current

$$\begin{aligned} \dot{Q}_1 &= - I_1 \\ \dot{Q} &= I_1 - I_2 \ , \end{aligned} \tag{5-14}$$

so that, after differentiating Equations 5-12 and assuming a harmonic time dependence, the inductance is seen to be related to the ringing frequency, ω, through

$$(\omega^2 L)^2 - A(\omega^2 L) + B = 0 \ , \tag{5-15}$$

where

$$\begin{aligned} A &= (E_{11} - E_{15}) + 2(E_{11} - E_{12} - E_{13} + E_{14}) \\ B &= (E_{11} - E_{13})(E_{11} - E_{15}) - E_{12} - E_{14})^2 \ . \end{aligned}$$

Because of the equal spacing between segments, the internode elastances are related simply:

$$\begin{aligned} E_{13} &= \frac{1}{2} E_{12} \\ E_{14} &= \frac{1}{3} E_{12} \\ E_{15} &= \frac{1}{4} E_{12} \ . \end{aligned} \tag{5-16}$$

In terms of the self-elastance, E_{11}, and the largest internode elastance, E_{12}, the coefficients A and B become

$$A = 3(E_{11} - \frac{29}{36} E_{12})$$

$$B = E_{11}^2 - \frac{3}{4} E_{11}E_{12} - \frac{23}{72} E_{12}^2 \ . \qquad (5\text{-}17)$$

The internode elastance is proportional to $1/\Delta\ell$, while the self-elastance is proportional to $(\Omega - 1)/\Delta\ell$, so that their ratio is

$$\frac{E_{11}}{E_{12}} = \Omega - 1 \ , \qquad (5\text{-}18)$$

where Ω is defined in Equation 5-8. It was shown above that a "thin" object is one for which $(h/a) > 7$, or $\Omega > 5.3$. Structurally, this is really quite a thick rod, i.e., most rods used in a satellite or other structure are thinner than this ratio. Even in this case, the ratio of self-elastance to mutual elastance is relatively large ($E_{11}/E_{12} = 4.3$) and the mutual elastances can be effectively ignored. The coefficients A and B reduce to

$$A \simeq 3E_{11}$$

$$B \simeq E_{11}^2 \ . \qquad (5\text{-}19)$$

When the internode elastances can be ignored, the self-capacitance is approximately equal to the reciprocal of the self-elastance (see Section 4). Therefore, for the purpose of defining inductance values to give the proper resonance frequency, the nodal model is equivalent to using a lumped parameter representation of a transmission line model. To show the equivalence, we will derive such a model.

In a transmission line model, the rod would be assigned a capacitance per unit length (C') and an inductance per unit length (L') such that

$$L'C' = 1/c^2 \ . \qquad (5\text{-}20)$$

The approximate values given by Equations 5-6 and 5-7 satisfy this relationship (since they were forced to). In this way, the total inductance and total capacitance will be such that the undamped ringing frequency will correspond

to the inverse of the time required for light to traverse the length of the rod and back, i.e.,

$$\ell^2 L'C' = 1/\omega^2 \ . \qquad (5\text{-}21)$$

If one chooses to represent this transmission line model with a lumped parameter model, the circuit would look like that shown in Figure 17, where a model with five capacitors was chosen to correspond to the five node model analyzed above. Using standard circuit solution techniques, the equation relating L, C, and ω is seen to be

$$(\omega^2 L)^2 - \frac{3}{C}(\omega L) + \frac{1}{C^2} = 0 \ . \qquad (5\text{-}22)$$

Comparison with Equations 5-15 and 5-19 shows that this model is equivalent to the nodal model, in the thin rod limit where the internode elastances can be ignored, one can use the capacitance to infinity, or its inverse, in each case.

The solution to Equation 5-22 shows that

$$LC = \frac{(3 - \sqrt{5})}{2\omega^2} \ , \qquad (5\text{-}23)$$

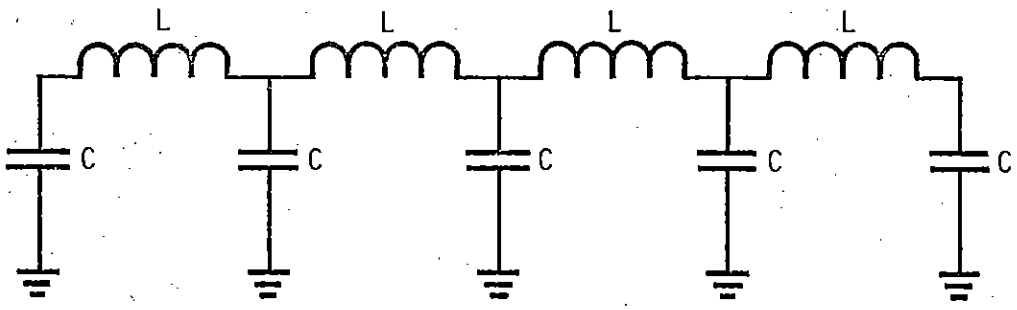

Figure 17. Lumped parameter representation of the transmission line model of a thin rod. A model with five capacitors was chosen for comparison with the nodal model shown in Figure 16.

where, in analogy to the nodal model

$$C = \frac{1}{E_{11}} = \frac{\Delta\ell}{4\pi\varepsilon_0(\Omega - 1)} , \qquad (5\text{-}24)$$

$$\Delta\ell = \ell/5 .$$

The product LC is considerably larger than would be expected if one could use the L and C corresponding to the size of the rod segment represented, in which case one would have the relation

$$LC = \frac{1}{20\omega^2} . \qquad (5\text{-}25)$$

In other words, when constructing an LC model for a thin rod, one cannot simply take the total capacitance, divide it by the number of segments represented by capacitances and also take the total inductance divided by the number of segments represented by inductances and expect to force the model to resonate at the proper frequency. The same is true for the nodal model, in which the capacitances are replaced by elastances.

We now investigate the second technique for finding inductance values which make the nodal model ring at the proper frequency. This technique is mathematically simpler and can be used for fat objects where the concept of elastance per unit length cannot be applied. In this case, we allow no charge to accumulate at the inner nodes, so that there is no contribution to the potentials from them and the current is constant as a function of distance along the rod. This assumption necessitates the use of different inductances between different pairs of nodes, in this case, two inductances (L_1 and L_2). The open circuit voltage equations, analogous to Equations 5-9, are

$$V_1 = (E_{11} - E_{15})Q_1$$

$$V_2 = (E_{12} - E_{14})Q_1$$

$$V_3 = 0 \qquad (5\text{-}26)$$

$$V_4 = - V_2$$

$$V_5 = - V_1 \ .$$

Now, the charge Q_2 is equal to zero. Therefore, the current is given by

$$L_1 \frac{dI}{dt} = [(E_{11} - E_{15}) - (E_{12} - E_{14})]Q_1 \ , \qquad (5\text{-}27)$$

$$L_2 \frac{dI}{dt} = (E_{12} - E_{14})Q_1 \ . \qquad (5\text{-}28)$$

Using the same definition of positive current, we obtain, after differentiation

$$\omega^2 L_1 = E_{11} - E_{12} + E_{14} - E_{15} = E_{11} - \frac{11}{12} E_{12} \ , \qquad (5\text{-}29)$$

$$\omega^2 L_2 = E_{12} - E_{14} = \frac{2}{3} E_{12} \ . \qquad (5\text{-}30)$$

If the internode elastance is ignored as a first approximation, the inductance L_2 can be replaced by a short circuit and inductance L_1 is proportional to the self-elastance. The average inductance is

$$L_{avg} = \frac{1}{2} (L_1 + L_2) = \frac{E_{11}}{2\omega^2} \ . \qquad (5\text{-}31)$$

The constant inductance calculated using the first technique was (Equation 5-23, with $C = 1/E_{11}$)

$$L \simeq \frac{0.76E_{11}}{2\omega^2} \ , \qquad (5\text{-}32)$$

or, about 25 percent smaller.

Both techniques yield the same current on the end segments, when the initial charge is the same, i.e.,

$$I = I_1 = - i\omega Q_0 e^{i\omega t} , \qquad (5\text{-}33)$$

where Q_0 is the charge initially placed on segment 1 and $-Q_0$ is the charge initially placed on segment 5. The inner current, I_2, developed when equal inductances are used, is given approximately by

$$I_2 \simeq \frac{1}{2}(1 + \sqrt{5})I_1 = 1.62I_1 . \qquad (5\text{-}34)$$

In terms of the end current, $I = I_1$, the average current running on the equal inductance rod is

$$I_{avg} = 1.31\ I . \qquad (5\text{-}35)$$

The fact that the average current is about 30 percent larger than the equal current model is consistent with the fact that the average inductance of the equal current model is about 30 percent larger than that of the equal inductance model.

SECTION 6

THE SPHERE AND CYLINDER

In the previous section, the difference in treatment between thin objects and "fat" objects was considered. "Thin" and "fat" were defined in terms of the approximations which could be used to estimate the capacitance to infinity of the object, namely, the logrithmic and area approximations. In this section, we concentrate on the representation of fat objects, specifically the sphere and fat cylinder. These are certain aspects to the problem of modeling fat objects which are not encountered in the thin rod problem. One of these was discussed in Section 5: the method by which one chooses to solve the inductance-current distribution problem. There is also the problem of spacing the nodes properly, one which did not occur with the thin rod because the node radius, in most practical cases, is much less than the internode distance. The problem of the sphere has already been thoroughly explored by Longmire (Reference 10), but it will be explored here from a somewhat different viewpoint. Its symmetry makes it a nice problem to solve, but also prevents it from lending much insight into the solution of real problems. That is why the fat cylinder will also be considered.

One of the first questions encountered when trying to model an object for SGEMP predictions is that of how many nodes to use. From the aspect of trying to force a single, uncomplicated structure to ring in its lowest mode, a basic two-node representation will suffice. However, other considerations are involved. First, the inverse separation distance approximation for the internode elastances will only be valid if the nodes are

separated by a distance which is sufficiently great, compared to the radius used to calculate the self-elastance. A rule yielding reasonable results is to have the centers of any two neighboring nodes separated by three times the average radius of the two nodes. This assumes that the two node radii in question are not grossly different (they would not be in any reasonably thought-out representation). We will return to this subject briefly in the next paragraph. The second consideration is that of the detail desired in the structural current distribution. The distribution will normally be dominated by the driving source, i.e., the currents leaving the structure and returning from space, rather than by any ringing modes excited on the structure. Therefore, the number of nodes, and their placement will be determined in large part by the expected current flow due to the electron emission rather than the desire to resolve standing waves.

As an example of how the node spacing becomes a factor because of the internode elastance approximation, consider the problem of representing a right circular cylinder with flat endcaps. Assume that a two-node representation is acceptable as a first approximation to the current flow across the cylinder's equator. The question becomes one of whether the nodes representing each end of the cylinder are far enough apart to allow the elastance approximation. To check this we first calculate the half-area of the cylinder to be

$$A_h = \pi r(d + r) \ , \qquad (6\text{-}1)$$

where d is the cylinder length and r is its radius. The node radius is that of a sphere with the same surface area, i.e.,

$$a = \frac{r}{2}\sqrt{1 + d/r} \ , \qquad (6\text{-}2)$$

where a is the equivalent radius. If we require that the nodes be centered on the centers of the endcaps, a distance, d, apart, and that $d \geq 3a$, we

find that the ratio of $d/r \geq 3$ must be observed. If the cylinder is fatter than this, it must be broken into smaller segments in both the azimuthal and longitudinal directions. As mentioned above, this would probably be done for purposes of resolving the current distribution anyway. See Figures 1, 2, and 3 for an example.

As a partial justification for the node separation ($d/a \geq 3$) rule, consider the Maxwell capacitance coefficient for two metal spheres. Using the inverse distance approximation for the elastance, we have (Equation 4-24)

$$C_{12} = C_{21} \simeq - 4\pi\varepsilon_0 \frac{a^2}{d} , \tag{6-3}$$

where a is the sphere radius (equal spheres) and d is the separation between sphere centers. The correct relation is (Reference 11)

$$C_{12} = C_{21} = 4\pi\varepsilon a \sinh\beta \sum_{n=1}^{\infty} \operatorname{csch}(2n\beta) , \tag{6-4}$$

where $\cosh \beta \equiv \frac{d}{2a}$. For reference, the self-capacitance is given by

$$C_{11} = C_{22} = 4\pi\varepsilon a \sinh \sum_{n=1}^{\infty} \operatorname{csch}[(2n - 1)\beta] . \tag{6-5}$$

Equations 6-3 and 6-4 are compared in Figure 18. It indicates that $d/a \geq 3$ is a reasonable separation rule for invoking the inverse distance approximation.

In Section 5 we showed that the capacitance of "fat" cylinders was very close to the capacitance of a sphere with the same area. Reference 6 indicates that this is true, for "fat" shapes in general, including thin disks. We now show that, by conserving area in a nodal representation of such an object, and using the inverse distance approximation for the mutual elastance, that one can expect a reasonable value for the static potential calculated at the node. We will restrict ourselves to the case of a sphere, which is easy to solve, and assume that the conclusions will be valid in

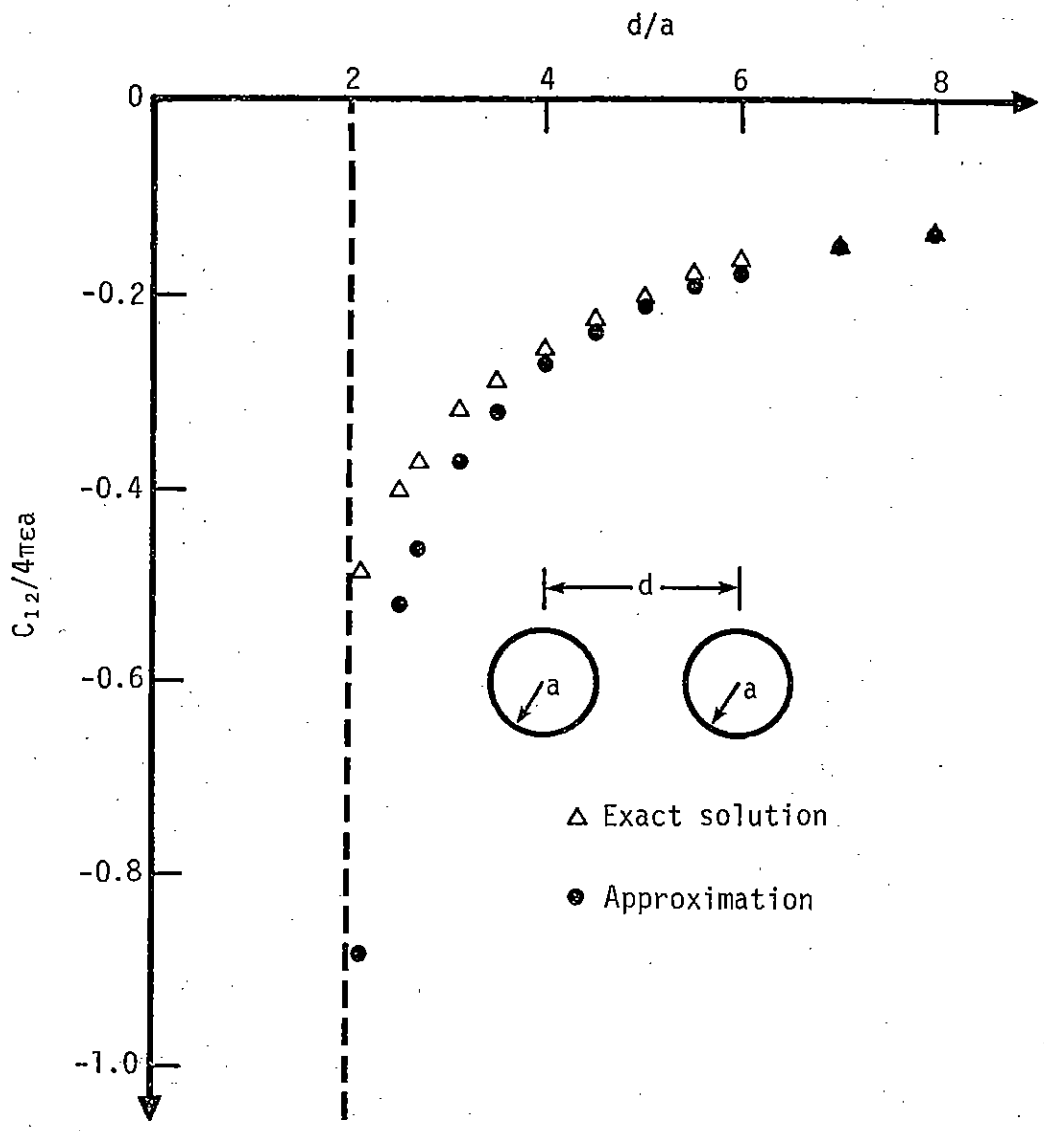

Figure 18. Comparison between the mutual capacitance coefficient (C_{12}) for a pair of spheres calculated exactly and using the inverse distance approximation.

general. Before proceeding, however, we will find the minimum number of nodes that can be used with the mutual elastance approximation. Since two nodes would be the minimum desirable number, we check that first. Consider a sphere of radius, r. The radius of a sphere with half this area is

$$a = r/\sqrt{2} \ . \tag{6-6}$$

If the two nodes with this diameter are located a diameter apart, i.e., d = 2r, then the separation distance to radius ratio is

$$d/a = 2\sqrt{2} \simeq 2.8 \ . \tag{6-7}$$

This is close to the desirable ratio of 3, so we conclude that a minimum of two equally spaced nodes can be used to represent a sphere, using the inverse distance mutual elastance approximation.

The potential at any point on the surface of a sphere with charge Q is

$$V = \frac{Q}{4\pi\varepsilon_0 r} \ . \tag{6-8}$$

If we picture the sphere as being divided into N segments of equal area, each with charge $Q_0 = Q/N$, then the potential at a point on the i^{th} segment is

$$V_i = \frac{1}{4\pi\varepsilon_0} \ \frac{N}{r} \ Q_0 \ . \tag{6-9}$$

Now represent each of these N area segments by a node such that the potential at the i^{th} node is

$$V_i = \sum_{n=1}^{N} E_{in} Q_0 \ , \tag{6-10}$$

and we have the test for the accuracy of the node model, i.e., how well is the relation

$$4\pi\varepsilon_0 \sum_{n=1}^{N} E_{in} = \frac{N}{r} \ . \tag{6-11}$$

satisfied?

With a_i the radius of the i^{th} node and r_{in} the distance between the i^{th} and n^{th} node, the test becomes

$$\frac{1}{a_i} + \sum_{n \neq i}^{N} \frac{1}{r_{in}} = \frac{N}{r} . \tag{6-12}$$

In the case of a two-node representation, we have $N = 2$, $a_1 = a_2 = r/\sqrt{2}$, and $r_{12} = r_{21} = 2r$. Then

$$\frac{1}{a_1} + \frac{1}{r_{12}} = \frac{\sqrt{2} + \frac{1}{2}}{r} \simeq \frac{1.91}{r}, \tag{6-13}$$

which is very close to the desired $2/r$, i.e., within 4.5 percent. By increasing the number of nodes to $N = 6$, we maintain a configuration in which all adjacent nodes are the same distance apart, which is nice for some calculations which we will perform later. After numbering the nodes as shown in Figure 19, with nodes 1 and 6 at the poles and 2 through 5 around the equator, the relevant distances are

$$a_1 = a_2 = \ldots = a_6 = r/\sqrt{6} , \tag{6-14}$$

$$r_{in}(\text{n adjacent}) = \sqrt{2}\, r$$

$$r_{in}(\text{n opposite}) = 2r .$$

Equation 6-12 yields

$$\frac{\sqrt{6}}{r} + \frac{4}{\sqrt{2}\, r} + \frac{1}{2r} = \frac{5.78}{r} , \tag{6-15}$$

which is within 3.7 percent of the desired value of $6/r$.

The nodal model improves as we look at potentials farther out in space since the object begins to look more like a point charge. Thus, we have good reason to believe that the node model will be reasonable representation in the static limit.

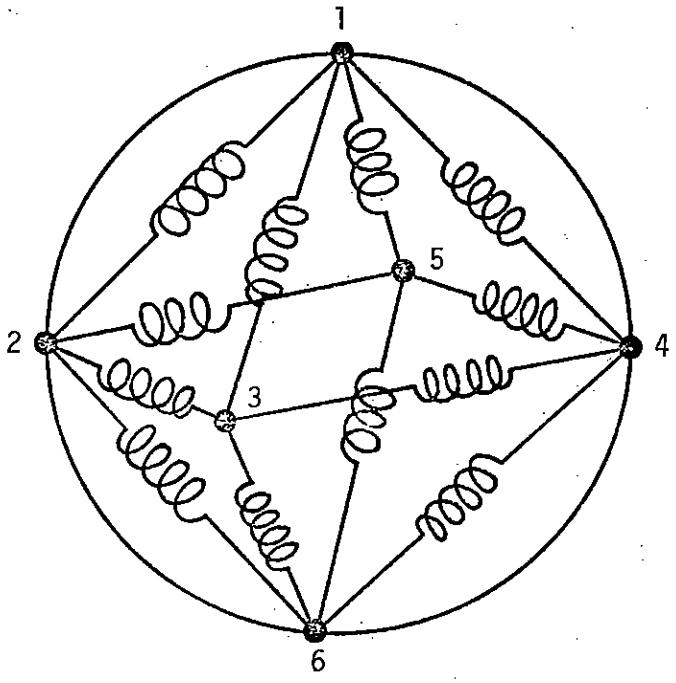

Figure 19. Six-node model of a sphere.

The first mode, or dipole response, of the sphere is extremely easy to represent in the case of the six-node model. The inductances are connected as shown in Figure 19, although the inductances parallel to the equator can be eliminated from the inductance calculation, since the azimuthally symmetric dipole mode will not excite currents in that direction. Also, with six equally spaced nodes, all inductances are equal, all currents are equal. Therefore, instead of solving the six-node sphere, which is done elsewhere (Reference 10), or solving a more complicated spherical representation, we choose to look at the fat cylinder. The basic nodal model is the fourteen node model shown in Figures 1 through 3. The nodes are arranged in two azimuthal planes, yielding four identical arms with the two end nodes (numbered 1 and 14 in Figure 1) in common. Each arm has five nodes, including the two common end-nodes. One node is at each corner and one is at the equator. In the model used as a test problem in QUASI, the end nodes represented half the end-cap area. The eight nodes at the corners each represented $1/8^{th}$

the end-cap area plus $1/16^{th}$ the area of the side of the cylinder. The four nodes around the equator each represent $1/8^{th}$ the side area.

In order to compute the inductances required to force the cylinder to ring at the proper frequency, a charge of +q will be placed on one end (node 1) and a charge of -q on the other (node 14). The symmetry of the problem allows us to consider only the current through one branch (nodes 1, 2, 6, 10, 14), $1/4^{th}$ of the total current flows through each arm. Further symmetry reduces the calculation to that of two inductances: the one connecting the end-node with a corner node (L_{12}) and the one connecting the corner node to the one at the equator (L_{26}). This particular calculation will not yield values for the inductances parallel to the equator, since the symmetry is such as to allow no current flow in that direction. A separate calculation, in which the cylinder is excited in this direction, e.g., by placing positive charges on nodes 2, 6, and 10, and negative charges on nodes 4, 8, and 12, would be necessary to obtain these values.

The impedances which connect the nodes consist of pairs of inductances and resistances in parallel. The inductances are calculated first, since the undamped ringing frequency can be estimated rather simply. This is done by fixing the wavelength of the oscillation as the distance around the cylinder, i.e.,

$$\lambda = 2(\ell + d) \ , \tag{6-16}$$

where ℓ is the cylinder height and d its diameter. The undamped ringing frequency is then

$$\omega_0 = 2\pi c/\lambda \ . \tag{6-17}$$

The damping rate, ν, must be estimated separately. This might be done in the general case by looking at the damping rate of an ellipsoid with similar size and dimension ratios. The solution is known for thin cylinders. In the course of calculating the inductances, an effective capacitance will be found which yields the relation

$$\omega_0 = \frac{1}{\sqrt{LC_{eff}}} \quad , \tag{6-17}$$

for each L. This effective capacitance, given in terms of the elastance coefficients, can then be used to calculate the parallel resistance through Equation 3-3,

$$R = \frac{1}{2\nu C_{eff}} \quad . \tag{6-18}$$

The cylinder will then ring with the damped frequency

$$\omega_r = \sqrt{\omega_0^2 - \nu^2} \quad . \tag{6-19}$$

Continuing with the example of the cylinder, we have the problem shown in Figure 20 to solve. The cylinder radius is r = d/2 and length ℓ = 2h. Therefore, the area of each end-cap is

$$A_c = \pi r^2 \quad , \tag{6-20}$$

and that of the cylinder body is

$$A_b = 4\pi rh \quad . \tag{6-21}$$

The area represented by each end-node is

$$A_1 = \frac{\pi}{2} r^2 \quad . \tag{6-22}$$

The area represented by each corner node is

$$A_2 = \frac{\pi}{8} r^2 + \frac{\pi}{4} rh \quad . \tag{6-23}$$

The nodes around the equator each represent the area

$$A_3 = \frac{\pi}{2} rh \quad . \tag{6-24}$$

The corresponding node radii are

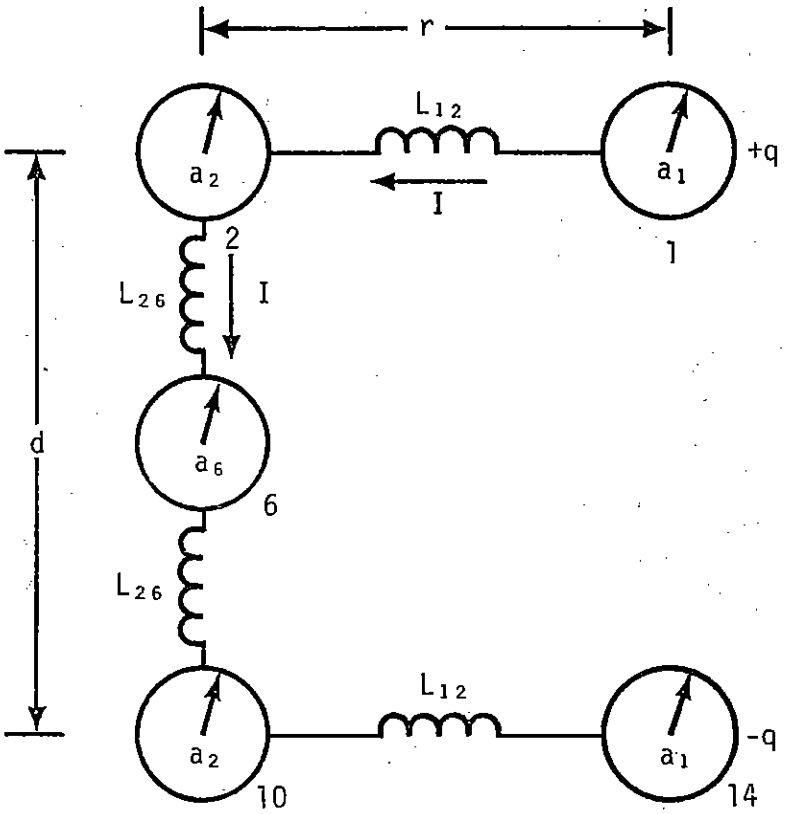

Figure 20. Single arm of node representation of cylinder. One fourth of total current flows down each arm. It is assumed that no charge accumulates at the corner nodes. The cylinder has radius r and length ℓ.

$$a_1 = \frac{r}{\sqrt{8}} , \tag{6-25}$$

$$a_2 = \frac{r}{4}\sqrt{\frac{h}{r} + \frac{1}{2}} , \tag{6-26}$$

$$a_3 = \frac{1}{2}\sqrt{\frac{rh}{2}} . \tag{6-27}$$

In order to simplify the calculation, we assume that the current is continuous around the corner, i.e., there is no charge accumulation. The three relevant potentials are

$$V_1 = q(E_{1,1} - E_{1,14}) \ , \tag{6-28}$$

$$V_2 = q(E_{1,2} - E_{2,14}) \ , \tag{6-29}$$

$$V_6 = 0 \ . \tag{6-30}$$

The elastances are given by

$$4\pi\epsilon_0 E_{1,1} = 1/a \ , \tag{6-31}$$

$$4\pi\epsilon_0 E_{1,2} = 1/r \ , \tag{6-32}$$

$$4\pi\epsilon_0 E_{1,14} = 1/\ell \ , \tag{6-33}$$

$$4\pi\epsilon_0 E_{2,14} = 1/\sqrt{\ell^2 + r^2} \ . \tag{6-34}$$

Noting that $I = -1/4\ dq/dt$, we have the equations for the inductances

$$\omega_0^2 L_{12} = 4[(E_{1,1} - E_{1,2}) - (E_{1,14} - E_{2,14})] \ , \tag{6-35}$$

$$\omega_0^2 L_{26} = 4(E_{1,2} - E_{2,14}) \ . \tag{6-36}$$

The effective capacitances are then

$$4C_{12} = [(E_{1,1} - E_{1,2}) - (E_{1,13} - E_{2,14})]^{-1} \tag{6-37}$$

$$4C_{26} = (E_{1,2} - E_{2,14})^{-1} \ . \tag{6-38}$$

Equation 6-18 can be used to calculate the two necessary resistances R_{12} and R_{26}, which appear in parallel with L_{12} and L_{26}. To do this, an estimate of ν must be made. An upper limit is given by the damping rate of a sphere with the same surface area as the object under consideration (Equation 3-21). This is a reasonable approximation when the object is fat and not convoluted. In general, however, the damping rate is not an important parameter in SGEMP problems and can be ignored. Its importance can be bracketed by solving the problem twice, once with no resistance term and once with a resistance which gives the damping rate of a sphere of equal area.

REFERENCES

1. Mautz, J. R., and R. F. Harrington, Generalized Network for Bodies of Revolution, Air Force Weapons Laboratory, EMP Interaction Note 187, May 1968.

2. Hutchins, R. L., K. S. Kunz, and T. H. Lehman, Electromagnetic Coupling Critique, Braddock, Dunn, and McDonald, Inc., Albuquerque, New Mexico, BDM/A-176-73-TR, December 1973.

3. Marin, L., Natural Modes of Certain Thin-Wire Structures, Air Force Weapons Laboratory, EMP Interaction Note 186, August 1974.

4. Stratton, J. A., Electromagnetic Theory, McGraw-Hill Company, New York, 1941.

5. Marin, L., A Cylindrical Post Above a Perfectly Conducting Plate, I (Static Case), Air Force Weapons Laboratory, EMP Sensor and Simulation Note 134, July 1971.

6. Shumpert, T. H., Capacitance Calculations for Satellites, Part I. Isolated Capacitances of Ellipsoidal Shapes With Comparisons to Some Other Simple Bodies, Air Force Weapons Laboratory, EMP Sensor and Simulation Note 157, September 1972.

7. Marin, L., Natural Mode Representation of Transient Scattering from Rotationally Symmetric, Perfectly Conducting Bodies and Numerical Results for a Prolate Spheroid, Air Force Weapons Laboratory, EMP Interaction Note 119, September 1972.

8. Lee, S. W., and B. Leung, The Natural Resonance Frequency of a Thin Cylinder and its Application to EMP Studies, Air Force Weapons Laboratory, EMP Interaction Note 96, February 1972.

9. Marin, L., Natural Modes of Certain Thin-Wire Structures, Air Force Weapons Laboratory, EMP Interaction Note 186, August 1974.

10. Longmire, C. L., Note on Equivalent Circuits for Conducting Sphere, Mission Research Corporation, Santa Barbara, California, MRC-N-152, September 1974.

11. Smyth, W. R., Static and Dynamic Electricity, McGraw-Hill Company, 1968.

APPENDIX 2

QUASI: A HYBRID QUASI-STATIC CODE FOR CALCULATING SGEMP STRUCTURAL REPLACEMENT CURRENTS — THEORY AND RESULTS

NOTE: This appendix is self-contained and all mention of sections, figures, tables, equations, and references refers only to items contained herein. This appendix has not been published as a separate document.

TABLE OF CONTENTS

LIST OF ILLUSTRATIONS

SECTION 1

INTRODUCTION

When photons from an exoatmospheric nuclear burst hit an orbiting satellite, electrons are knocked off exposed surfaces. Electrons may move away from the satellite, escaping to infinity, or they may return to the satellite's surface, although not necessarily to the point where they were emitted. In any case, a spatial current density is produced which results in electromagnetic fields in space and currents on the conducting surfaces of the satellite. Such currents are labeled replacement currents, since this charge flow, in one sense, "replaces" the emitted electrons. The situation is more complicated than simple charge replacement, however. Emitted electrons have not moved very far from the satellite at early times and their presence affects the charge distribution on the satellite. Furthermore, the resulting electromagnetic fields will influence the electron trajectories, pulling many of the emitted electrons back to the satellite in some cases. The whole SGEMP problem is thus quite complicated, requiring, in general, a self-consistent calculation of electron motion and electromagnetic fields along with the proper boundary conditions as determined by the geometrical configuration of satellite conductors.

The electron dynamics problem is complicated by the fact that satellites are typically quite complex electromagnetic structures. Conductors rarely are in the form of simple geometries and often various pieces of the satellite are connected by struts or rods. In general, three-dimensional effects may also be important.

One thus has two primary computational problems in trying to calculate SGEMP replacement currents on a satellite. The first is the problem of calculating the self-consistent electron trajectories in sufficient detail to define the spatial current densities and charge distribution in the space outside the satellite, while the second problem is proper modeling of the complex geometrical structure of a real system.

A number of techniques can conceptually be used for calculating SGEMP replacement currents on complex structures. One of these techniques is the finite difference approximation for solving Maxwell's equations in a three-dimensional grid combined with Newton's law for following electron trajectories. Such finite-difference techniques have been used for some time in calculating the EMP fields produced by nuclear weapons[1-3], and more recently for two-dimensional SGEMP calculations[4-6]. The main problem in extending these finite difference calculations to a complex three-dimensional geometry is the fact that a very fine mesh would be required to describe parts of a complex geometry (e.g., struts or rods). When working in three dimensions the mesh size can easily become prohibitively large for use with existing computers.

Another calculational technique that has been used in the past for SGEMP calculations is the equivalent circuit method[7,8]. This method treats both the satellite itself and the surrounding space as an electrical circuit. Emitted electrons become current sources and existing circuit codes are used to find the transient response of the equivalent circuit. The advantage of such methods is that detailed geometries can sometimes be modeled by a few simple circuit elements (e.g., a thin rod may just be modeled as a single inductor); in addition, methods for solving circuit equations are readily available and generally understood. The disadvantages of circuit equivalent methods is that a rigorous treatment of both the satellite and the surrounding space requires a very large number of circuit elements whereas existing circuit solution techniques limit the analyst to relatively few elements, requiring much intuition in setting up the models.

Another set of calculational methods might be grouped under the general heading of electromagnetic scattering codes. Such techniques include moment methods, integral equation solutions, and singularity expansion calculations. These methods have been used for high altitude EMP interaction calculations where the incident fields are well known (usually incident plane waves). Thus these tools have been primarily used outside the source region, while for the SGEMP problem one must integrate over the spatial current density outside the satellite (due to emitted electrons) to determine the incident electromagnetic field at each conducting boundary. Scattered fields are then calculated so that the proper EM boundary conditions are obtained. The fact that one must obtain the incident fields due to external electrons at each time step severely limits the usefulness of these techniques at higher fluences where space charge limiting effects are important.

One can combine several of these calculational techniques into what might be called a hybrid method. Such hybrids can be designed to include the advantages of several other methods while attempting to minimize the limitations. Such a hybrid technique was used in constructing the structural return current code discussed in this report.

The method used is to divide the SGEMP problem into two parts. The space outside of a satellite is treated using finite difference techniques. Quasi-static fields are calculated and electron trajectories are followed by use of finite-difference approximations of Newton's law. The satellite itself, however, is treated as an equivalent circuit where currents depend on the voltages between circuit nodes and the connecting impedances. Simple circuits can model fairly complex structures so that realistic satellite geometries can be considered. We thus combine the good treatment of external space provided by finite difference techniques with the capability of handling complex geometries by circuit modeling. The main problem is mating these two methods so that self-consistent replacement current calculations are made.

The code developed for doing these calculations is called QUASI. This report first describes the basic theory used and various approximations made. A description of the code and numerical methods used is then given. This is then followed by a discussion of typical results.

SECTION 2

BASIC THEORY

As with any electromagnetics problem, a basic starting point is Maxwell's equations (in MKS units)

$$\nabla\times\vec{E} + \frac{\partial\vec{B}}{\partial t} = 0 \tag{2-1}$$

$$\nabla\times\vec{H} - \frac{\partial\vec{D}}{\partial t} = \vec{J} \tag{2-2}$$

$$\nabla\cdot\vec{B} = 0 \tag{2-3}$$

$$\nabla\cdot\vec{D} = \rho \tag{2-4}$$

where $\vec{B} = \mu\vec{H}$ and $\vec{D} = \epsilon\vec{E}$ (2-5)

The electromagnetic fields can be written in terms of scalar and vector potentials, ϕ and $\vec{A}$, where

$$\vec{E} = -\nabla\phi - \frac{\partial\vec{A}}{\partial t} \tag{2-6}$$

and

$$\vec{H} = \frac{1}{\mu}\nabla\times\vec{A} \tag{2-7}$$

The potentials ϕ and $\vec{A}$ can be related in several ways. If we use the Lorentz gauge, then

$$\nabla \cdot \vec{A} + \varepsilon\mu \frac{\partial \phi}{\partial t} = 0 \qquad (2\text{-}8)$$

which gives

$$\nabla^2 \phi - \varepsilon\mu \frac{\partial^2 \phi}{\partial t^2} = - \frac{\rho}{\varepsilon} \qquad (2\text{-}9)$$

and

$$\nabla^2 \vec{A} - \varepsilon\mu \frac{\partial^2 \vec{A}}{\partial t^2} = - \mu \vec{J} \quad . \qquad (2\text{-}10)$$

This then implies that, in free space,

$$\phi(\vec{x},t) = \frac{1}{4\pi\varepsilon} \int \frac{[\rho(x',t')]_{ret}}{|\vec{x}-\vec{x}'|} \, d^3x' \qquad (2\text{-}11)$$

and

$$\vec{A}(\vec{x},t) = \frac{\mu}{4\pi} \int \frac{[\vec{J}(\vec{x}',t')]_{ret}}{|\vec{x}-\vec{x}'|} \, d^3x' \qquad (2\text{-}12)$$

where $[\ ]_{ret}$ means that t' is to be evaluated at $t=t - \frac{|\vec{x}-\vec{x}'|}{c}$.

Up to this point all equations used have been exact. One approximation used in the code, however, is implied by the name QUASI. This name refers to the quasi-static approximation, which is equivalent to assuming that the $\partial\vec{A}/\partial t$ term in Equation 2-6 is relatively small. The scalar potential is then given by solving Poisson's equation. In this approximation, in free space,

$$\phi(\vec{x},t)_{\text{Quasi-static}} = \frac{1}{4\pi\varepsilon} \int \frac{\rho(\vec{x}',t)}{|\vec{x}-\vec{x}'|} \, d^3x' \qquad (2\text{-}13)$$

This equation is identical with Equation 2-11 when retardation effects are ignored. Thus, the quasi-static approximation implies that we assume $\partial\vec{A}/\partial t$ is zero and that retardation effects can be ignored.

Note that Equation 2-13 is the solution of Poisson's equation in free space, i.e., the solution of

$$\nabla^2\phi(\vec{x},t) = \frac{1}{\varepsilon}\rho(\vec{x},t) \tag{2-14}$$

This integral (Equation 2-13) can be applied to the SGEMP problem if we include charges on the various satellite surfaces in the charge distribution $\rho(\vec{x}',t)$. If we think of $\rho(\vec{x}',t)$ as a number of point charges in space the integral in Equation 2-13 just becomes a summation

$$\phi(\vec{x},t) = \frac{1}{4\pi\varepsilon}\sum_i \frac{Q_i(t)}{|\vec{x}-\vec{x}_i|} \tag{2-15}$$

This expression is equivalent to the relationship between voltage and charge on a system of N conductors first written down by Maxwell[9]

$$\phi_i = \sum_{j=1}^{N} S_{ij}\, Q_j \tag{2-16}$$

where ϕ_i is the potential on the i^{th} conductor, Q_j is the charge on the j^{th} conductor and S_{ij} is called the elastance coefficient.

The elastance coefficient[9-10] S_{sr} is defined as the potential to which the r^{th} conductor is raised when a unit charge is placed on the s^{th} conductor, all other conductors being present but uncharged. Elastance values are thus related to the inverse of capacitance coefficients, and, in the limit as conductors go to point charges, elastance values just depend on the distance between two points (compare Equations 2-15 and 2-16).

Note that at this point we have made no distinction between points in space and points on the surface of a satellite. At points in space, Q_j in Equation 2-16 represents the charge due to emitted electrons while on conducting surfaces Q_j includes both the charge left behind when electrons were emitted and any redistribution of charge due to replacement current flow along conducting surfaces.

For a purely electrostatic problem, any conducting surface is an equipotential surface due to the fact that the time derivative of the vector potential in Equation 2-16 is zero. Since the tangential component of $\vec{E}$ is zero at the surface of a perfect conductor, then

$$\nabla \phi_{\text{tangential}} = 0 \tag{2-17}$$

and thus

ϕ = constant along the surface

In this case, Q_j on conducting surfaces is given by Equation 2-16 and the fact that ϕ_i is constant everywhere on the surface. (The Q_j at points off conducting surfaces are assumed known from particle following of emitted electrons.)

For a fully dynamic problem, however, the correspondence between voltage and scalar potential is more complicated. The voltage between two points is given by the line integral of the electric field; i.e.,

$$\Delta V_{21} = - \int_1^2 \vec{E} \cdot d\vec{\ell} \tag{2-18}$$

which, from Equation 2-6, becomes

$$\Delta V_{21} = \int_1^2 \left(\nabla\phi + \frac{\partial \vec{A}}{\partial t}\right) \cdot \vec{\ell}$$

$$= (\phi_2-\phi_1) + \frac{\partial}{\partial t} \int_1^2 \vec{A}\cdot d\vec{\ell} \qquad (2\text{-}19)$$

for time-varying fields, the second term in Equation 2-19 is path dependent.

Now, if the path of integration is along the surface of a perfect conductor, ΔV_{21} is zero, since the tangential component of $\vec{E}$ along the conductor is zero. This then implies that

$$\phi_2-\phi_1 = - \frac{\partial}{\partial t} \int_1^2 \vec{A}\cdot d\vec{\ell} \qquad (2\text{-}20)$$

The QUASI code is not fully quasi-static because the right hand side of Equation 2-20 is not assumed equal to zero. Instead, it is approximated by the expression $Z_{21}\cdot I_{21}$ where Z_{21} is some operator and I_{21} is the current flowing from point 2 to point 1. Equation 2-20 then becomes

$$\phi_2-\phi_1 = Z_{21}\cdot I_{21} \qquad (2\text{-}21)$$

This equation is just Ohm's law giving the voltage between two nodes of a circuit as the product of an impedance operator times the current through the branch connecting the nodes. We are thus treating the conducting surfaces of the satellite structure as an equivalent circuit. By proper choice of the circuit impedances, the resonant frequencies and decay times of the satellite structure can be approximated.

The first of these two equations gives us the potential at a point in space assuming we know the charge at various grid points and the various elastance coefficients. The charge at points outside the satellite is found by "following" various particles representing emitted electrons, while the charge on various portions of the satellite surface depends on the amount of charge left behind when electrons are emitted plus the amount of replacement current that has flowed up to the time being considered.

The second basic equation is used to determine replacement currents on the satellite structure. Various points are represented by circuit nodes connected by impedances. The potential difference, as found from Equation 2-16, and a predetermined impedance are used to calculate the replacement current at each time step.

Now that we have discussed the two basic equations of the QUASI code, we will consider some of the approximations made in more detail.

ELASTANCE COEFFICIENTS

The elastance coefficients are a set of numbers, depending only on geometrical considerations, that can be used to calculate the potential of a set of conductors when the charge on each of the conductors is known. For N conductors,

$$\phi_i = \sum_{j=1}^{N} S_{ij} Q_j \ , \qquad 1 \leq i \leq N \tag{2-22}$$

where the elastance coefficient, S_{ij} , is defined as the potential to which the j^{th} conductor is raised when a unit charge is placed on the i^{th} conductor. We have previously seen (Equation 2-15) that if each of the conductors is made so small as to approach a point charge, then

$$S_{ij} = \frac{1}{4\pi\epsilon_0} \frac{1}{|\vec{x}_i - \vec{x}_j|} \tag{2-23}$$

and

$$S_{ij} = 0 \tag{2-24}$$

since Equation 2-22 then just becomes the expression for the potential from a set of N point charges.

In general, however, each of the N conductors can have an arbitrary shape. The set of equations for voltage can also be solved for charge, with the result that

$$Q_i = \sum_{j=1}^{N} C_{ij} V_j \tag{2-25}$$

where C_{ij} are the capacitance coefficients of a multi-conductor system[10]. [For our purposes, it is usually easier to deal with the elastance matrix since it is easier to calculate. The charge, rather than voltage, is also more readily available from other calculations in the code.]

As an example of the elastance concept, let us consider a simple two conductor system consisting of two spheres of radii a and b (Figure 2-1) separated by the distance r

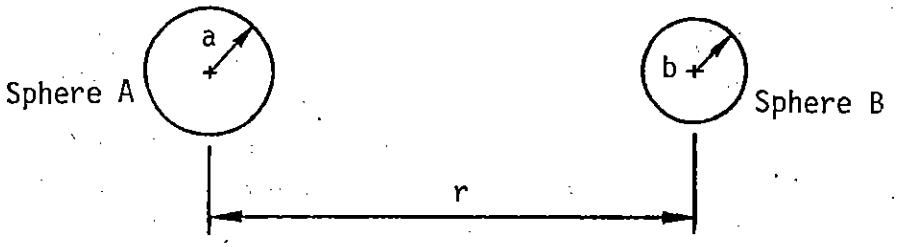

Figure 2-1. Geometry for elastance coefficient calculations.

The capacitance of a single sphere of radius R with respect to infinity is

$$C = 4\pi\varepsilon_0 R \tag{2-26}$$

Therefore,

$$C_A = 4\pi\varepsilon_0 a \tag{2-27}$$

$$C_B = 4\pi\varepsilon_0 b \tag{2-28}$$

Let us first assume that $r >> a$ and $r >> b$. If we charge sphere B to a charge Q_B, the potential at sphere A is about $Q_B/4\pi\varepsilon_0 r$. Thus

$$S_{BA} \simeq S_{AB} \simeq \frac{1}{4\pi\varepsilon_0 r} \tag{2-29}$$

A charge of opposite sign to Q_B and order of magnitude $Q_B(a/r)$ will be induced on the near side of sphere A and an opposite charge on the far side. This dipole-like charge distribution will have little effect on the potential of sphere B. Therefore

$$S_{BB} \simeq \frac{1}{C_b} \tag{2-30}$$

likewise

$$S_{AA} \simeq \frac{1}{C_a} \tag{2-31}$$

For any combination of charges on the two spheres, the potentials are thus given by

$$\phi_A = \frac{1}{4\pi\varepsilon_0}\left[\frac{1}{a} Q_A + \frac{1}{r} Q_B\right] \tag{2-32}$$

$$\phi_B = \frac{1}{4\pi\epsilon_0} \left[\frac{1}{r} Q_A + \frac{1}{b} Q_B \right] \tag{2-33}$$

These two equations can then be solved for Q_A and Q_B and the resulting coefficients of ϕ_A and ϕ_B are just the capacitance coefficients of the system; namely

$$C_{AB} = C_{BA} \simeq - 4\pi\epsilon_0 \frac{ab}{r} \tag{2-34}$$

$$C_{AA} \simeq 4\pi\epsilon_0 \frac{r^2 b}{r^2 - ab} \tag{2-35}$$

$$C_{BB} \simeq 4\pi\epsilon_0 \frac{r^2 a}{r^2 - ab} \tag{2-36}$$

To obtain these relationships, we assumed that the separation distance, r, was relatively large. It is possible to solve for the capacitance coefficients exactly by using an infinite set of image charges. From Reference 10, the exact solutions, when a = b, are given by

$$C_{AA} = C_{BB} = 4\pi\epsilon_0 \, a \sinh\beta \sum_{n=1}^{\infty} \operatorname{csch} [(\partial n - 1)\beta] \tag{2-37}$$

$$C_{AB} = C_{BA} = - 4\pi\epsilon_0 \, a \sinh\beta \sum_{n=1}^{\infty} \operatorname{csch} (\partial n \beta) \tag{2-38}$$

where $$\cosh\beta = \frac{r}{2a} \tag{2-39}$$

For convenience, a was set equal to one meter and the normalized capacitance matrix elements were calculated as a function of sphere separation r. The results are shown in Figure 2-2. It appears that the approximations used in calculating Equations 2-34 to 2-36 are fairly accurate for $r \geq 3a$.

The approximations used in obtaining Equations 2-29 to 2-31 can easily be extended to a system with N conductors as long as the separation

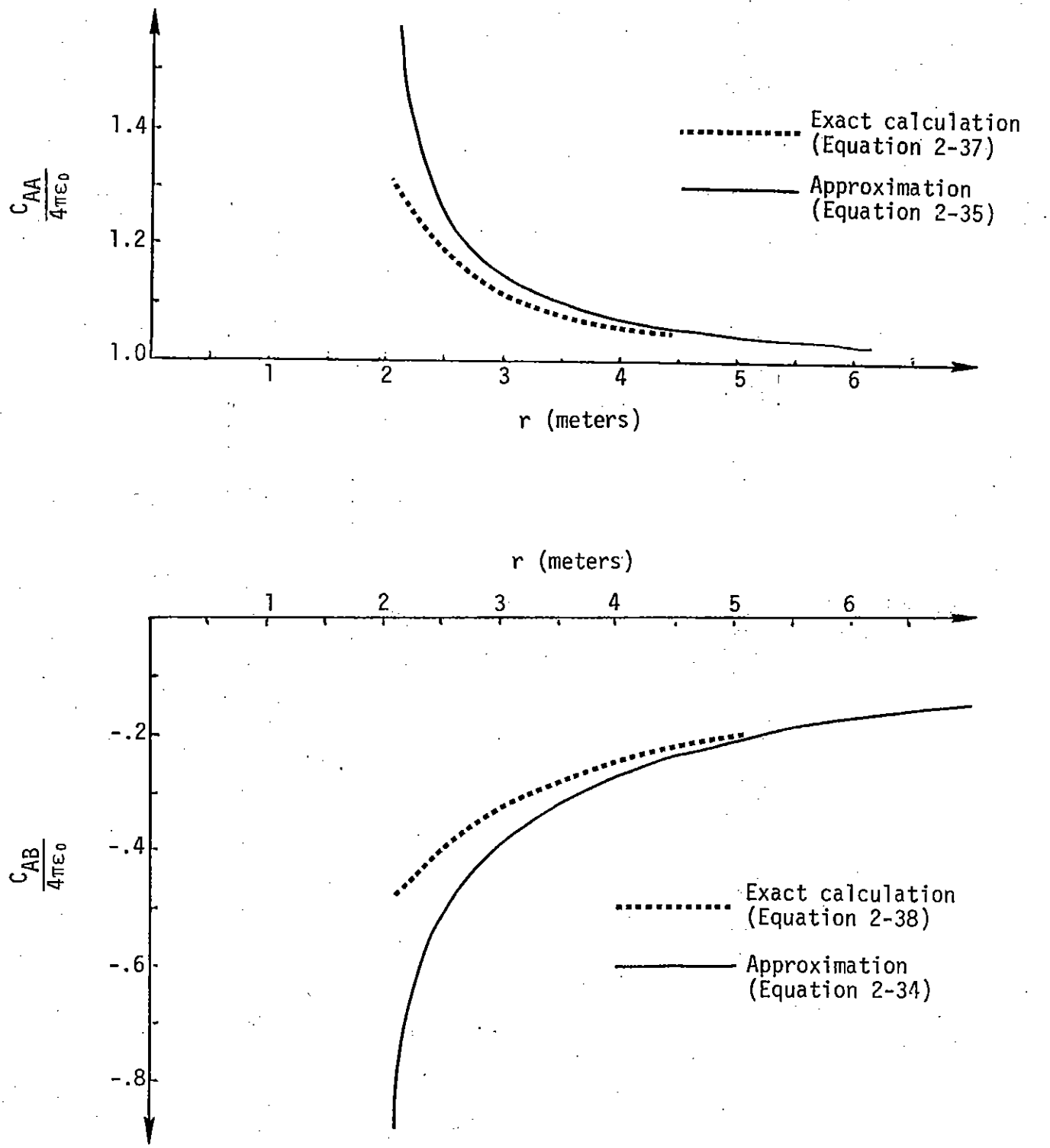

Figure 2-2. Comparison of exact and approximate capacitance coefficients for the geometry shown in Figure 2-1 with a = b = 1 meter.

between conductors is relatively large. The mutual elastance, S_{ij}, just depends on the distance, r_{ij}, and the self-elastance of a conductor is approximated by the inverse of its capacitance to infinity; i.e.,

$$S_{ij} = \frac{1}{4\pi\varepsilon_0 r_{ij}} \tag{2-40}$$

$$S_{jj} = \frac{1}{C_j} \tag{2-41}$$

One should also note that the capacitance of a conductor of any shape can be approximated rather well by the capacitance of a sphere having equal surface area (see Reference 11). For example, if an irregular conductor has a surface area A, then a sphere of radius

$$r_{eq} = \sqrt{\frac{A}{4\pi}} \tag{2-42}$$

will have a capacitance to infinity very nearly equal to that of the original conductor. (The capacitance of the sphere is just $[4\pi\varepsilon_0 r_{eq}]^{-1}$).

ELECTRON EMISSION

When incident photons hit the surface of a satellite, electrons are emitted. The number of electrons emitted per unit area and the initial electron energy distribution depend upon the incident photon spectrum, the total incident photon fluence, and the emission material. The various electron emission parameters are calculated separately and used as input to the QUASI code.

Electron emission at a given point is described by the expression

$$N_e(W,\theta,\phi,t) = F(w)\ \Theta(\theta,\phi)\ g(t) \tag{2-43}$$

where N_e is the number of electrons emitted per unit area, per unit incident fluence, per unit energy (w), per unit solid angle (θ,ϕ), per unit time (t).

For photoelectrons, one can separate the various terms so that F(w) is the electron yield per unit energy, $\Theta(\theta,\phi)$ is the angular distribution of electrons with respect to the surface normal (θ and ϕ are measured from the surface normal), and G(t) is the time history of electron emission, which is usually assumed to just follow the time history of the incident x-ray pulse. For convenience, one usually normalizes the angular distribution and time history so that

$$\int_{\theta=1}^{\pi}\int_{\phi=1}^{\pi} \Theta(\theta,\phi)\, d\theta d\phi = 1 \qquad (2\text{-}44)$$

and

$$\int_{0}^{\infty} G(t)\, dt = 1 \qquad (2\text{-}45)$$

The total electron yield is then just

$$Y_e = \int_{0}^{\infty} F(w)\, dw \qquad (2\text{-}46)$$

F(w) is a function of the emitting material and the incident x-ray spectrum. To first order, however, the electron energy distribution is independent of the photon angle of incidence. The function F(w) can be found from any of a number of codes, including GRAP, NORM, and QUICKE2.

The QUASI code actually uses an integrated electron energy distribution defined by

$$IF(w) = \int_{w}^{\infty} F(w)\, dw \qquad (2\text{-}47)$$

IF(w) is then the number of electrons having energy greater than w.

Except at a glancing angle of incidence, the angular distribution of backscattered photoelectrons can be fairly accurately described by

$$\Theta(\theta,\phi) = \frac{\sin\theta\cos\phi}{\pi} \, d\theta d\phi \tag{2-48}$$

where θ is measured from the surface normal.

The time history, G(t), could be any of a variety of analytic functions or generated from a numerical table. One useful analytic function is the trapezoidal time history

$$\begin{aligned} G(t) &= G_0 \left(\frac{t}{t_1}\right) && 0 \le t \le t_1 \\ &= G_0 && t_1 \le t \le t_2 \\ &= G_0 \left(1 - \frac{t}{t_3}\right) && t_2 \le t \le t_3 \end{aligned} \tag{2-49}$$

where, for normalization,

$$G_0 = \frac{2}{t_3 + t_2 - t_1} \tag{2-50}$$

PARTICLE FOLLOWING

For following the trajectories of emitted particles, one just uses Newton's law

$$m \frac{d\vec{v}}{dt} = e \, (\vec{E} + \vec{v} \times \vec{B}) \tag{2-51}$$

For the low energy electrons, which are dominant in SGEMP calculations, the turning force due to the magnetic field is much smaller than the force due to the electric field. Thus the $\vec{v}\times\vec{B}$ term in the above equation is dropped from the particle-following calculations in the QUASI code. The velocity and position of each particle is simply obtained by numerically integrating the acceleration vector, $d\vec{v}/dt$.

SECTION 3

CODE DESCRIPTION

A simple flow diagram outlining the main sections of the QUASI code is shown in Figure 3-1. Each of the blocks in this diagram will be described in this section of the report. First, however, let us consider some basic assumptions regarding the spatial grid and how the satellite circuit model sits inside this grid.

A Cartesian grid is used with constant cell dimensions of Δx, Δy, and Δz. Let

NX = number of nodes along x-axis

NY = number of nodes along y-axis

and

NZ = number of nodes along z-axis .

The word node is used to refer to corners of each Cartesian cell. Each node is assigned a single number, counting first along the x-axis, then along the y-axis, and finally along the z-axis. If

IX = number of Δx's from the origin

IY = number of Δy's from the origin

and

IZ = number of Δx's from the origin

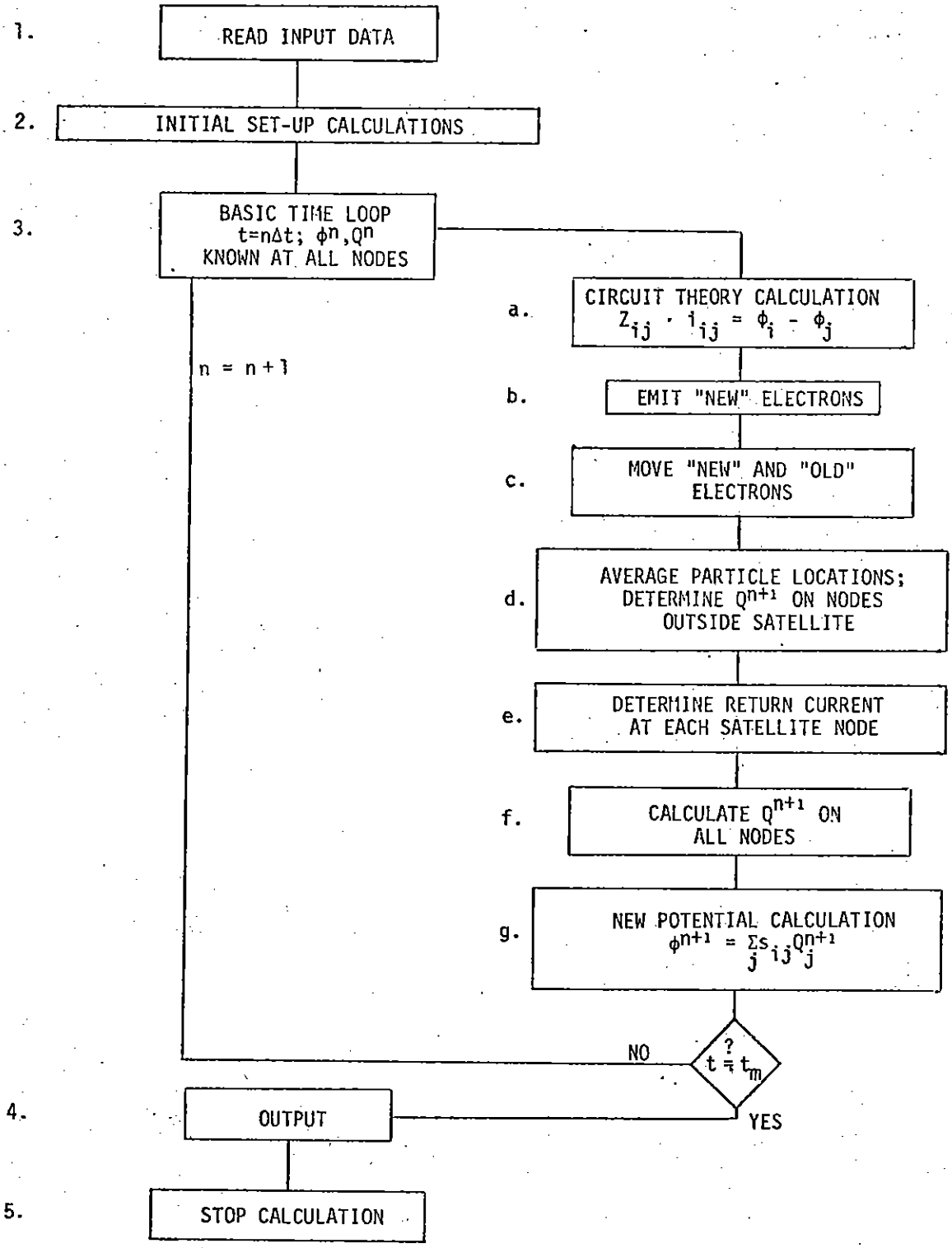

Figure 3-1. Flow chart of the QUASI code.

then the

$$\text{node number} = (IX+1) + NX*(IY) + NX*NY*(IZ) \ . \qquad (3\text{-}1)$$

Each spatial cell is also assigned a number; that number being the smallest of the node numbers of the eight nodes forming the corners of the cell.

The equivalent circuit used to model the electromagnetic structure of a satellite is constrained to "fit" the spatial mesh; i.e., circuit nodes must coincide with spatial nodes. Circuit branches (and thus the various R, L, and C impedances) are connected between the spatial nodes. A two-dimensional example is shown in Figure 3-2.

At first glance, it appears that we are constrained to satellite geometries that can be fit into a Cartesian grid. Strictly speaking, this is not true since the values of elements in the equivalent circuit depend upon the actual geometry rather than the coordinate system used for field and particle following calculations. Also, additional data describing the actual geometry of those spatial nodes representing satellite surfaces are part of the input information used by the QUASI code.

BLOCK 1—INPUT DATA

The QUASI code requires a large number of input parameters in order to fully specify the problem under consideration. Included among these parameters are:

1. General grid and time-step information
2. Descriptions of satellite surface and connecting impedances
3. Descriptions of electron emission points and electron spectram and time-history.

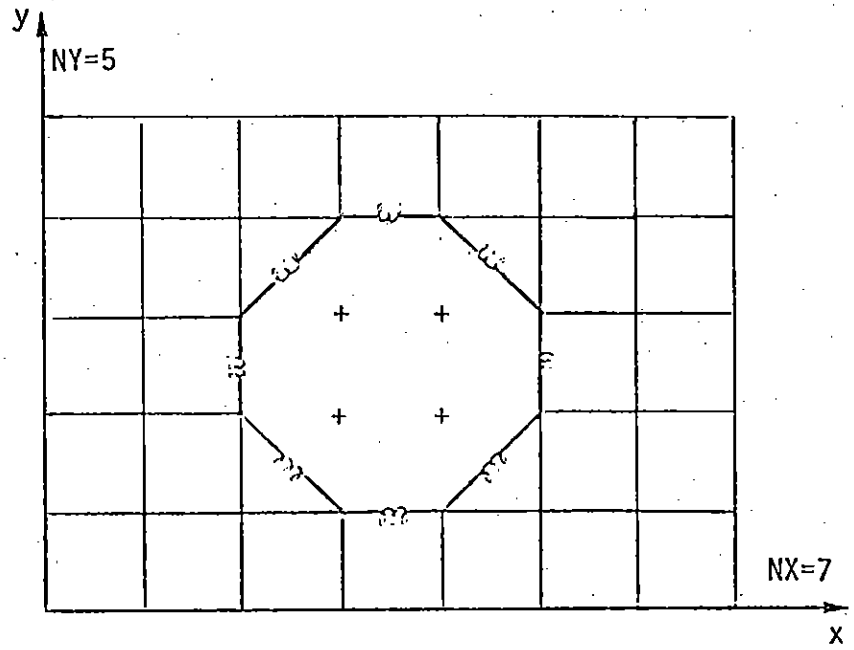

A. Grid model of cylinder

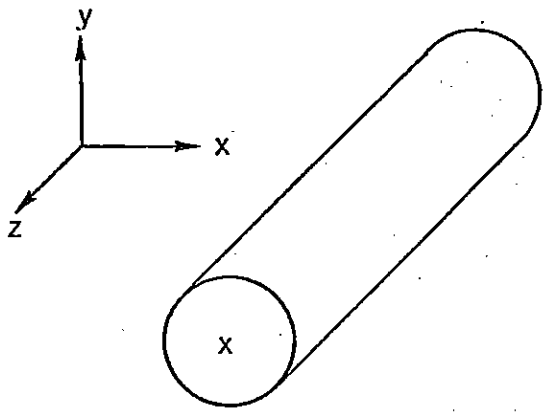

B. Actual geometry

Figure 3-2. Two-dimensional grid/circuit model of infinite cylinder.

Each of these three areas will now be described in more detail.

(1) Grid and Time-Step Information

Input parameters in this group include NX, NY, and NZ, the number of spatial nodes along the x-, y-, and z-axes. QUASI is presently configured to handle up to a 10 × 10 × 10 grid but this grid size could be increased if sufficient storage is available. The cell dimensions, Δx, Δy, and Δz are also read in at the start of the problem. The choice of values for Δx, Δy, and Δz will depend on the size of the satellite and the number of elements used in the equivalent circuit model. The time step interval, Δt, must also be read in. The size of Δt must be kept fairly small to insure that the various difference equations are stable. In addition, the total number of time cycles for the problem is an input parameter. The maximum problem time is then the number of cycles times the time step interval, Δt.

(2) Satellite Equivalent Circuit Description

A number of items regarding the equivalent circuit of the satellite are input parameters of the QUASI code. The subroutine SETUP reads the input satellite information and processes it for further use later in the code.

The first set of data read by SETUP describes the surface nodes of the satellite model. The location of each node in the grid, in terms of the integers IX, IY, and IZ (integral number of cells from the origin) is first read in, along with the surface area each node represents. IX, IY, and IZ, along with Equation 3-1 are used to calculate the spatial node to which each surface node corresponds. The area of the node is used to calculate the self-elastance of those nodes that represent the satellite. If the area represented is A, then a sphere having equal surface area has a radius of

$$r_{eq} = \sqrt{\frac{A}{4\pi}} \quad . \tag{3-2}$$

The self elastance is then given by

$$S_{ii} \simeq [4\pi\varepsilon_0 r_{eq}]^{-1} \quad . \tag{3-3}$$

Note that each surface node is specified by two index numbers, its surface node number and the corresponding spatial node number. The two indices are related by the array IA(I). When I is the surface node number, the value of IA(I) is the corresponding spatial node number.

The next set of data read in describes the direction of a vector normal to the surface at each cell bounding the surface of the satellite model. This surface normal data is used to determine when an electron in space is moving toward a surface where it will hit and be deposited. The surface normal data is indexed by cell number rather than node number since any particle in a cell bounding a surface may hit that surface. This makes the input of data somewhat confusing since the spatial node number of a surface node does not necessarily correspond to the cell number just outside the surface.

The IX, IY, and IZ of boundary cells are read in directly. These values are chosen to give the smallest node number of the cell and thus the cell number itself. Three direction cosines are also read in for each boundary cell. These numbers give the direction of the surface normal with respect to the x-, y-, and z-axes. Up to three surface normals may be assigned to any one cell so that concave geometries can be modeled, if not too complicated. This data is stored in the arrays NØRM and CN.

The final set of input data for describing the satellite gives the type and values of impedances that connect the various surface nodes. Thus, this data describes the branches of the equivalent circuit which is used

to model the satellite. Each branch is numbered and the two surface nodes which are connected by the branch given. (The order in which these nodes are input determines the direction of positive current flow.) Also, the predetermined inductance, resistance, and capacitance for each branch is given. These values are used to calculate various constants used in solving for currents in the circuit.

(3) Electron Emission Data

This last group of input information describes electron emission from the satellite. First of all, the emission time history parameters are given. A simple trapezoidal time history is assumed, and the time function constants indicated in Equation 2-49 are read in. Next, the integrated X-ray spectrum (Equation 2-47) is read into the array XIF(I), where I is the electron energy in units of 1 keV. [The XIF(I) array is normalized to 1.0 keV/cm^2 incident fluence, but the actual incident fluence, in cal/cm^2, is read in elesewhere in the code, and the unit conversion is automatically taken care of.] Several different XIF arrays can be read in to account for the different electron emission spectra of different materials.

The other input emission parameters describe where electrons are emitted and in what direction. In the present code configuration, electrons can be emitted only from surface nodes. For each emission node, the x, y, and z position of the node is given, along with two angles, a retardation time, and an emission area. The two angles, θ and ϕ, give the direction of the surface normal vector around which electrons are emitted. θ and ϕ are standard polar and azimuthal angles as measured from the x-, y-, and z-axes (see Figure 3-3). The retardation time is the time after the start of the problem at which a given point begins emitting electrons. This retardation time factor is used to account for the transit time of the incident X-ray pulse across the satellite. The emission area is used to find the total number of electrons that should be emitted per unit time (since the

electron yield is a function of exposed area). Since the code actually emits particles representing large numbers of electrons, several other parameters are also read into storage. These parameters are: n_w, the number of particle energies to be used; n_θ, the number of polar emission angles to be sampled; and n_ϕ, the number of azimuthal emission angles to be used.

Emission node relationships to surface node numbers are contained in the IB array. If I is the emission node number, then IB(I) is the corresponding surface node number. The spatial node number is then given by IA(IB(I)).

BLOCK 2—INITIAL SET-UP CALCULATIONS

Many calculations in this code need be carried out only once. The set-up section of the QUASI code does these one-time calculations and stores the results for use within the time stepping loop. A number of different set-up calculations are done. We shall describe here only those most important to understanding the overall operation of the QUASI code.

Some of these initial calculations have already been mentioned. The subroutine SETUP takes input data describing the satellite and calculates the IA array for referencing surface node indices to spatial node indices. This subroutine also begins setting up the NØRM array, which describes the surface normal vectors in each cell of the spatial grid. SETUP also calculates certain constants (the D(i) array) used in solving for the current through each branch of the satellite's equivalent circuit.

For calculational purposes the outer boundaries of the Cartesian grid system used in QUASI are treated in the same manner as surface cells representing the satellite. The reason for this is the fact that, when

electrons reach the outer boundary of the spatial mesh, we have decided to stop following their motion and simply let the charge represented "stick" at the point where it hits the outer boundary. If the outer boundary is not too close to the satellite, such an approximation is fairly accurate.

In order to have charge deposited on the outer boundary, one must assign surface normals to all outer boundary cells. Each outer face of the mesh has one surface normal, each outer edge two, and each outer corner three. Nodes on the outer boundary are then also included in the IA array (so that charge can collect on these "surface" nodes). The first NS elements of the IA array will always be surface nodes of the satellite model itself. The elements NS + 1 to NSN refer to nodes at the outer boundary.

For each spatial node the array TYPE(I) is also defined. If I is the spatial index of a surface node (satellite surface or outer boundary), TYPE(I) = 0.0. If I refers to a node in space, then TYPE(I) = 1.0.

The next set of set-up calculations are for the purpose of calculating the initial injection parameters of electrons emitted from the satellite's surface. These set-up calculations are carried out in the subroutine TRANTP, which assumes that emitted electrons have a $\cos\theta$ distribution with respect to the surface normal.

The original direction of an emitted particle depends on n_θ and n_ϕ as well as the direction of the surface normal with respect to the coordinate system of the problem. Let us assume the coordinates shown in Figure 3-3.

In this figure, z' represents the local surface normal, which is rotated from the (x,y,z) system by the angles θ and ϕ. The angular distribution of electrons is measured with respect to the z' axis. Thus these angles will be labeled with a prime.

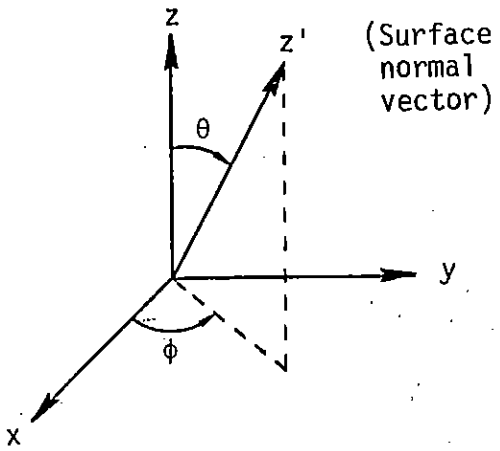

Figure 3-3. Emission geometry.

First of all, the ϕ' angles are given by

$$\phi'_1 = 0.0 \ ,$$

$$\phi'_{i_\phi} = (i_\phi - 1)(2\pi/n_\phi) \ , \qquad (3\text{-}4)$$

where

$$2 \le i_\phi \le n_\phi \ .$$

Furthermore, the n_θ equally probable θ' angles are given by

$$\theta'_{i_\theta} = (\theta_{i_\theta+1} + \theta_{i_\theta})/2 \ , \qquad (3\text{-}5)$$

where

$$\theta_1 = 0.0$$

$$\theta_2 = \sin^{-1}(\Delta\theta)$$

$$\Delta\theta = 1.0/\sqrt{n_\theta}$$

$$\theta_k = \sin^{-1}(\sqrt{k-1}\ \Delta\theta) \quad , \quad 3 \le k \le n_\theta$$

$$\theta_{n_\theta+1} = \frac{\pi}{2} \ .$$

A set of direction cosines are then calculated in the primed coordinate system using

$$z' = \cos\theta'$$
$$y' = \sin\theta'\sin\phi' \qquad (3\text{-}6)$$
$$x' = \sin\theta'\cos\phi' \ .$$

These coordinates are then transformed to the unprimed system by

$$x = x'\cos\theta\cos\phi + y'(-\sin\phi) + z'\sin\theta\cos\phi$$
$$y = x'\cos\theta\sin\phi + y'\cos\phi + z'\sin\theta\sin\phi \qquad (3\text{-}7)$$
$$z = x'(-\sin\theta) + z'\cos\theta \ .$$

These direction cosines are then just multiplied by the magnitude of the initial particle velocity to get the components of the velocity vector in the (x,y,z) coordinate system.

These direction cosines are stored in the arrays CX, CY, and CZ which are indexed by the emission node number and the particular θ' and ϕ' used in calculating their value.

Another group of set-up calculations are done to determine the values of the elastance coefficients (Equation 2-16). The self-elastance coefficients of satellite surface nodes are calculated using Equations 3-2 and 3-3. The self-elastance of spatial nodes is found by assuming that charge is uniformly distributed around each spatial node in a sphere having the same volume as a unit cell (see Reference 12). As a result of this approximation, the self-elastance for spatial cells is given by

$$S_{ii} \simeq [8\pi\varepsilon_0 a_i]^{-1} \ , \qquad (3\text{-}8)$$

where

$$a_i = \left[\frac{3\Delta x\Delta y\Delta z}{4\pi}\right]^{1/3} \ . \qquad (3\text{-}9)$$

As discussed in Section 2 of this report, the mutual elastance between two points just depends upon the distance between the two points. However, for a $10 \times 10 \times 10$ three-dimensional grid, there are 10^6 elastance coefficients. It is not practical to store this many numbers or to recalculate the elastance values every time step. In a uniform Cartesian grid, however, it is possible to use certain symmetry properties to greatly simplify the problem.

We have previously shown (Equation 2-40) that

$$S_{ij} \simeq \frac{1}{4\pi\epsilon_0 r_{ij}} , \tag{3-10}$$

wher r_{ij} is the distance between point i and point j. Now, in a Cartesian system

$$r_{ij} = \sqrt{(x_i - x_j)^2 + (y_i - y_j)^2 + (z_i - z_j)^2} . \tag{3-11}$$

Now

$$\begin{aligned} x_i &= k_i \Delta x \\ x_j &= k_j \Delta x \\ y_i &= \ell_i \Delta y \\ y_j &= \ell_j \Delta y \\ z_i &= m_i \Delta z \\ z_j &= m_j \Delta z , \end{aligned} \tag{3-12}$$

so that

$$r_{ij} = \sqrt{(k_i - k_j)^2(\Delta x)^2 + (\ell_i - \ell_j)^2(\Delta y)^2 + (m_i - m_j)^2(\Delta z)^2} . \tag{3-13}$$

Note that r_{ij}, and thus S_{ij}, depends only on the three numbers $(k_i - k_j)$, $(\ell_i - \ell_j)$ and $(m_i - m_j)$. For a $10 \times 10 \times 10$ grid there are only 1000 such

numbers, rather than the 10^6 possible S_{ij} values (i.e., in Cartesian system many of the elastance coefficients are identical in value). In the set-up calculations the, S_{ij} values are calculated and indexed to the $(k_i - k_j)$, $(\ell_i - \ell_j)$, and $(m_i - m_j)$ values.

BLOCK 3—TIME ITERATION LOOP

The vast majority of calculations carried out by QUASI are done inside the time iteration loop. The various parameters of interest are calculated in a time-stepping procedure. All parameters are assumed known for the n^{th} time cycle (at time $t = n\Delta t$) when the loop is entered. The values of voltage, current, charge, etc., are then calculated for the $n + 1$ time cycle. The time loop can be broken down into a number of distinct steps, as shown in Figure 3-1. In this section, we will discuss each of these steps.

Block 3a—Circuit Theory Calculation

This part of the code calculates the current in each branch of the equivalent circuit that is used to represent the satellite's surface. The potential at each end of every circuit branch is known from the previous pass through the time loop. The potential difference across the branch is then

$$\Delta V_k^n = \phi_i^n - \phi_j^n \ , \qquad (3\text{-}14)$$

where ϕ_i is the potential at the i^{th} node (one end of the branch) and ϕ_j is the potential at the j^{th} node (the other end of the branch). The current through the branch at $t = (n + 1)\Delta t$ is then given by a general equation of the form

$$I_k^{n+1/2} = [D_k(1)\ V_k^n + D_k(2) I_k^{n-1/2} + D_k(3) q_k^{n-1/2}] D_k(4) \quad . \quad (3\text{-}5)$$

(The n+1/2 and n-1/2 superscripts indicate that branch currents are actually calculated at times one-half time step different than spatial voltages.) In this equation,

k = branch number

n = time step

q_k^n = total charge transferred between nodes up to $t = n\Delta t$

and

D_k = constants depending upon the impedances associated with the k^{th} branch.

Three types of impedances have been considered initially: R, RL, and RLC where R, L, and C refer to resistance, inductance, and capacitance respectively (always connected in series).

CASE I: Z = R

$$I_k^n = \frac{\Delta V_k^{n-1/2}}{R} , \quad (3\text{-}16)$$

therefore

$$D_k(1) = 1/R ,$$

$$D_k(2) = D_k(3) = 0 , \quad (3\text{-}17)$$

$$D_k(4) = 1 .$$

CASE II: $Z = L \frac{d}{dt} + R$

$$L \frac{dI}{dt} + RI = \Delta V$$

$$\frac{dI}{dt} + \frac{R}{L} I = \Delta V/L \tag{3-18}$$

$$I_k^n = \frac{\Delta V_k^{n-1/2}}{R} (1 - e^{-R/L \Delta t}) + I_k^{n-1} e^{-R/L \Delta t}$$

therefore

$$D_k(1) = \frac{1}{R} (1 - e^{-R/L \Delta t})$$

$$D_k(2) = e^{-R/L \Delta t} \tag{3-19}$$

$$D_k(3) = 0$$

$$D_k(4) = 1 .$$

CASE III: $Z = L \frac{d}{dt} + RI + \frac{1}{C} \int_0^t dt$

$$L \frac{dI}{dt} + RI + \frac{1}{C} \int_0^t Idt = V(t) \tag{3-20}$$

$$L \frac{dI}{dt} + RI + \frac{1}{C} \int_{t^{n-1}}^{t^n} Idt = V(t) - \underbrace{\frac{1}{C} \int_0^{t^{n-1}} Idt}_{Q_k^{n-1}}$$

$$L\left(\frac{1}{\Delta t}\right)\left(I_k^n - I_k^{n-1}\right) + R\left(\frac{1}{2}\right)\left(I_k^n + I_k^{n-1}\right) + \frac{\Delta t}{C}\left(\frac{1}{2}\right)\left(I_k^n + I_k^{n-1}\right)$$

$$= \Delta V_k^{n-1/2} - \frac{Q_k^{n-1}}{C}$$

$$I^n = \frac{\frac{\Delta V_k^{n-1/2}}{L}\Delta t + I^{n-1}\left[1 - \frac{1}{2}\left(\frac{R\Delta t}{L} + \frac{\Delta t^2}{LC}\right)\right] - \frac{Q_k^{n-1}}{LC}\Delta t}{1 + \frac{1}{2}\left(\frac{R\Delta t}{L} + \frac{\Delta t^2}{LC}\right)}$$

therefore

$$D_k(1) = \frac{\Delta t}{L}$$

$$D_k(2) = 1 - \frac{1}{2}\left(\frac{R\Delta t}{L} + \frac{\Delta t^2}{LC}\right)$$

$$D_k(3) = -\frac{\Delta t}{LC}$$

$$D_k(4) = 1./\left[1 + \frac{1}{2}\left(\frac{R\Delta t}{L} + \frac{\Delta t^2}{LC}\right)\right] .$$

Since an analytic solution is used for the RL circuit (Case II), assuming constant ΔV over the time increment, it will be wise to use this one whenever possible. This means ignoring a series capacitance which might be used to give a rod its own resonance frequency, for example.

A finite difference solution is used for the RLC circuit. This will become unstable for large Δt, on the order of L/R or $\sqrt{LC}$.

The D_k parameter in Equation 3-15 is calculated for each branch in the subroutine SETUP and stored in the array D(k,m) where k is the branch number and m ranges from 1 to 4. In addition, the branch-to-surface node array, NØDE (I,K) is also precalculated in SETUP. In this array, I is 1 or 2, depending on which end of the branch one is at, and K is the branch number. For each I and K, the value of NØDE equals the corresponding surface node index.

The actual calculation of the new current in each circuit branch is carried out in the subroutine LOAD. This subroutine also calculates the amount of charge added or subtracted to each surface node during the time step due to current flow through the circuit branches. This charge is added or subtracted to the previous charge on each node so that the new charge distribution can be determined.

The charge that is actually located on each surface node is given by the value of the QQ array. When the charge that has flowed through a given branch in one time step is calculated, that same amount of charge is added to the value of QQ at the node at one end of the branch and subtracted from the QQ value at the node at the other end.

Block 3b—Emit New Electrons

During each time step in which electrons are being emitted from the exposed surfaces of the satellite, particles representing these electrons must be emitted from emission nodes in the QUASI grid. This part of the code calculates the initial parameters that are to be assigned to these newly emitted particles.

In the QUASI code electrons in space are represented by particles with given locations, velocities, and charges. Each particle represents a certain number of electrons as indicated by the total charge of the particle (also called the weight of the particle). When particles are injected from emission surfaces, the original velocity vectors and particle weights are calculated from the electron emission distributions.

Inputs to the QUASI code include

n_w = number of different energy particles to be emitted

n_θ = number of different θ emission angles

and

$$n_\phi = \text{number of different } \phi \text{ emission angles} .$$

Using these parameters, the original velocity vector and particle weights are chosen so that all particles emitted at a given time step represent the same number of particles.

To calculate the energy of emitted particles, the total yield is divided by $2n_w$; i.e.,

$$\alpha = \frac{IF(w_{min})}{2n_w} , \tag{3-22}$$

where IF(w) is defined in Equation 2-47 and w_{min} is the minimum electron energy considered (1 keV in most cases). The emission energies, w_i, are then determined by

$$\begin{aligned} IF(w_1) &= \alpha \\ IF(w_2) &= 3\alpha \\ IF(w_n) &= (2n - 1)\alpha . \end{aligned} \tag{3-23}$$

Thus each emission energy represents an equal number of electrons (the number being 2α per unit area).

Once the original kinetic energy is known, the non-relativistic velocity is given by

$$v = c\sqrt{\frac{2w}{mc^2}} , \tag{3-24}$$

Since we have calculated initial angles and energies to be equally probable, the weight assigned to each ejected particle is just

$$WT = e\,\frac{(A_r)(IF(w_{min}))}{n_w n_\theta n_\phi}\,G(t) , \tag{3-25}$$

where A_r is the area of the emission surface, G(t) is the emission rate at the time being considered, and e is the electron charge.

Note that, if w_{min} is not a function of time, all of the above parameters, except G(t), can be calculated outside of the time loop. The time history, G(t), is evaluated at any given time by a call to the FUNCTION subprogram FTIME.

The above calculations are carried out for each emission node. Each initial velocity is multiplied by the direction cosines calculated in the TRANTP subroutine to give the initial x-, y-, and z- components of the velocity vector. The initial position is just that of the emission point.

When charge is emitted from a surface node, an equal amount of charge of opposite sign must be added to the QQ array at that point. This accounts for the positive charge left behind when electrons are emitted.

Block 3c—Move "New" and "Old" Electrons

This block of the code involves a loop over all particles (electrons) in space outside the satellite. New positions and velocities are calculated for each particle using Newton's law. To understand this section of the code, let us first consider how the particle parameters are defined.

For each particle, seven parameters are stored. The three position components are written as

```
XP = IX.XFF
YP = IY.YFF                                              (3-26)
```

and

```
ZP = IZ.ZFF  ,
```

where IX is the integer number of cells from the origin, measured along a line parallel to the x-axis and XFF is the fractional distance across the IX^{th} cell. YP and ZP are similarly defined. Thus

$$XP = \frac{\text{actual x-component}}{\Delta x} ,$$

$$YP = \frac{\text{actual y-component}}{\Delta y} , \qquad (3\text{-}27)$$

$$ZP = \frac{\text{actual z-component}}{\Delta z} .$$

In addition, for each particle, the three velocity components, VX, VY, and VZ, and the particle's weight (charge), WT, are stored and updated as needed.

The motion of a particle is determined by Newton's law

$$\vec{F} = m\vec{a} = m\dot{\vec{v}} . \qquad (3\text{-}28)$$

In the QUASI code, it is assumed that the only force acting on a particle is due to the local electric field. Therefore

$$\dot{\vec{v}} = \left(\frac{e}{m}\right)\vec{E} , \qquad (3\text{-}29)$$

where $\vec{E}$ is the local electric field vector and (e/m) is the ratio of electron charge to electron mass. If we convert this equation to finite difference notation

$$v^{n+1/2} = \left(\frac{e}{m} E\right)\Delta t + v^{n-1/2} . \qquad (3\text{-}30)$$

This new velocity component is integrated once more to obtain the new particle location

$$x^{n+1} = v^{n+1/2}\,\Delta t + x^{n} . \qquad (3\text{-}31)$$

In the code itself, one first determines what cell the particle is

initially in. This cell number is given by

$$I = IX + 1 + NY*IY + NX*NY*IZ \ , \qquad (3\text{-}32)$$

where IX, IY, and IZ are the integer parts of the particle's location at the start of the time step. The new x-components of the velocity and position vectors are then given by (in FORTRAN notation)

$$VX(J) = VS(J) + \left(\frac{e\Delta t}{m}\right)*EX(I) \ , \qquad (3\text{-}33)$$

$$XP(J) = XP(J) + \left(\frac{\Delta t}{\Delta x}\right)*VX(J) \ , \qquad (3\text{-}34)$$

where J is the index of the particle being considered. Similar expressions apply for the y- and z-components of velocity and position.

EX(I) is the x-component of the electric field in the I^{th} cell. Before any particles are "moved," the three components of electric field are calculated for each cell using the relationship

$$\vec{E} = - \nabla\phi \ . \qquad (3\text{-}35)$$

Note that it is at this point we make the quasi-static assumption that $\partial\vec{A}/\partial t = 0$ (compare the above equation with Equation 2-6).

Each cell is numbered according to the smallest node number of its eight vertices. Using the potentials at the corners of each cell, four values of each component of $\vec{E}$ are calculated. These four values are then averaged and this average electric field used to calculate the acceleration of all particles within the cell.

Consider the single cell shown in Figure 3-4. The z-component of electric field is then approximated by

$$E_z \simeq -\frac{1}{4\pi}\Big[\phi(5) - \phi(1) + \phi(6) - \phi(2) + \phi(7) - \phi(3) + \phi(8) - \phi(4)\Big] . \qquad (3\text{-}36)$$

where $\phi(i)$ is the potential of the i^{th} cell corner. E_x and E_y are similarly calculated for each cell.

The cell corner labeled 1 in Figure 3-4 has the node number that is used to label the cell under consideration. This cell number is given by Equation 3-32. If corner 1 is node I, the other seven node numbers are given by

```
I1 = I + 1 = corner 2
I2 = I + NX = corner 3
I3 = I + NX*NY = corner 5
I4 = I + NX + 1 = corner 4                    (3-37)
I5 = I + NX + NX*NY = corner 7
I6 = I + NX*NY + 1 = corner 6
I7 = I + NX + NX*NY + 1 = corner 8 .
```

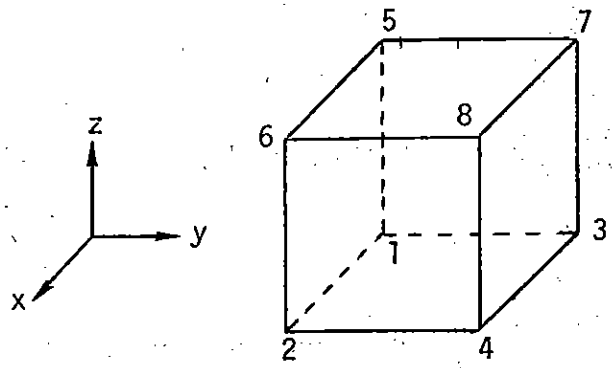

Figure 3-4. Unit cell geometry.

These numbers then give the proper indices for use in calculating the potential gradients used to find the average electric field components in each cell.

Blocks 3d and 3e—Average Particle Locations and Determine Return Currents

Due to the way calculations are carried out it is useful to discuss both block 3d and block 3e of Figure 3-1 at the same time. In actual fact, blocks 3c to 3e are all carried out in the subroutine MP which loops over all of the particles emitted from the satellite's surface.

Once a particle's new position has been calculated, this "new" position is used to calculate a "new" charge distribution. All charge within a given cell is assigned to the eight cell corners linearly interpolating according the actual particle location within the cell. In this way, the expression relating charge to potential (Equation 2-16) needs only be summed over the spatial nodes, rather than over all particles.

This "averaging" of each particle's location is carried out in the following way. Since the particle's new position is indicated by

$$\begin{aligned} XP &= IX.XFF \\ YP &= IY.YFF \\ ZP &= IZ.ZFF \ , \end{aligned} \tag{3-38}$$

the integer parts of XP, YP, and ZP are used to calculate the new number of the cell which contains the particle, using Equation 3-32. The following quantities are then calculated using the fractional parts of the particles location:

```
FQ(1) = (XFF)*(1.0 - YFF)*(1.0 - ZFF)*WT
FQ(2) = (1.0 - XFF)*(1.0 - ZFF)*(YFF)*WT
FQ(3) = (1.0 - XFF)*(ZFF)*(1.0 - YFF)*WT
FQ(4) = (XFF)*(YFF)*(1.0 - ZFF)*WT
FQ(5) = (XFF)*(1.0 - YFF)*(ZFF)*WT
FQ(6) = (1.0 - XFF)*(ZFF)*(YFF)*WT
FQ(7) = (XFF)*(YFF)*(ZFF)*WT
FQ(8) = (1.0 - XFF)*(1.0 - ZFF)*(1.0 - YFF)*WT ,
```

(3-39)

where WT is the weight (charge) of the particle being considered.

After a little thought, it becomes apparent that FQ(i) is just the fractional amount of charge that is given to each corner of the cell, using linear interpolation. For $1 \leq i \leq 7$, i just refers to the node number Ii given in Equation 3-37, while i = 8 is the cell number given by Equation 3-32; i.e.,

```
I = (IX + 1) + NX*(IY) + NX*NY*(IZ) .
```

Now, the array Q(k) is used to store the charge attributed to each spatial node due to particles moving through space. Therefore, for each particle, the Q array is updated by the calculation

```
Q(I) = Q(I) + FQ(8)
Q(I1) = Q(I1) + FQ(1)
Q(I2) = Q(I2) + FQ(2)
Q(I3) = Q(I3) + FQ(3)
Q(I4) = Q(I4) + FQ(4)
Q(I5) = Q(I5) + FQ(5)
Q(I6) = Q(I6) + FQ(6)
Q(I7) = Q(I7) + FQ(7) .
```

(3-40)

The calculations described so far would complete the particle loop if one did not have to consider the possibility of the charge returning to the satellite's surface or hitting the outer boundary of the spatial mesh. When this happens, the amount of returning charge must be determined, and that amount of charge must be removed from the particle following calculation.

This procedure applies only when the particle being considered is in a cell adjoining a surface of the satellite or the outer boundary. The array NORM is used to determine when this is the case. If I is the cell number and NORM(I) = 0, then the particle is not near a surface and the particle calculation is complete. If NORM(I) $\neq$ 0, then the particle is near a surface and further checks must be made.

For each cell where NORM(I) $\neq$ 0, the components of a vector (or vectors) normal to the nearby surface (or surfaces) are stored in the CN array. For particles in such a cell, the dot product of each particle's velocity vector and the surface normal vector is calculated. If this dot product is positive, the particle is moving away from the surface and thus no further calculations need be carried out. If the dot product is negative, the particle is moving toward a surface and further calculations must be done to determine if it has yet hit the surface.

The surface normal array, CN, is then used to determine if a particle is within a certain distance of a surface. This distance, which is an input number, is some fraction of a cell size. For most cases, the surface the particle is approaching is just one of the cell boundaries, but surfaces diagonally dividing a cell are also allowed.

When the distance between the particle and the surface boundary is less than the specified distance, the following additional calculations are carried out.

First of all, the weight of the particle is recalculated, using the algorithm

$$\begin{aligned} WT(J) = {} & FQ(1)*TYPE(I1) + FQ(2)*TYPE(I2) \\ & + FQ(3)*TYPE(I3) + FQ(4)*TYPE(I4) \\ & + FQ(5)*TYPE(I5) + FQ(6)*TYPE(I6) \\ & + FQ(7)*TYPE(I7) + FQ(8)*TYPE(I) \ , \end{aligned} \tag{3-41}$$

where

J is the particle index

I is the cell number

and the array TYPE(i) is 0.0 if i is a node in free space or 1.0 if i is a surface node. The weight of the particle is thus decreased to account for part of the charge it represents returning to a surface node.

At the same time, this returning charge must be added to the QQ array. This is done by expressions of the form

$$QQ(j) = QQ(j) + FQ(k)*(1.0 - TYPE(j)) \ , \tag{3-42}$$

where j varies over the eight surface nodes bounding the cell and k is the index corresponding to j as determined by Equations 3-37 and 3-39.

Similarly, the same amount of charge must be subtracted from the Q array, since it was previously added (Equation 3-40) when it was assumed that the particle was not returning to a surface.

When these calculations have been completed for all particles in space, the particle loop (blocks 3c to 3e of Figure 3-1) is completed. New values of particle location, velocity, and wieght have been calculated, the charge distributed to spatial nodes determined, and the charge returned to surfaces has also been calculated.

One other point regarding the particle loop calculations needs to be considered; namely, when do we stop following a given particle's motion? This is determined by a check on the weight of the particle at the beginning of the particle loop. If the weight is less than 1 percent of the average particle weight, which is recalculated every time step, the particle is assumed unimportant and is no longer considered.

Block 3f—Calculate Q^{n+1} on All Nodes

At this point in the time loop, the total charge of the system is contained in two arrays, Q(I) and QQ(I), where I is an index varying over all spatial nodes of the mesh.

The Q array represents only that part of the total charge due to electrons moving in space, i.e., the emitted charge. Part of this charge may be assigned to nodes that are also surface nodes since many particles are expected to be near emission surfaces at early times. This charge may move away from surface nodes at later times, however. The Q array depends only on particle locations and weights. Therefore, this array is set equal to zero at the beginning of each time step and recalculated as particles move in space.

The QQ array, on the other hand, represents charge actually residing on the various surface nodes of the satellite and the outer grid boundary. These charges may redistribute themselves by flowing through the various circuit elements, but, at any given time, the total sum of charge in the QQ array plus that in the Q array should equal the initial total charge of the entire system (which is usually zero). Note also that QQ(I) is always zero when I is not a surface node. Also unlike the Q array, the values of QQ(I) must be saved from one time step to the next since there is no other place where equivalent data is stored. (The Q array can always be recalculated from particle data.)

For calculating the new potential at each node, however, one requires the total charge at each node. Thus, after all particle motion calculations have been completed, the two charge arrays are just summed, with the resulting total charge for each node stored in the Q array. At this point then, the numbers in the Q array change their meaning from that previously discussed. (Note, however, that Q(I) changes only for those I values that represent surface nodes with non-zero QQ(I) values.)

Block 3g—New Potential Calculation

The final step in the time loop is to calculate the new potential values at each node in the spatial grid. This new potential is given by

$$\phi_i^{n+1} = \sum_j S_{ij} Q_j^{n+1}$$

where Q_j^{n+1} is the total charge at t^{n+1} on the j^{th} node as calculated in block 3f of the time loop.

Calculation of ϕ_i^{n+1} is straightforward, but the operation can be quite time-consuming since there are j multiplications for each value of i. However, in many cases Q_j^{n+1} will be zero for many of the nodes in the mesh. Therefore, the code first checks to see if Q_j^{n+1} is zero. If this is so, j is just iterated to its next value. If not, S_{ij} is determined by calculating the Δk, $\Delta \ell$, and Δm values defined in Equations 3-13.

When this calculation is completed, the time loop is also finished. The code then checks to see if the maximum desired time has been reached. If not, the time loop is repeated.

BLOCK 4—OUTPUT

There are obviously a tremendous number of output parameters that one might be interested in obtaining. As a result, the various charges,

potentials, electric fields, and branch currents are written on an output tape at every specified time step. The desired output parameters can then be pulled off of this output tape.

In order to avoid exceedingly long printed outputs, only a limited number of parameters are actually printed at the end of the output listing. One output cell is specified. The potential and total charge (after Q and QQ have been summed) are printed for each of the eight corners of the cell. The three components of the average electric field within the cell are also printed. In addition, a number of specified branch currents are printed at specified cycle numbers. If the primary interest is in calculated replacement currents (i.e., the branch currents), this printed output may be sufficient for the user.

SECTION 4

SAMPLE PROBLEM AND RESULTS

In order to check out the calculations made by the QUASI code, a sample problem was used. This sample problem was calculating the SGEMP response of a right circular cylinder emitting electrons from one end. This simple two-dimensional geometry was chosen because calculations for such a geometry had previously been carried out using the SEMP code, which uses purely finite-difference techniques for finding skin currents on the cylinder. We can thus directly compare the replacement currents calculated by QUASI with those given by a rather finely meshed finite difference calculation.

The geometry considered and the equivalent circuit used by the QUASI code are shown in Figures 4-1a and 4-1b. The points where skin currents were calculated with the SEMP code are indicated in Figure 4-1c and the QUASI surface node numbering scheme is shown in Figure 4-1d.

It should be noted that the grid size in the SEMP calculation is approximately 15 centimeters, while for QUASI, $\Delta x = \Delta y = 1.5$ meters and $\Delta z = 0.75$ meter. We are thus using a rather coarse grid in QUASI. This implies that the current in each branch of the QUASI equivalent circuit is, in some sense, an "average" of the current across the area of the cylinder that the branch represents. Thus, a one-to-one comparison of QUASI and SEMP results is not possible.

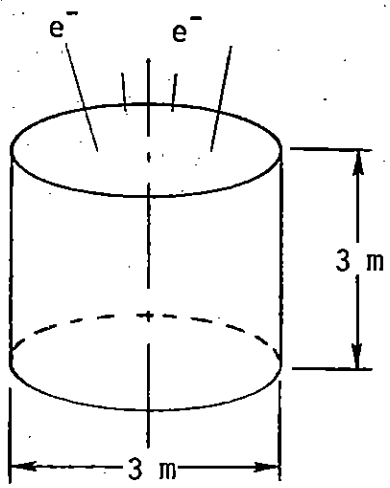

a. Geometry considered

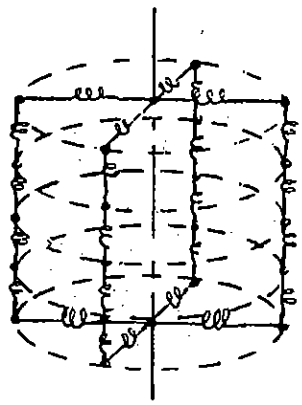

b. QUASI circuit model

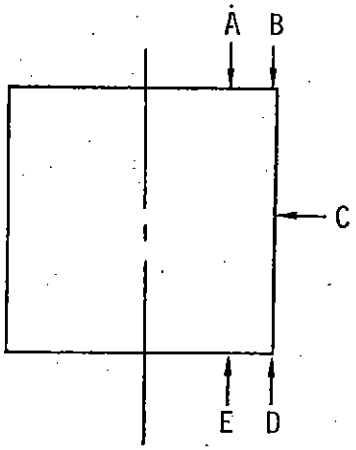

c. Locations where skin current was calculated using the SEMP code.

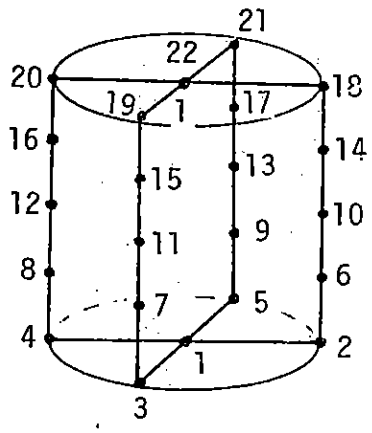

d. Node numbers of the QUASI equivalent circuit

Figure 4-1. Sample problem: comparison of finite difference calculation (SEMP) and QUASI.

For comparison purposes, identical electron emission data was used in both the SEMP and QUASI calculations. Although the geometry of the problem was two-dimensional, no attempt was made to require azimuthal symmetry in the QUASI calculation. In fact, azimuthal circuit elements were at first used in the QUASI circuit model, but they were later dropped for simplicity when it was determined that azimuthal currents were, indeed, quite small. Calculations also show that the currents in each of the four parallel circuit paths of the QUASI code are very nearly equal even when the azimuthal circuit elements are absent.

A comparison of replacement currents on the emission surface of the cylinder is shown in Figure 4-2 where an incident fluence of 10^{-5} cal/cm^2 was assumed. In this case, the current calculated by QUASI does indeed look like the "average" of the current calculated at points A and B by the SEMP code. (Each of the branch currents from QUASI has been multiplied by four to account for the four parallel circuit branches.)

Figure 4-3 compares the SEMP current at point B with QUASI results at adjacent circuit branches. One would expect the SEMP results to be the "average" of the two QUASI currents. In this case, the QUASI calculations appear to be a little high, but not unreasonably so considering the large size of the QUASI grid.

Results on the back side of the cylinder are shown in Figure 4-4. Again, the comparison is not at all bad.

It should be noted that a few time points were calculated by QUASI beyond those shown in Figures 4-2 to 4-4. At these later times, the currents appear to be becoming unstable and results begin to diverge from the SEMP calculations. The reason for this phenomenon is not fully understood at this time.

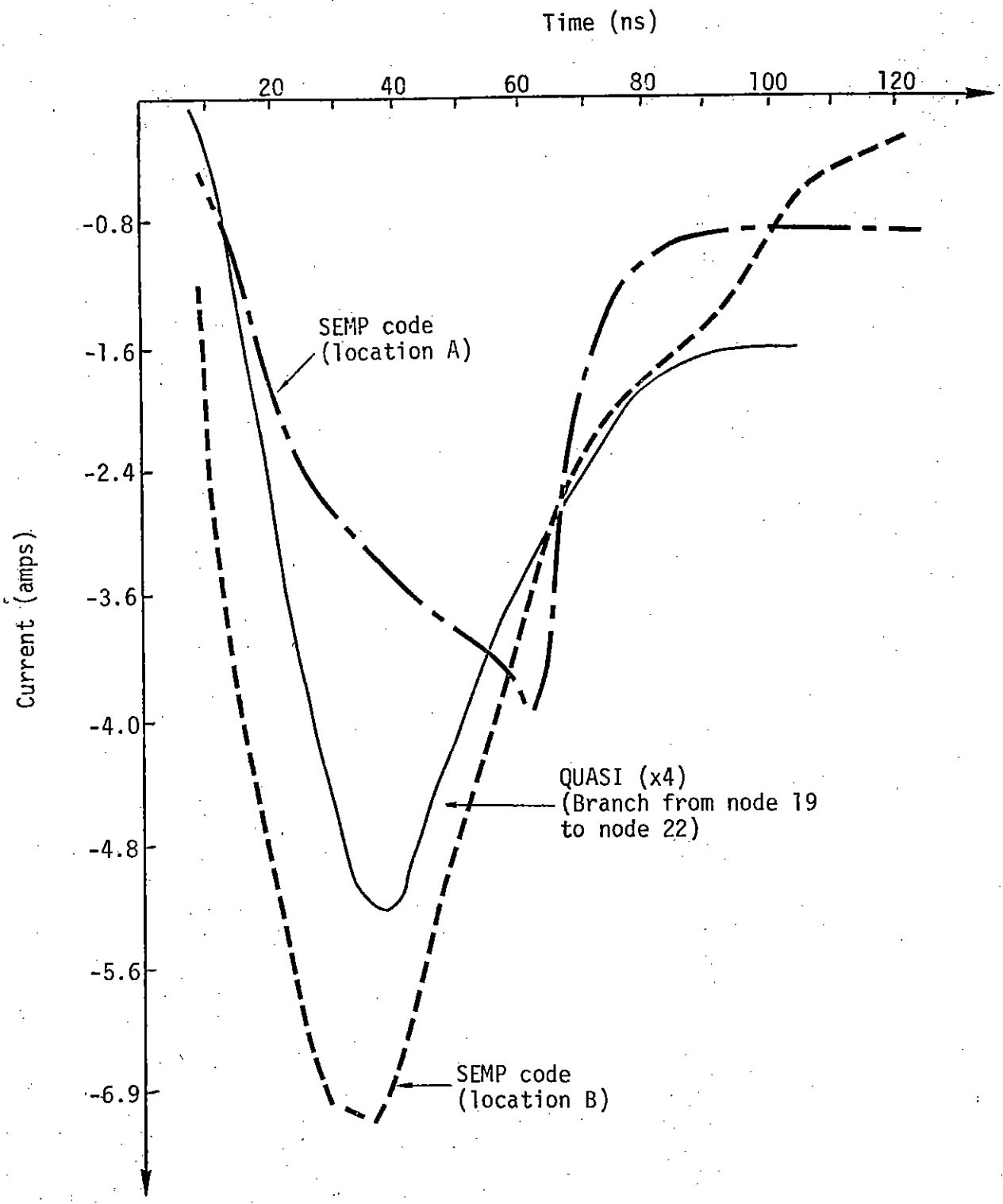

Figure 4-2. Comparison of calculated skin currents: incident fluence = 10^{-5} cal/cm^2.

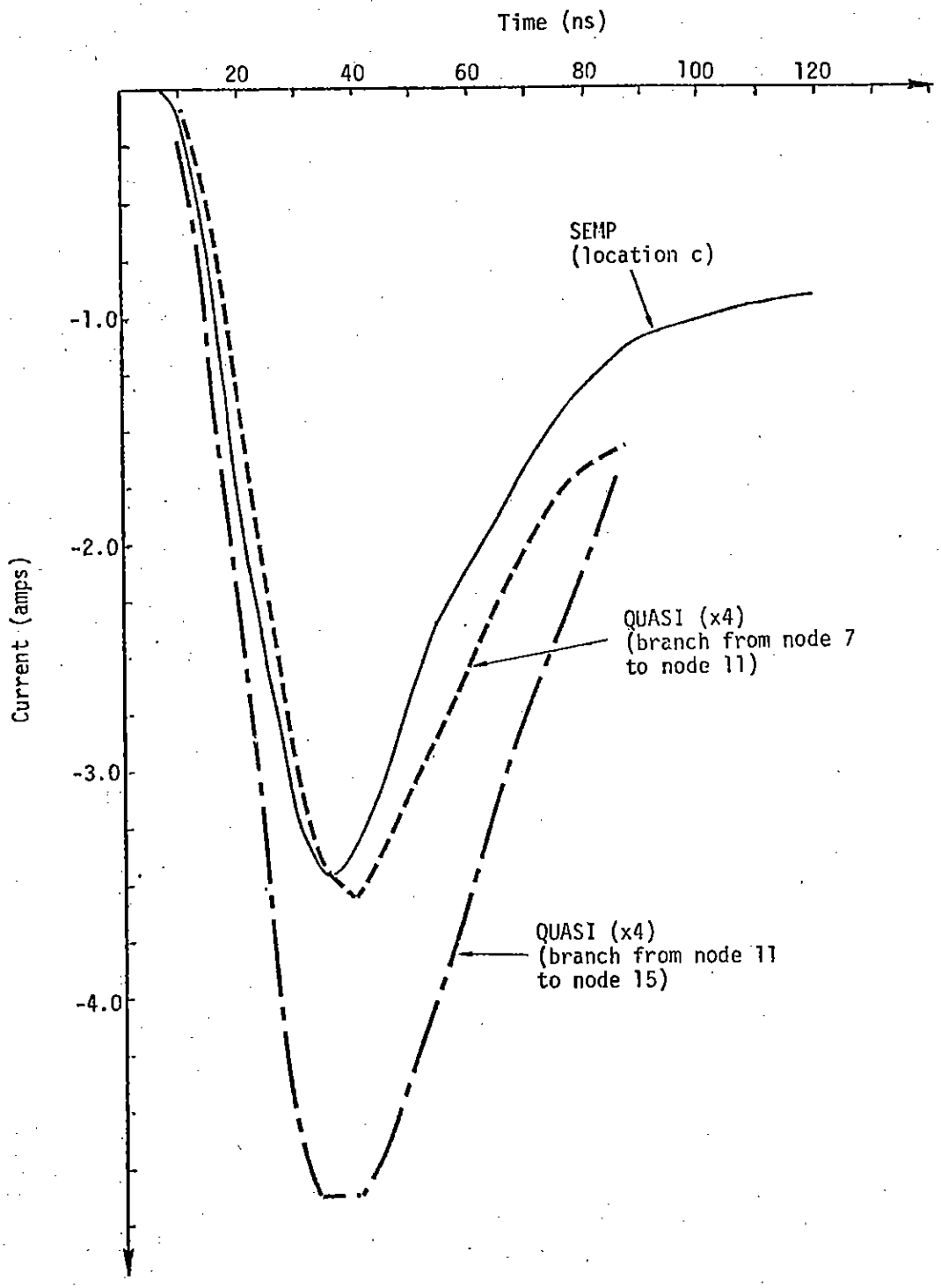

Figure 4-3. Comparison of calculated skin currents: incident fluence = 10^5 cal/cm^2.

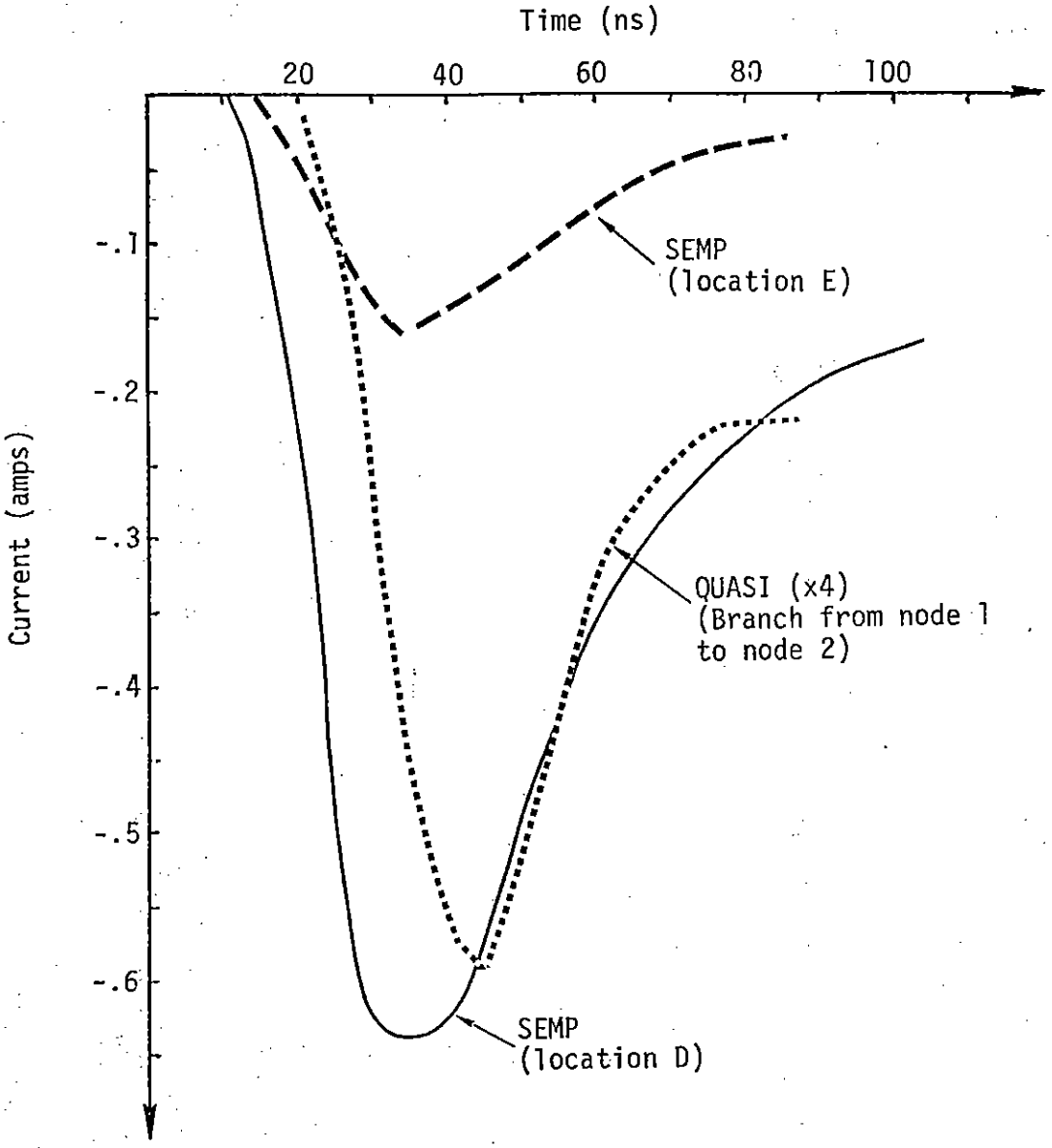

Figure 4-4. Comparison of calculated skin currents: incident fluence = 10^{-5} cal/cm^2.

The total CP time for this QUASI run on the CDC 7600 was less than 4 minutes and the total number of particles emitted was about 5000. The QUASI code is thus capable of giving reasonably accurate structural replacement currents at low fluences without using excessive amounts of computer time.

The same sample problem was also considered at a somewhat higher incident fluence (10^{-4} cal/cm^2). A comparison of results is shown in Figure 4-5. In this case, the QUASI results are a factor of 2 to 3 times greater than the SEMP results.

This disagreement is thought to be due to the fact that the cells in QUASI are relatively large and a uniform electric field is used to move all particles within each cell. However, at higher fluences, where space charge limiting effects become important, electric field gradients are fairly steep near emission surfaces. For example, the SEMP calculation gives a peak electric field of about 2.5×10^4 volts/m at a distance of 15 cm from the emission surface and a peak field of 6.1×10^3 volts/m at 45 cm. The QUASI cell, however, has a minimum dimension of 75 cm. The peak calculated electric field in a cell adjacent to the emission surface was about 6.0×10^3 volts/m, which is about right for a point at the center of the cell.

However, for moving those electrons in the half of the cell closest to the emission surface, this electric field has too small of a value. Thus, space charge limiting effects will be under-estimated and one therefore expects the QUASI currents to be somewhat high. A proposed method for correcting this large cell size problem is given in Reference 13.

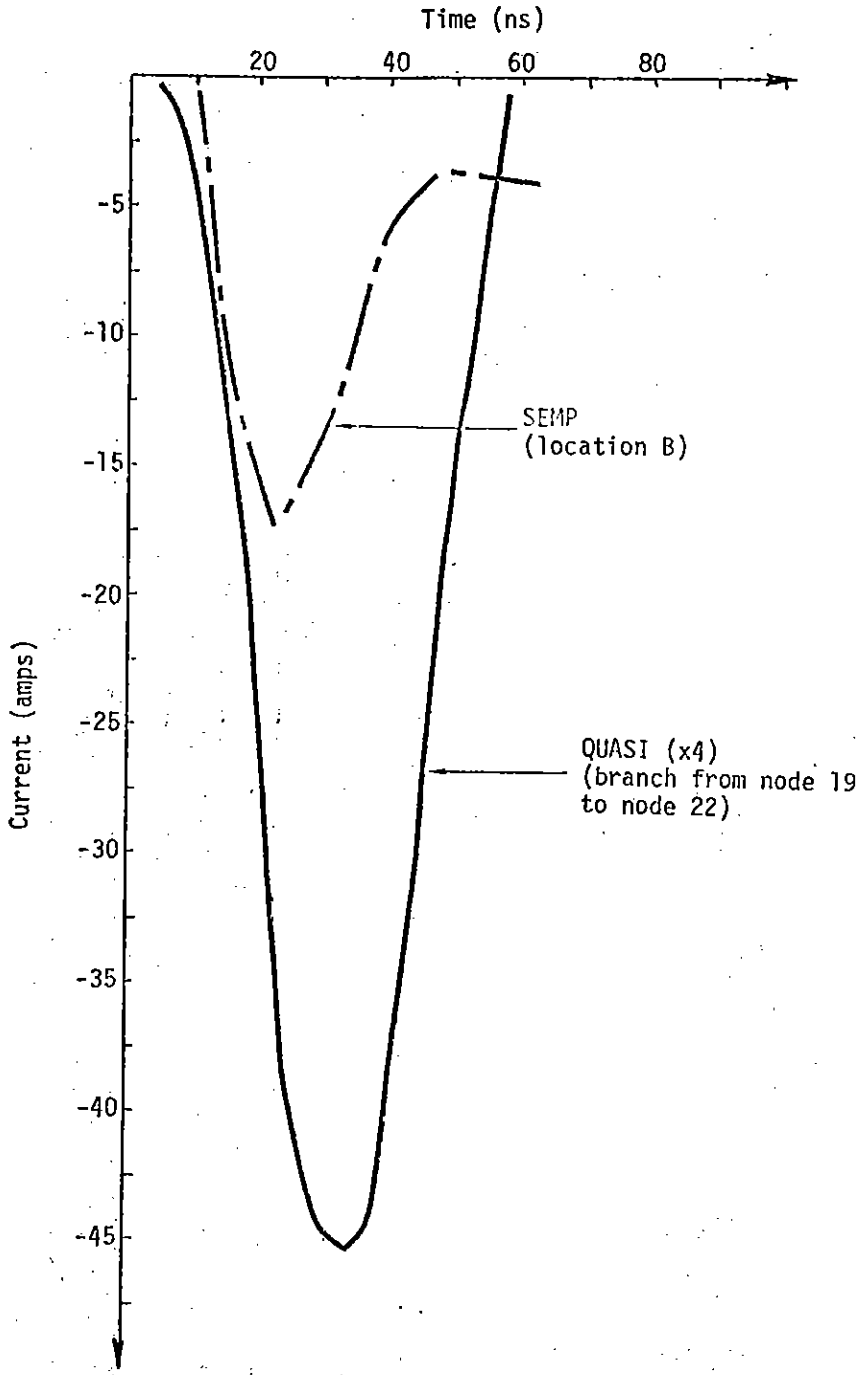

Figure 4-5. Comparison of calculated skin currents: incident fluence = 10^{-4} cal/cm^2.

SECTION 5

CONCLUSIONS

In this report, we have discussed the basic theory of a three-dimensional, hybrid electromagnetic/circuit theory code for calculating SGEMP replacement currents. The code QUASI has been written for carrying out such calculations and the basic structure of the QUASI code has been outlined. Results of a sample problem have also been presented and compared with the results of a different calculational technique. The calculated replacement currents compare quite favorably at low fluences.

From the limited amount of calculated data that has been generated so far, it appears that the QUASI code is a valid and useful tool for calculating SGEMP replacement currents on relatively complicated structures. The code has some obvious limitations and a number of improvements are certainly possible. One needs to exercise the code for a number of different geometries to determine its ultimate usefulness.

REFERENCES

1. Graham, W. R., The Electromagnetic Fields Produced by a General Current Distribution in a Conductive Environment Under Certain Symmetry Conditions, Air Force Weapons Laboratory, Theoretical Note TN 21, January 1975.

2. Longley, H. J., and C. L. Longmire, Development and Testing of LEMP 1, Air Force Weapons Laboratory, Theoretical Note TN 75, April 1970.

3. Longley, H. J., and C. L. Longmire, Development of the GLANC EMP Code, Mission Research Corporation, DNA 3221T, December 1973.

4. Lopez, O., and W. F. Rich, "Dynamic Internal Electromagnetic Pulse Calculations in Three Spatial Dimensions", IEEE Tran. Nucl. Sci., NS-20, No. 6, pp. 14-19 (1973).

5. dePlomb, E. P., and A. J. Woods, TEDIUM-RZ and RΘ: Two Dimensional Time-Dependent IEMP Computer Codes, Intelcom Rad Tech, DNA 3140F, March 1973.

6. Stettner, R., and D. F. Higgins, X-ray Induced Currents on the Surface of a Conducting Sphere, Mission Research Corporation, MRC-N-111, September 1974.

7. Wenaas, E. P., "Lumped-Element Modeling of Satellite SGEMP Excitation," IEEE Tran. Nucl. Sci., NS-21, pp. 271-275 (1974).

8. Kron, G., "Equivalent Circuit of the Field Equations of Maxwell-I," Proc. I.R.E., Vol. 32, pp.289-299 (May 1944).

9. Maxwell, J. C., A Treatise on Electricity and Magnetism, pp. 87-118 of the Dover reprint of the Third Edition (Originally published 1891), New York, 1954.

10. Smythe, W. R., Static and Dynamic Electricity, Third Edition, pp. 35-39 and pp. 128-131, McGraw-Hill, New York, 1968.

11. Shumpert, T. H., Capacitance Calculations for Satellites: Part I Isolated Capacitances of Ellipsoidal Shapes with Comparisons to Some Other Simple Bodies, Air Force Weapons Laboratory, Sensor and Simulation Note SSN 157, September 1972.

12. Messier, M. A., The Quasi-static Method Applied to Satellite Structural Return Current Analysis: Surface Node Analysis, Mission Research Corporation, MRC-R-179, March 1975.

13. Carron, N. J., Suggested Improvements in the QUASI Code, Mission Research Corporation, MRC-N-191, February 1975.

APPENDIX 3

USER'S MANUAL FOR THE QUASI COMPUTER CODE

NOTE: This appendix is self-contained and all mention of sections, figures, tables, equations, and references refers only to items contained herein. This appendix has not been published as a separate document.

TABLE OF CONTENTS

LIST OF FIGURES

1. INTRODUCTION

This document gives the information necessary for running the computer program QUASI. This code calculates structural return currents on a satellite due to system generated EMP effects. The theory used and a basic conceptual outline of the QUASI code are described in two companion documents[1,2] to this user's manual. The reader should refer to these documents for further information on the meaning of various input and output parameters described here.

2. OUTLINE OF CODE OPERATION

QUASI is a three dimensional code using an uniform Cartesian grid. The dimensions of a unit cell in the grid are specified by the three dimensions Δx, Δy, and Δz. The corner of each grid cell is called a node. To avoid triple indexing, each node is assigned a single index. Similarly, each cell is given an index number.

For a given node, the node number is assigned in the following manner:

Let IX = integer number of Δx's of node from yz-plane
IY = integer number of Δy's of node from xz-plane
IZ = integer number of Δz's of node from xy-plane

Then,

node number = IX+1 + NX*IY + NX*NY*IZ

and cell number = IX+1 + (NX-1)*IY + (NX-1)*(NY-1)*IZ

where NX and NY are the total number of nodes in the x and y directions, respectively.

A further description of the relationship between node numbers, cell numbers, surface nodes, and circuit branches is given in Reference 2.

A flow diagram of the QUASI code is shown in Figure 1. This flow diagram, along with the attached code listing should be sufficient information to enable an experienced programmer to understand how QUASI operates.

In order to consolidate the parameters of each problem and also to facilitate communication between routines, two arrays J(200) and C(200) have been included which hold many of the key fixed point and floating point parameters respectively. Although many J(I) and C(I) have been left unused for future modification or expansion, a list of some of the ones used with a definition of each is given in Tables 1 and 2.

Various other J's and C's are used as temporary storage to facilitate in setting up a problem. However, no other C's or J's are used once the time loop has been entered.

3. INPUT DATA

A number of input parameters are required by the QUASI code. This input data is broken down into nine data sets, each of which is described in the following pages.

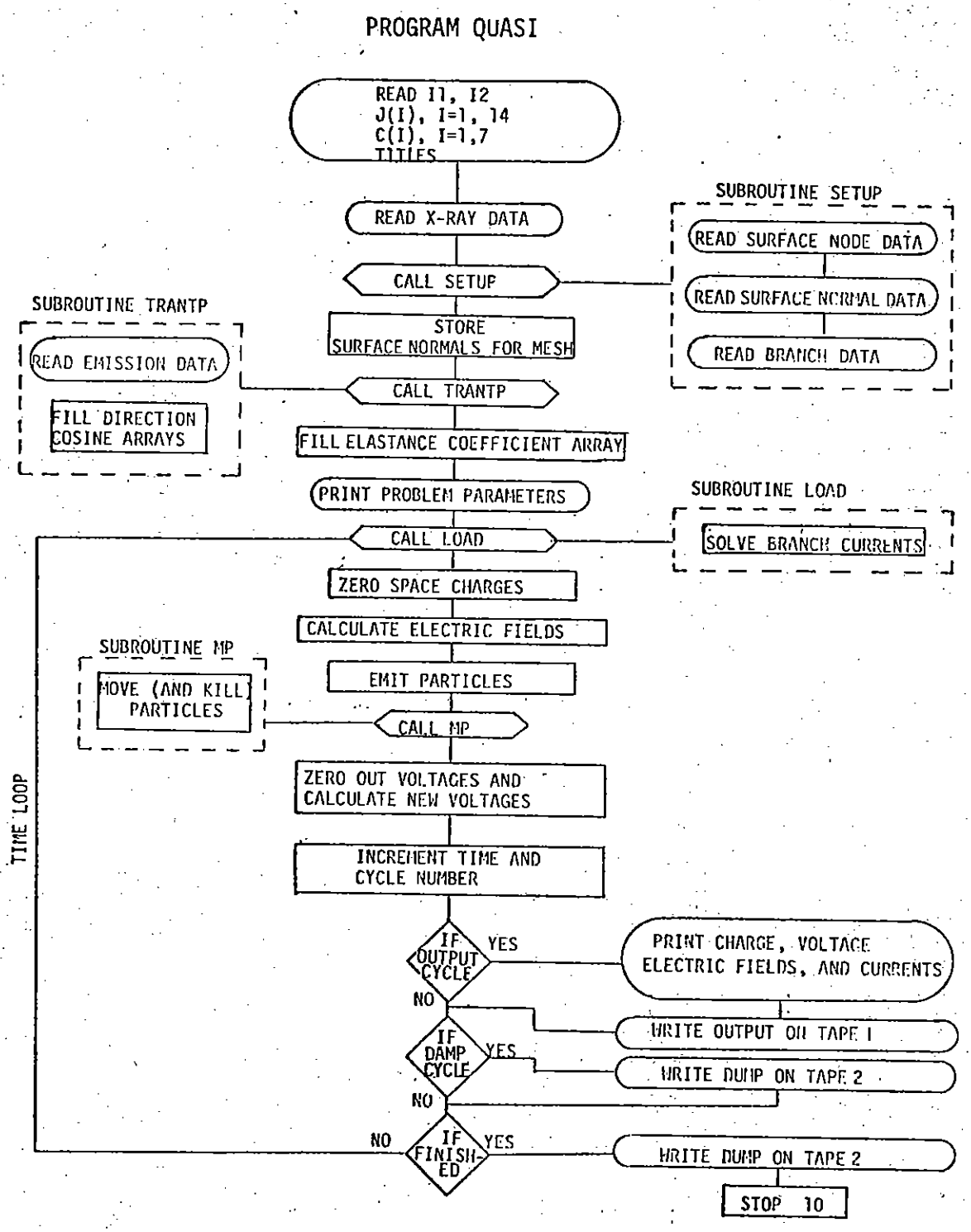

Figure 1. QUASI Flow Chart.

Table 1. Fixed Point Parameters

J(1) - NX = number of nodes in the x direction
J(2) - NY = " " " y "
J(3) - NZ = " " " z "
J(5) - total number of time cycles to run problem
J(6) - total number of output points requested
J(7) - number of theta emission angles
J(8) - number of phi emission angles
J(9) - number of energies for emission
J(10) - number of surface nodes (specimen only)
J(11) - number of branches
J(12) - number of surface normals (specimen only)
J(13) - output point number (this node plus the 7 associated nodes which make up a cell will have the voltage and charge printed at each output cycle along with the electric fields for that cell)
J(14) - problem number
J(29) - cycle number
J(30) - maximum number of particles for which storage has been allotted
J(31) - buffer size for reading or writing particle information
J(33) - number of surface nodes (including outer mesh boundary)
J(34) - number of surface normals (including outer mesh boundary)
J(40) - total number of particles
J(41) - output cycle flag
J(42) - output cycle counter
J(51) - number of particles emitted in the J(29)th cycle
J(101) - total number of angles for emitting particles (J(7)·J(8))
J(102) - 2*J(9)-1
J(103) - J(1)+J(2)-1
J(104) - number of branch current values to be printed at each output cycle
J(110) - (NXNY = J(1)*J(2))

Table 1 (continued) Fixed Point Parameters

J(111) - (NXNYNZ = J(1)*J(2)*J(3)) total number of nodes
J(112) - (KX = NX-1) number of cells in x direction
J(113) - (KY = NY-1) " " y "
J(114) - (KZ = NZ-1) " " z "
J(115) - (NN = KX*KY*KZ) total number of cells
J(116) - (KXKY = J(112)*J(113))
J(120) - J(127) - node numbers of the eight voltages and charges to be printed
J(129) - cell number of electric field to be printed
J(199) - number of dumps

Table 2. Floating Point Parameters

C(1) - DX = distance between nodes in x direction in meters
C(2) - DY = " " " y " "
C(3) - DZ = " " " z " "
C(4) - DT = time elapsed between cycles in seconds
C(5) - real time elapsed between dumps in seconds
C(6) - electron fluence in cal/cm^2
C(7) - fraction of distance from surface for particle turn-off (i.e., if C(7) = 0.01 any particle within 1% of a DX, DY, DZ - or combination of these as indicated by a surface normal - will have its charge returned to the surface charge and will subsequently be killed)
C(64)-C(70) - title of X-ray spectra used
C(71)-C(77) - title of specimen used
C(85) - 1 cal/cm^2 in units of KeV/m^2
C(86) - 1*/(2*J(9))
C(90) - $1*/(4\pi\epsilon_0)$
C(91) - self elastance of a node in space
C(92) - time in seconds
C(93) - charge on an electron (-1.6021E-19 coul)
C(94) - mass of an electron (9.1083E-31 kg)
C(95) - speed of light (2.9979E+8 m/sec)
C(96) - absolute value of C(93)*C(4)
C(97) - reciprocal of electron rest mass in KeV (1.0/511.0)
C(98) - minimum charge on particle for calculating purposes (updated each time cycle). Any particle having less than this amount of charge is considered negligible and is dropped (killed) from calculations
C(99) - C(93)·C(4)/C(94)

Table 2 (continued) Floating Point Parameters

C(100) - C(4)/C(1)
C(101) - C(4)/C(2)
C(102) - C(4)/C(3)
C(103) - C(4)*C(93)/J(101)
C(106) - -1.0/(4*C(1))
C(107) - -1.0/(4*C(2))
C(108) - -1.0/(4*C(3))
C(113) - NX
C(114) - NY
C(115) - NZ

DATA SET 1

Data set 1 is one card which is read in a 2I5 format

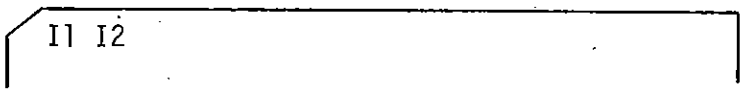

I1 - integer flag to indicate an initiating run or a dump start

I1 = 0 initiating run
I1 > 0 start from dump number I1

I2 - maximum number of minutes that problem will run

DATA SET 2

Data set 2 is one card which is read in a 14I5 format

J(1)	J(2)	J(4)	J(5)	J(6)	J(7)	J(8)	J(9)	J(10)	J(11)	J(12)	J(13)	J(14)

J(1) - number of nodes in the x direction
J(2) - " " " y "
J(3) - " " " z "
J(4) - not used
J(5) - total number of time cycles for problem
J(6) - total number of output points to be put on TAPE1
J(7) - number of theta emission angles
J(8) - " phi " "
J(9) - number of energies for emission
J(10) - number of surface nodes
J(11) - number of current branches
J(12) - number of surface normals
J(13) - node number for output print cell
J(14) - problem number

DATA SET 3

Data set 3 is one card which is read in a 7E10.3 format

C(1)	C(2)	C(3)	C(4)	C(5)	C(6)	C(7)

C(1) - Δx in meters
C(2) - Δy in meters
C(3) - Δz in meters
C(4) - Δt in seconds
C(5) - time between dumps in seconds
C(6) - fluence in calories/cm^2
C(7) - not used

DATA SET 4

Data set 4 is two cards which are used in a 7A10 format

50 KEV BREMSSTRAHLUNG	stored in C(64) - C(71)
3 METER X 3 METER CYLINDER	stored in C(72) - C(79)

C(64)-C(71) - description of X-ray source
C(72)-C(79) - " " specimen

DATA SET 5

Data set 5 is made up of 1 card followed by one or more other cards read in a 7E10.3 format

FT1(k)	FT2(k)	FT3(k)	FMNY	FLG

FT1(k) - first point of trapezoidal time pulse in seconds
FT2(k) - second point of trapezoidal time pulse
FT3(k) - third point of trapezoidal time pulse

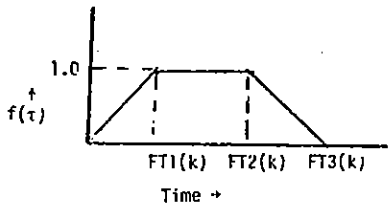

FMNY - number of data points in electron spectrum which will follow

FLG - flag for reading another electron spectrum and time function (i.e., if FLG > 0 another set of data will be read)

	. . . .	XIF(FMNY)
XIF(8)	. . . .	XIF(14)
XIF(1) XIF(2)	. . . .	XIF(7)

XIF(I) - integral of electron fluence normalized to 1 KeV of incident fluence (i.e., XIF(I) = number of electrons ≥ "I" KeV in energy)

DATA SET 6

Data set 6 contains surface node data (one card for each node) read in a 315, E10.3 format

IX IY IZ AREA

IX, IY, IZ - integer distances from the origin of the coordinate system in x-direction, y-direction, and z-direction respectively (the equation for the node number corresponding to IX, IY, IZ is NN = IX + 1 + NX*IY + NXNY * IZ)

AREA - effective area in square meters allotted to this node for current calculations (the total AREA's input to QUASI must equal the physical surface area in square meters of the object)

DATA SET 7

Data set 7 contains surface normal data (one card for each cell) read in a 3I5, 3E10.3 format

IX	IY	IZ	CN(N)	CN(N+1)	CN(N+2)

IX, IY, IZ - integer distances from the origin of the coordinate system in the x-direction, y-direction, and z-direction respectively. (the equation for the cell number corresponding to IX, IY, IZ is cell no. = IX + 1+KX*IY + KX*KY*IZ)

CN - an array which holds the surface normal vectors, i.e., $\vec{S} = CN(N)\cdot\vec{1}_x + CN(N+1)\cdot\vec{1}_y + CN(N+2)\cdot\vec{1}_z$

DATA SET 8

Data set 8 contains branch data (one card for each branch) read in a 3I5, 3E10.3 format

NODE(1,k)	NODE(2,k)	ITYPE	R	AL	CC

NODE(I,k) - integer node number of starting point and ending point of the branch

ITYPE - integer to indicate type of circuit in this branch

ITYPE = 1, R circuit
2, RL series circuit
3, RLC series circuit

R - resistance of the circuit in this branch

AL - inductance of the circuit

CC - capacitance of the circuit

DATA SET 9

Data set 9 contains emission data (one card for each emission point) in a I5, 7E10.3 format

IEM(I)	XEP(I)	YEP(I)	ZEP(I)	THEP(I)	PHEP(I)	FRT(I)	AR(I)

IEM(I) - integer to indicate which electron spectrum is to be used at this point. i.e., IEM(I) = 1 implies that the first electron spectrum will be used

XEP(I), YEP(I), ZEP(I) - the floating point distance from the origin of the coordinate system in the x-direction, y-direction and z-direction respectively

THEP(I) - the first angle of emission measured from the x-axis of the surface

PHEP(I) - the second angle of emission measured from the normal to the surface.

FRI(I) - the time in seconds that the Ith emission point is retarded from emitting electrons with respect to the first emitting time.

AR(I) - the area of the surface in square meters over which the Ith emission point is emitting (i.e., the Ith emission point represents emission over this area).

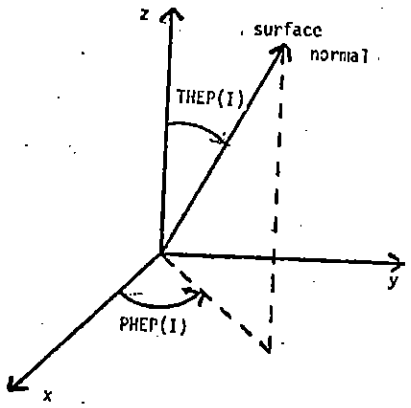

4. OUTPUT

Two binary tapes are created by QUASI. TAPE 1 is an output tape which, for each output cycle, contains the cycle number, the number of particles, and all of the currents, charges, potentials and electric fields at that time. TAPE 2 is a dump start tape. Several dumps may be written and QUASI may be restarted from any one.

A number of output parameters are also printed along with the code listing. The first part of such printed output data just lists the various input parameters and the results of certain set-up calculations. A sample of this problem definition data is given in Appendix A.

A second set of data is printed at each output cycle. This printed data is a sample of the more complete set of data being written on the output tape, TAPE 1.

An example of the information printed at each output cycle is shown in Figure 2. The first line contains the following data:

CYCLE NO.	=	cycle number (number of times the time loop has been iterated)
NO. PART.	=	number of particles currently being followed
TIME	=	time at which output parameters were calculated (TIME = cycle number x time step)
PART./CYCLE	=	number of particles emitted per time cycle
SPACE Q	=	sum of all charge in space (outside the satellite)
TOTAL Q	=	sum of charge in space plus charge on surface nodes; i.e., total charge on system
AVG. Q	=	average charge of particle in space divided by 100 (particles with less than this amount of charge are dropped from the calculation.

The next three lines refer to a previously specified spatial cell (this cell number is stored in J(13)). The first of these three lines is the total charge on each of the eight nodes of the specified cell at the end of the time cycle being considered. The second line gives the calculated voltages at each of these nodes. (The order in which the nodes are printed is indicated in Figure 2.) The first three numbers in the third line are the calculated Ex, Ey, and Ez components of the electric field, respectively, for the specified cell. The fourth number in this line is the sum of the charges on the eight nodes divided by the cell volume (in cm^3) and the fifth number is just the fourth divided by the electron charge.

The final line of data for each output cycle is the current in amps flowing through certain specified branches of the equivalent circuit which represents the satellite structure. These currents, then, are the so-called structural replacements currents due to SGEMP. The specified branches to which these currents correspond are printed just before the output data for each cycle begins (see Appendix A).

```
CYCLE NO. =    5 NC. PART. =  100 TIME = 1.500E-09PART./CYCLE =   20 SPACE Q =-3.043E-08 TOTAL Q = 1.655E-21 AVG. Q =-3.043E-12
        3.662E-10      4.718E-11      6.719E-11     -1.593E-10     -1.633E-11     -5.826E-11     -6.081E-11     -6.845E-13
        3.708E+00      1.431E+00      1.442E+00      2.493E+00      3.965E-01      5.616E-01      5.668E-01     -1.678E-03
        6.172E-01      6.200E-01      7.072E-01      1.280E+09      7.583E+02
   1.088E-05      1.078E-05     -1.426E-04     -2.353E-04     -4.472E-04     -4.336E-04     -3.527E-04     -3.891E-04
CYCLE NO. =   10 NC. PART. =  200 TIME = 2.750E-09PART./CYCLE =   20 SPACE Q =-1.116E-07 TOTAL Q = 9.942E-21 AVG. Q =-5.579E-12
        2.219E-09      4.103E-10      4.103E-10     -7.232E-10     -9.611E-11     -3.474E-10     -3.352E-10     -6.047E-12
        2.469E+01      9.362E+00      9.346E+00      1.587E+01      2.878E+00      4.016E+00      3.938E+00      4.705E-01
        4.546E+00      4.357E+00      5.053E+00      9.550E+09      5.659E+03
   1.715E-04      1.714E-04     -1.666E-03     -2.729E-03     -5.172E-03     -5.151E-03     -4.286E-03     -4.482E-03
CYCLE NO. =   15 NC. PART. =  300 TIME = 4.000E-09PART./CYCLE =   20 SPACE Q =-2.034E-07 TOTAL Q = 2.609E-20 AVG. Q =-8.115E-12
        6.691E-09      1.251E-09      1.251E-09     -2.468E-09     -2.931E-10     -1.014E-09     -1.113E-09     -2.635E-11
        7.169E+01      2.758E+01      2.776E+01      4.690E+01      8.010E+00      1.111E+01      1.163E+01      8.385E-01
        1.474E+01      1.462E+01      1.687E+01      2.669E+10      1.582E+04
   7.719E-04      7.721E-04     -7.709E-03     -1.260E-02     -2.374E-02     -2.372E-02     -1.988E-02     -2.072E-02
```

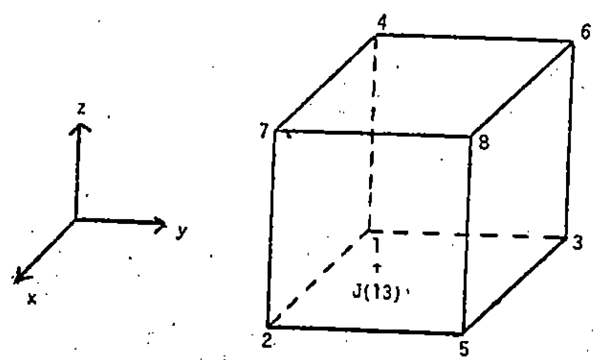

Numbers indicate order in which charge and potential are printed

Figure 2. Example of output data printed each output cycle.

APPENDIX A

SET-UP DATA FOR SAMPLE PROBLEM

Results for a sample QUASI run were given in Reference 2. This appendix shows the various parameters used in that problem as they are printed out by the code itself. This listing includes all of the data printed out by the code prior to the beginning of the time loop.

The geometry considered, the equivalent circuit and the corresponding node numbers for the problem are shown in Figure A-1.

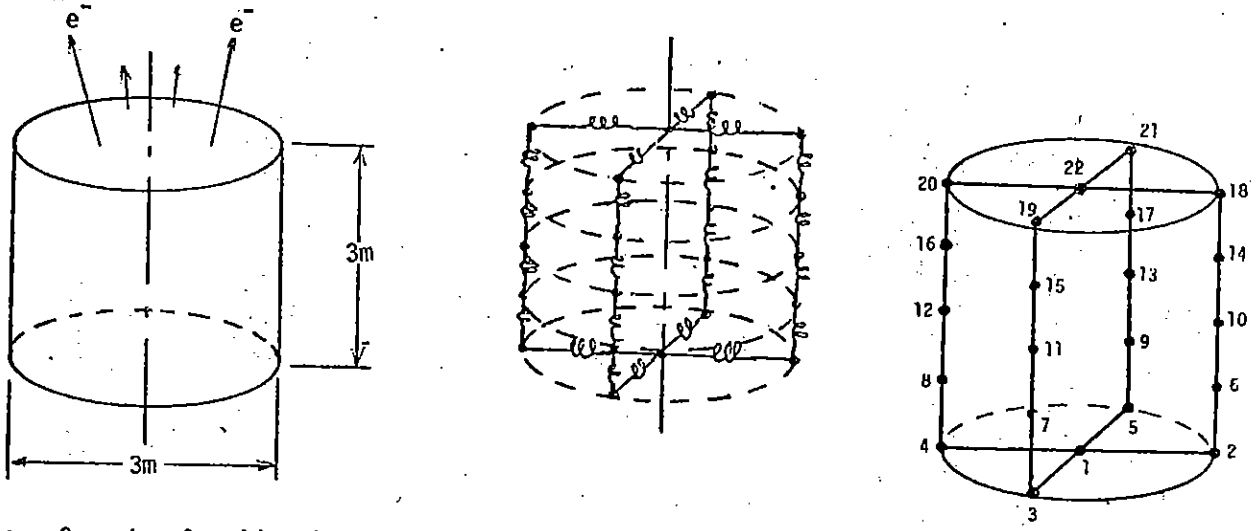

a. Geometry Considered

b. Equivalent Circuit

c. Node Numbers

Figure A-1. Problem Definition.

PROGRAM CHASI PROBLEM NO. = 26

10 10 10 -0 500 100 1 4 6 22 24 24 556 26

1.500E+00 1.500E+00 7.500E-01 2.500E-10 2.000E+02 1.000E-04 1.00AE-02

2 KEV BLACKBODY AT A FLUENCE OF 10-4 CAL/CM2

INCIDENT ON A CYCLINDER 3M X 3M

X-RAY DATA

FT1	FT2	FT3	FT4	NO. OF PTS.
7.000E-09	1.800E-08	6.000E-09	2.817E+07	1.000E+02

XIF(I)

2.720E-04	1.411E-04	9.696E-05	5.833E-05	3.432E-05	1.978E-05	1.115E-05	5.936E-06	4.350E-06	2.573E-06
1.527E-06	9.052E-07	5.395E-07	3.205E-07	1.919E-07	1.140E-07	6.877E-08	4.116E-08	2.493E-08	1.504E-08
9.189E-09	5.591E-09	3.434E-09	2.079E-09	1.268E-09	7.945E-10	4.925E-10	3.070E-10	1.947E-10	1.188E-10
6.999E-11	4.070E-11	2.436E-11	1.551E-11	9.476E-12	5.585E-12	3.241E-12	1.940E-12	1.239E-12	7.588E-13
4.476E-13	2.898E-13	1.554E-13	9.936E-14	6.086E-14	3.586E-14	2.07AE-14	1.240E-14	7.945E-15	4.872E-15
2.871E-15	1.6A2E-15	9.936E-16	6.363E-16	3.926E-16	2.322E-16	1.35AE-16	8.117E-17	5.253E-17	3.267E-17
1.967E-17	1.17AE-17	7.352E-18	4.944E-18	3.314E-18	2.191E-18	1.477E-18	1.044E-18	7.731E-19	5.571E-19
3.88AE-19	2.59AE-19	1.649E-19	9.812E-20	5.387E-20	2.702E-20	1.28AE-20	6.892E-21	5.117E-21	3.695E-21
2.580E-21	1.728E-21	1.099E-21	6.539E-22	3.585E-22	1.789E-22	6.39AE-23	4.439E-23	3.285E-23	2.360E-23
1.A33E-23	1.076E-23	6.689E-24	3.807E-24	1.908E-24	7.742E-25	2.02AE-25	0.	0.	0.

SURFACE NODE DATA

CARD NODE

NO.	NO.	IX	IY	IZ	AREA
1	156	5	5	1	3.534E+00
2	146	5	4	1	1.767E+00
3	155	4	5	1	1.767E+00
4	166	5	6	1	1.767E+00
5	157	6	5	1	1.767E+00
6	247	6	5	2	1.767E+00
7	246	5	4	2	1.767E+00
8	255	4	5	2	1.767E+00
9	266	5	6	2	1.767E+00
10	346	5	4	3	1.767E+00
11	355	4	5	3	1.767E+00
12	366	5	6	3	1.767E+00
13	357	6	5	3	1.767E+00
14	457	6	5	4	1.767E+00
15	466	5	6	4	1.767E+00
16	455	4	5	4	1.767E+00
17	446	5	4	4	1.767E+00
18	546	5	4	5	1.767E+00
19	555	4	5	5	1.767E+00
20	566	5	6	5	1.767E+00
21	557	6	5	5	1.767E+00
22	556	5	5	5	3.534E+00

SURFACE NORMAL DATA

POSITION IX	IY	IZ	NORMAL TO X-AXIS	Y-AXIS	Z-AXIS
5	5	0	0.	0.	-1.000E+00
5	4	0	0.	0.	-1.000E+00
4	5	0	0.	0.	-1.000E+00
4	4	0	0.	0.	-1.000E+00
5	5	5	0.	0.	1.000E+00
5	4	5	0.	0.	1.000E+00
4	5	5	0.	0.	1.000E+00
4	4	5	0.	0.	1.000E+00
5	5	1	1.000E+00	1.000E+00	0.
5	5	2	1.000E+00	1.000E+00	0.
5	5	3	1.000E+00	1.000E+00	0.
5	5	4	1.000E+00	1.000E+00	0.
5	4	1	1.000E+00	-1.000E+00	0.
5	4	2	1.000E+00	-1.000E+00	0.
5	4	3	1.000E+00	-1.000E+00	0.
5	4	4	1.000E+00	-1.000E+00	0.
4	5	1	-1.000E+00	1.000E+00	0.
4	5	2	-1.000E+00	1.000E+00	0.
4	5	3	-1.000E+00	1.000E+00	0.
4	5	4	-1.000E+00	1.000E+00	0.
4	4	1	-1.000E+00	-1.000E+00	0.
4	4	2	-1.000E+00	-1.000E+00	0.
4	4	3	-1.000E+00	-1.000E+00	0.
4	4	4	-1.000E+00	-1.000E+00	0.

BRANCH DATA

BRN NO.	FROM CARD	TO CARD	ITYPE	R	L	C	D1	D2	D3	D4
1	1	2	2	1.547E+02	1.727E-06	-0.	1.432E-04	9.779E-01	0.	1.000E+00
2	1	3	2	1.547E+02	1.727E-06	-0.	1.432E-04	9.779E-01	0.	1.000E+00
3	1	4	2	1.547E+02	1.727E-06	-0.	1.432E-04	9.779E-01	0.	1.000E+00
4	1	5	2	1.547E+02	1.727E-06	-0.	1.432E-04	9.779E-01	0.	1.000E+00
5	2	6	2	2.405E+01	2.685E-07	-0.	9.208E-04	9.779E-01	0.	1.000E+00
6	3	7	2	2.405E+01	2.685E-07	-0.	9.208E-04	9.779E-01	0.	1.000E+00
7	4	8	2	2.405E+01	2.685E-07	-0.	9.208E-04	9.779E-01	0.	1.000E+00
8	5	9	2	2.405E+01	2.685E-07	-0.	9.208E-04	9.779E-01	0.	1.000E+00
9	6	10	2	2.405E+01	2.685E-07	-0.	9.208E-04	9.779E-01	0.	1.000E+00
10	7	11	2	2.405E+01	2.685E-07	-0.	9.208E-04	9.779E-01	0.	1.000E+00
11	8	12	2	2.405E+01	2.685E-07	-0.	9.208E-04	9.779E-01	0.	1.000E+00
12	9	13	2	2.405E+01	2.685E-07	-0.	9.208E-04	9.779E-01	0.	1.000E+00
13	10	14	2	2.405E+01	2.685E-07	-0.	9.208E-04	9.779E-01	0.	1.000E+00
14	11	15	2	2.405E+01	2.685E-07	-0.	9.208E-04	9.779E-01	0.	1.000E+00
15	12	16	2	2.405E+01	2.685E-07	-0.	9.208E-04	9.779E-01	0.	1.000E+00
16	13	17	2	2.405E+01	2.685E-07	-0.	9.208E-04	9.779E-01	0.	1.000E+00
17	14	18	2	2.405E+01	2.685E-07	-0.	9.208E-04	9.779E-01	0.	1.000E+00
18	15	19	2	2.405E+01	2.685E-07	-0.	9.208E-04	9.779E-01	0.	1.000E+00
19	16	20	2	2.405E+01	2.685E-07	-0.	9.208E-04	9.779E-01	0.	1.000E+00
20	17	21	2	2.405E+01	2.685E-07	-0.	9.208E-04	9.779E-01	0.	1.000E+00
21	18	22	2	1.547E+02	1.727E-06	-0.	1.432E-04	9.779E-01	0.	1.000E+00
22	19	22	2	1.547E+02	1.727E-06	-0.	1.432E-04	9.779E-01	0.	1.000E+00
23	20	22	2	1.547E+02	1.727E-06	-0.	1.432E-04	9.779E-01	0.	1.000E+00
24	21	22	2	1.547E+02	1.727E-06	-0.	1.432E-04	9.779E-01	0.	1.000E+00

EMISSION DATA

EMISSION NO.	X POSITION	Y POSITION	Z POSITION	THETA POSITION	PHI POSITION	RETARD TIME	AREA
1	5.000E+00	5.000E+00	5.000E+00	-0.	-0.		3.534E+00
1	5.000E+00	4.000E+00	5.000E+00	-0.	-0.		8.836E-01
1	6.000E+00	5.000E+00	5.000E+00	-0.	-0.		8.836E-01
1	5.000E+00	6.000E+00	5.000E+00	-0.	-0.		8.836E-01
1	4.000E+00	5.000E+00	5.000E+00	-0.	-0.		8.836E-01
-0.	-0.	-0.	-0.	-0.	-0.	-0.	

FLOATING POINT PARAMETERS (C*8)

1.500E+00	1.500E+00	7.500E-01	2.500E-10	2.000E+02	1.000E-04	1.000E-02	0.	0.	0.
0.	0.	0.	0.	0.	0.	0.	0.	0.	0.
0.	0.	0.	0.	0.	0.	0.	0.	0.	0.
0.	0.	0.	0.	0.	0.	0.	0.	0.	0.
0.	0.	0.	0.	0.	0.	0.	0.	0.	0.
0.	0.	0.	0.	0.	0.	0.	0.	0.	0.
0.	0.	0.	-4.841E+62	1.406+234	1.967+262	1.387E+03	2.681E-52	-7.174E+57	-7.174E+57
-1.387F+69	3.518F-01	2.189E-24	8.701+287	-7.174E+57	-7.174E+57	-7.174E+57	0.	0.	0.
0.	0.	0.	0.	2.619E+16	8.333E-02	3.142E+00	5.926E-07	6.242E+18	8.987E+09
6.080E+09	2.500F-10	-1.602E-10	9.108E-31	2.998E+08	4.005E-29	1.957E-03	0.	-4.397E+01	1.667F-10
1.667E-10	3.333F-10	-1.001E-29	0.	0.	-1.667E-01	-1.667E-01	-3.333E-01	0.	0.
0.	0.	1.000E+01	1.000E+01	1.000E+01	0.	0.	0.	0.	0.
0.	0.	0.	0.	0.	0.	1.000E+00	-1.000E+00	1.000E+00	-1.000E+00
0.	0.	0.	1.000E+00	1.000E+00	-1.000E+00	-1.000E+00	0.	0.	0.
1.000E+00	-1.000E+00	-1.000E+00	-1.000E+00	1.000E+00	1.000E+00	1.000E+00	-1.000E+00	1.000E+00	1.000E+00
-1.000E+00	-1.000E+00	-1.000E+00	1.000E+00	-1.000E+00	1.000E+00	1.000E+00	1.000E+00	1.000E+00	-1.000E+00
-1.000E+00	-1.000E+00	1.000E+00	-1.000E+00	0.	0.	0.	0.	0.	0.
0.	0.	0.	0.	0.	0.	0.	0.	0.	0.
0.	0.	0.	0.	0.	0.	0.	0.	0.	0.
0.	0.	0.	0.	0.	0.	0.	0.	0.	0.

FIXED POINT PARAMETERS (J*8)

10	10	10	-0	500	100	1	4	6	22	24	24	556	26	0	0	0	0	0	0
0	0	0	0	0	0	0	0	0	30000	1023	0	510	1531	0	0	0	0	0	0
5	0	0	0	0	0	0	0	0	0	0	0	0	0	0	0	0	0	0	0
0	0	0	0	0	0	0	0	0	0	0	0	0	0	0	0	0	0	0	0
0	0	0	0	0	0	0	0	0	0	0	0	0	0	0	0	0	0	0	0
4	11	19	3	1531	0	0	0	0	100	1000	9	9	9	729	81	0	0	0	0
557	566	656	567	666	657	667	0	456	0	0	0	0	0	1	0	0	2	2	556
1	9	81	729	721	649	73	657	0	8	8	8	1	9	81	1	73	649	721	1
9	649	657	1	9	73	81	0	0	0	0	0	0	0	0	0	0	0	0	0
0	0	0	0	0	0	0	0	0	0	0	0	0	0	0	0	0	0	0	0

INDIRECT ADDRESSING (IBES) FOR EMISSION NODES,
I.E. CHARGE IS EMITTED FROM NO(IA(IB(I)))

22	18	21	20	19

INDIRECT ADDRESSING (IA*S) FOR SURFACE NODES,
I.E. SURFACE CHARGE IS REDISTRIBUTED BY SUB. LOAD FOR QQ(IA(I))

156	146	155	146	157	257	256	255	246	346	355	366	357	457	466	455	446	546	555	566
557	554	1	10	101	110	201	210	301	310	401	410	501	510	601	610	701	710	801	810
901	910	11	20	111	120	211	220	311	320	411	420	511	520	611	620	711	720	811	820
911	920	21	30	121	130	221	230	321	330	421	430	521	530	621	630	721	730	821	830
921	930	31	40	131	140	231	240	331	340	431	440	531	540	631	640	731	740	831	840
931	940	41	50	141	150	241	250	341	350	441	450	541	550	641	650	741	750	841	850
941	950	51	60	151	160	251	260	351	360	451	460	551	560	651	660	751	760	851	860
951	960	61	70	161	170	261	270	361	370	461	470	561	570	661	670	761	770	861	870
961	970	71	80	171	180	271	280	371	380	471	480	571	580	671	680	771	780	871	880
971	980	81	90	181	190	281	290	381	390	481	490	581	590	681	690	781	790	881	890
981	990	91	100	191	200	291	300	391	400	491	500	591	600	691	700	791	800	891	900
991	1000	2	92	102	192	202	292	302	392	402	492	502	592	602	692	702	792	802	892
902	992	3	93	103	193	203	293	303	393	403	493	503	593	603	693	703	793	803	893
903	993	4	94	104	194	204	294	304	394	404	494	504	594	604	694	704	794	804	894
904	994	5	95	105	195	205	295	305	395	405	495	505	595	605	695	705	795	805	895
905	995	6	96	106	196	206	296	306	396	406	496	506	596	606	696	706	796	806	896
906	996	7	97	107	197	207	297	307	397	407	497	507	597	607	697	707	797	807	897
907	997	8	98	108	198	208	298	308	398	408	498	508	598	608	698	708	798	808	898
908	998	9	99	109	199	209	299	309	399	409	499	509	599	609	699	709	799	809	899
909	999	12	912	22	922	32	932	42	942	52	952	62	962	72	972	82	982	13	913
23	923	33	933	43	943	53	953	63	963	73	973	83	983	14	914	24	924	34	934
44	944	54	954	64	964	74	974	84	984	15	915	25	925	35	935	45	945	55	955
65	965	75	975	85	985	16	916	26	926	36	936	46	946	56	956	66	966	76	976
86	986	17	917	27	927	37	937	47	947	57	957	67	967	77	977	87	987	18	918
28	928	38	938	48	948	58	958	68	968	78	978	88	988	19	919	29	929	39	939
49	949	59	959	69	969	79	979	89	989										

TYPE OF EACH NODE,I.E. TYPE=0.(SURFACE NODE)
TYPE=1.0 (SPACE NODE)

0.	0.	0.	0.	0.	0.	0.	0.	0.	0.
0.	0.	0.	0.	0.	0.	0.	0.	0.	0.
0.	0.	0.	0.	0.	0.	0.	0.	0.	0.
0.	0.	0.	0.	0.	0.	0.	0.	0.	0.
0.	0.	0.	0.	0.	0.	0.	0.	0.	0.
0.	0.	0.	0.	0.	0.	0.	0.	0.	0.
0.	0.	0.	0.	0.	0.	0.	0.	0.	0.
0.	0.	0.	0.	0.	0.	0.	0.	0.	0.
0.	0.	0.	0.	0.	0.	0.	0.	0.	0.
0.	0.	0.	0.	0.	0.	0.	0.	0.	0.
0.	0.	0.	0.	0.	0.	0.	0.	0.	0.
0.	1.000E+00	1.000E+00	1.000E+00	1.000E+00	1.000E+00	1.000E+00	1.000E+00	1.000E+00	0.
0.	1.000E+00	1.000E+00	1.000E+00	1.000E+00	1.000E+00	1.000E+00	1.000E+00	1.000E+00	0.
0.	1.000E+00	1.000E+00	1.000E+00	1.000E+00	1.000E+00	1.000E+00	1.000E+00	1.000E+00	0.
0.	1.000E+00	1.000E+00	1.000E+00	1.000E+00	0.	1.000E+00	1.000E+00	1.000E+00	0.
0.	1.000E+00	1.000E+00	1.000E+00	0.	0.	0.	1.000E+00	1.000E+00	0.
0.	1.000E+00	1.000E+00	1.000E+00	1.000E+00	0.	1.000E+00	1.000E+00	1.000E+00	0.
0.	1.000E+00	1.000E+00	1.000E+00	1.000E+00	1.000E+00	1.000E+00	1.000E+00	1.000E+00	0.
0.	1.000E+00	1.000E+00	1.000E+00	1.000E+00	1.000E+00	1.000E+00	1.000E+00	1.000E+00	0.
0.	0.	0.	0.	0.	0.	0.	0.	0.	0.
0.	0.	0.	0.	0.	0.	0.	0.	0.	0.
0.	1.000E+00	1.000E+00	1.000E+00	1.000E+00	1.000E+00	1.000E+00	1.000E+00	1.000E+00	0.
0.	1.000E+00	1.000E+00	1.000E+00	1.000E+00	1.000E+00	1.000E+00	1.000E+00	1.000E+00	0.
0.	1.000E+00	1.000E+00	1.000E+00	1.000E+00	1.000E+00	1.000E+00	1.000E+00	1.000E+00	0.
0.	1.000E+00	1.000E+00	1.000E+00	1.000E+00	0.	1.000E+00	1.000E+00	1.000E+00	0.
0.	1.000E+00	1.000E+00	1.000E+00	0.	1.000E+00	0.	1.000E+00	1.000E+00	0.
0.	1.000E+00	1.000E+00	1.000E+00	1.000E+00	0.	1.000E+00	1.000E+00	1.000E+00	0.
0.	1.000E+00	1.000E+00	1.000E+00	1.000E+00	1.000E+00	1.000E+00	1.000E+00	1.000E+00	0.
0.	1.000E+00	1.000E+00	1.000E+00	1.000E+00	1.000E+00	1.000E+00	1.000E+00	1.000E+00	0.
0.	0.	0.	0.	0.	0.	0.	0.	0.	0.
0.	0.	0.	0.	0.	0.	0.	0.	0.	0.

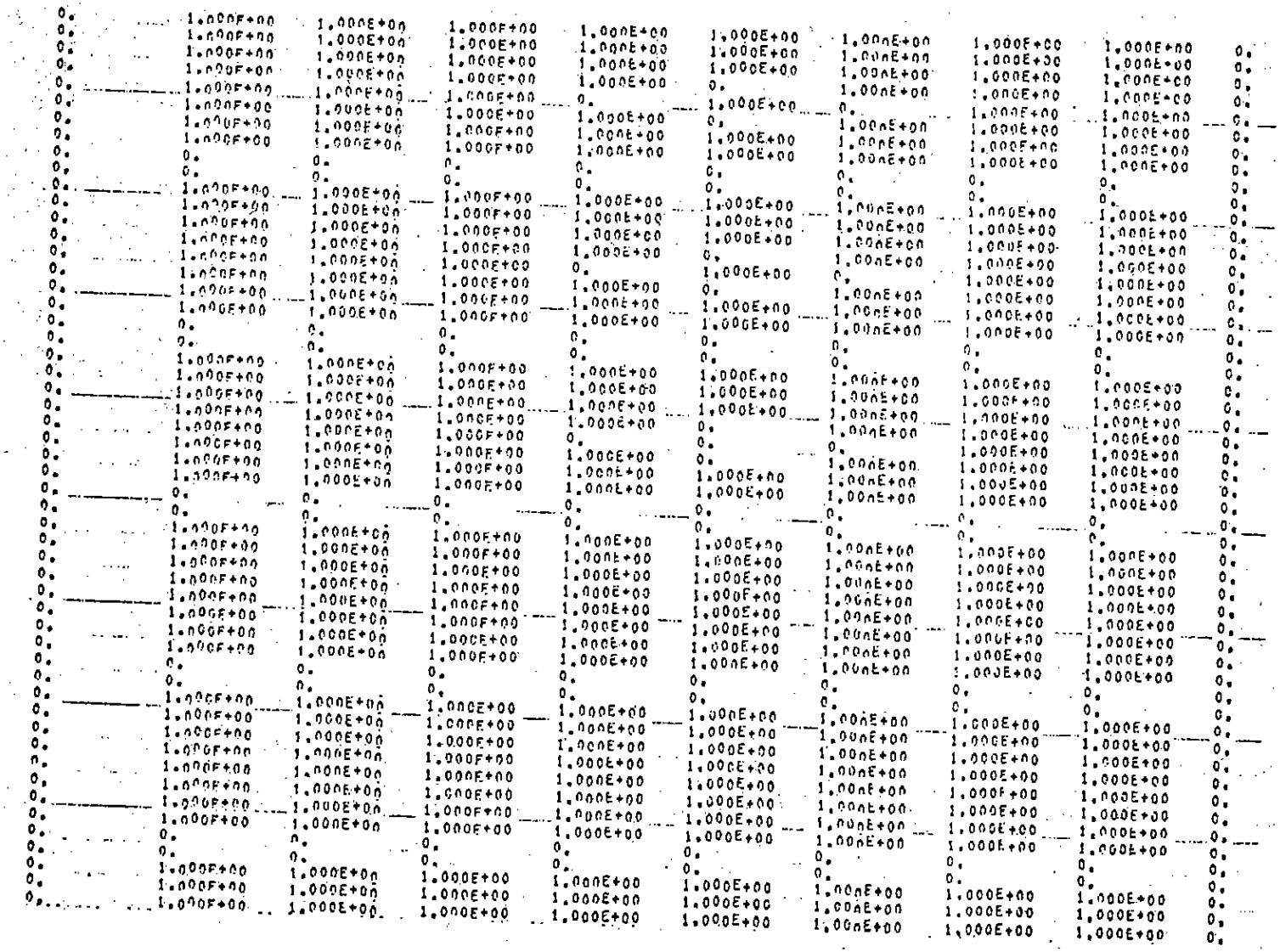

```
     0.          1.000E+00   1.000E+00   1.000E+00   1.000E+00   1.000E+00   1.000E+00   1.000E+00   1.000E+00   0.
     0.          1.000E+00   1.000E+00   1.000E+00   1.000E+00   1.000E+00   1.000E+00   1.000E+00   1.000E+00   0.
     0.          1.000E+00   1.000E+00   1.000E+00   1.000E+00   1.000E+00   1.000E+00   1.000E+00   1.000E+00   0.
     0.          1.000E+00   1.000E+00   1.000E+00   1.000E+00   1.000E+00   1.000E+00   1.000E+00   1.000E+00   0.
     0.          1.000E+00   1.000E+00   1.000E+00   1.000E+00   1.000E+00   1.000E+00   1.000E+00   1.000E+00   0.
     0.          0.          0.          0.          0.          0.          0.          0.          0.          0.
     0.          0.          0.          0.          0.          0.          0.          0.          0.          0.
     0.          0.          0.          0.          0.          0.          0.          0.          0.          0.
     0.          0.          0.          0.          0.          0.          0.          0.          0.          0.
     0.          0.          0.          0.          0.          0.          0.          0.          0.          0.
     0.          0.          0.          0.          0.          0.          0.          0.          0.          0.
     0.          0.          0.          0.          0.          0.          0.          0.          0.          0.
     0.          0.          0.          0.          0.          0.          0.          0.          0.          0.
     0.          0.          0.          0.          0.          0.          0.          0.          0.          0.
#NORM# FOR EACH CELL,I.E.,
NORM=0 ( NO ADJACENT SURFACES)
              NORMAL COMPONENT      X-AXIS      Y-AXIS      Z-AXIS
NORM=IIII                           CN(III)     CN(III+1)   CN(III+2)

NORM=-2IIII            1ST          CN(III)     CN(III+1)   CN(III+2)
                       2ND          CN(III+3)   CN(III+4)   CN(III+5)

NORM=-3IIII            1ST          CN(III)     CN(III+1)   CN(III+2)
                       2ND          CN(III+3)   CN(III+4)   CN(III+5)
                       3RD          CN(III+6)   CN(III+7)   CN(III+8)
-30073-20145-20151-20157-20163-20169-20175-20181-30082
-20313  1237  1279  1321  1363  1405  1447  1489-20355
-20319  1243  1285  1327  1369  1411  1453  1495-20361
-20325  1249  1291  1333  1375  1417  1459  1501-20367
-20331  1255  1297  1339  1381  1423  1465  1507-20373
-20337  1261  1303  1345  1387  1429  1471  1513-20379
-20343  1267  1309  1351  1393  1435  1477  1519-20385
-20349  1273  1315  1357  1399  1441  1483  1525-20391
-30127-20187-20193-20199-20205-20211-20217-20223-30091
-20481   943   985  1027  1069  1111  1153  1195-20523
   649     0     0     0     0     0     0     0   652
   691     0     0     0     0     0     0     0   694
   733     0     0     0     0     0     0     0   736
   775     0     0     0    61    37     0     0   778
   817     0     0     0    49    25     0     0   820
   859     0     0     0     0     0     0     0   862
   901     0     0     0     0     0     0     0   904
-20565   946   988  1030  1072  1114  1156  1198-20607
-20487   949   991  1033  1075  1117  1159  1201-20529
   655     0     0     0     0     0     0     0   658
   697     0     0     0     0     0     0     0   700
   739     0     0     0     0     0     0     0   742
   781     0     0     0    64    40     0     0   784
   823     0     0     0    52    28     0     0   826
   865     0     0     0     0     0     0     0   868
   907     0     0     0     0     0     0     0   910
-20571   952   994  1036  1078  1120  1162  1204-20613
-20493   955   997  1039  1081  1123  1165  1207-20535
   661     0     0     0     0     0     0     0   664
   703     0     0     0     0     0     0     0   706
   745     0     0     0     0     0     0     0   748
   787     0     0     0    67    43     0     0   790
   829     0     0     0    55    31     0     0   832
   871     0     0     0     0     0     0     0   874
   913     0     0     0     0     0     0     0   916
-20577   958  1000  1042  1084  1126  1168  1210-20619
-20499   961  1003  1045  1087  1129  1171  1213-20541
   667     0     0     0     0     0     0     0   670
   709     0     0     0     0     0     0     0   712
```

```
   751     0     0     0     0     0     0     0   754
   793     0     0     0    70    46     0     0   796
   835     0     0     0    58    34     0     0   838
   877     0     0     0     0     0     0     0   880
   919     0     0     0     0     0     0     0   922
-20583   964  1006  1048  1090  1132  1174  1216-20625
-20505   967  1009  1051  1093  1135  1177  1219-20547
   673     0     0     0     0     0     0     0   674
   715     0     0     0     0     0     0     0   718
   757     0     0     0     0     0     0     0   760
   799     0     0     0    22    16     0     0   802
   841     0     0     0    19    13     0     0   844
   883     0     0     0     0     0     0     0   886
   925     0     0     0     0     0     0     0   928
-20589   970  1012  1054  1096  1138  1180  1222-20631
-20511   973  1015  1057  1099  1141  1183  1225-20553
   679     0     0     0     0     0     0     0   682
   721     0     0     0     0     0     0     0   724
   763     0     0     0     0     0     0     0   766
   805     0     0     0     0     0     0     0   808
   847     0     0     0     0     0     0     0   850
   889     0     0     0     0     0     0     0   892
   931     0     0     0     0     0     0     0   934
-20595   976  1018  1060  1102  1144  1186  1228-20637
-20517   979  1021  1063  1105  1147  1189  1231-20559
   685     0     0     0     0     0     0     0   688
   727     0     0     0     0     0     0     0   730
   769     0     0     0     0     0     0     0   772
   811     0     0     0     0     0     0     0   814
   853     0     0     0     0     0     0     0   856
   895     0     0     0     0     0     0     0   898
   937     0     0     0     0     0     0     0   940
-20601   982  1024  1066  1108  1150  1192  1234-20643
-30119-20229-20235-20241-20247-20253-20259-20265-30136
-20397  1240  1282  1324  1366  1408  1450  1492-20439
-20403  1246  1288  1330  1372  1414  1456  1498-20445
-20409  1252  1294  1336  1378  1420  1462  1504-20451
-20415  1258  1300  1342  1384  1426  1468  1510-20457
-20421  1264  1306  1348  1390  1432  1474  1516-20463
-20427  1270  1312  1354  1396  1438  1480  1522-20469
-20433  1276  1318  1360  1402  1444  1486  1528-20475
-30109-20271-20277-20283-20289-20295-20301-20307-30100
NODES OF BRANCHES FOR OUTPUT CURRENTS

OUTPUT POINT NO. =    1    2    3    4    5    6    7    8    9   10   11   12

        FROM NODE     1    1    4    7   10   13   16   19
        TO   NODE     2    5    8   11   14   17   20   22

                VELOCITIES AT WHICH PARTICLES ARE EMITTED
4.479E+07 3.612E+07 3.095E+07 2.669E+07 2.376E+07 2.055E+07
```

APPENDIX B

A LISTING OF THE QUASI CODE

```
      PROGRAM QUASI (INPUT,OUTPUT,TAPE1,TAPE2,TAPE5=INPUT,TAPE6=OUTPUT)
C           TAPE1=OUTPUT TAPE    ,    TAPE2=DUMP TAPE
      COMMON C(200),J(200),XTF(150,4),NMAX(4),YV(20),IB(30),EX(1000),EY(
     11000),EZ(1000),FT1(4),FT2(4),FT3(4),FT4(4),XP(1023),YP(1023),ZP(10
     223),VX(1023),VY(1023),VZ(1023),WT(1023),FQ(8),TYPE(1331),SIJ(1331)
     3,SII(1331),Q(1331)
      LARGE PX(30000),PY(30000),PZ(30000),PVX(30000),PVY(30000),
     1PVZ(30000),PWT(30000)
      COMMON /ENMSET/ NTHETA,NPHI,NEW,TEM(30),XEP(30),YEP(30),ZEP(30),TH
     1EP(30),PHEP(30),AR(30),FRT(30),CX(30,48),CY(30,48),CZ(30,48)
      COMMON /TABLE/ SUM(200),NODE(2,200),D(4,200),A(200),NORM(1000),CN(
     12500)
      COMMON /CONST/ DT,DX,DY,DZ,NT,NX,NY,NZ,KBRN,NS,NML
      COMMON /COUPLE/ V(1331),QQ(1331),CUR(200),IA(1000)
      IX=LOCF(J(200))+1
      IY=LOCF(Q(1331))-IX
      DO 10 I=1,IY
      J(200+I)=1777000000000000000B
   10 CONTINUE
      DO 20 I=1,200
      J(I)=0
      C(I)=0.0
   20 CONTINUE
      DO 30 I=1,1000
      NORM(I)=0
   30 CONTINUE
      READ (5,40) I1,I2
   40 FORMAT (14I5)
      PRINT 41,I2
   41 FORMAT(*1TIME LIMIT =*,I5,*MINUTES*)
      CALL SECOND (XCP1X)
      X1=FLOAT(I2)
      XCPXX=X1*60.0+10.0
      IF (I1) 190,190,50
C          DUMP START
   50 I3=I1+1
      REWIND 2
      IF (I3) 80,80,60
   60 DO 70 I=1,I3
      READ (2)
   70 CONTINUE
   80 READ (2) C,J,EX,EY,EZ,QQ,V,NORM,CN,NX,NY,NZ,KXKY,NEW,KX,KY,KZ,NXNY
     1,NXNYNZ,NN,TYPE,TA,AR,XTF,IB,IEM,XEP,ZEP,CX,CY,CZ,NMAX,SIJ,YEP,CUR
     2,D,NS,KBRN,DT,DX,DY,DZ,NSN,SUM,NODE,FRT,SII,FT1,FT2,FT3,FT4,PX,PY,
     3PZ,PVX,PVY,PVZ,PWT,A,NOP
      REWIND 2
      I2=0
   90 READ (2)
      IF (EOF,2) 110,100
  100 I2=I2+1
      GO TO 90
  110 BACKSPACE 2
      WRITE (6,120) I1,I2,J(10)
```

```
  120 FORMAT (42H    PROGRAM QUASI DUMP START FROM DUMP NO.,I3,/,18H TOT
     1AL NO. DUMPS =,I5,10H PROB NO.=,I5)
      J(199)=I2
      REWIND 1
      I2=0
  130 READ (1)
      IF (EOF,1) 150,140
  140 I2=I2+1
      GO TO 130
  150 J(198)=I2
      BACKSPACE 1
  160 FORMAT (1X,20I6)
  161 FORMAT(1X, 9I6)
  170 FORMAT (1X,10E13.3)
      I08=J(13)
      I01=I08+1
      I02=I08+NX
      I03=I08+NXNY
      I04=I01+NX
      I05=I02+NXNY
      I06=I03+1
      I07=I06+NX
      I1=I08/NXNY
      I09=J(13)-I1*J(103)-(J(13)-I1*NXNY)/NX
      J(121)=I01
      J(122)=I02
      J(123)=I03
      J(124)=I04
      J(125)=I05
      J(126)=I06
      J(127)=I07
      J(128)=I08
      J(129)=I09
      WRITE (6,160) J
      WRITE (6,170) C
      GO TO 370
C          END OF DUMP START
  190 J(30)=30000
      J(31)=1023
      J(135)=1
      J(136)=0
      J(137)=0
      J(138)=2
      J(139)=2
      J(140)=1
      J(141)=1
      J(153)=1
      J(156)=1
      J(160)=1
      J(164)=1
```

```
C          MKS UNITS
           C(87)=3.14159265359
           C(89)=1.0/1.6021E-19
           C(85)=2.6187E+20
           C(90)=8.9874E+9
           C(93)=-1.6021E-19
           C(94)=9.1083E-31
           C(95)=2.9979E+8
           C(96)=ABS(C(93))
           C(97)=1.0/511.0
           DO 200 I=1,3
           I1=144+I
           I2=156+I
           I3=120+7*I
           I4=141+I
           I5=150+I
           I6=141+7*I
           I7=159+I
           I8=142+7*I
           C(I1)=1.0
           C(I2)=1.0
           C(I3)=1.0
           C(I4)=-1.0
           C(I5)=-1.0
           C(I6)=-1.0
           C(I7)=-1.0
           C(I8)=1.0
   200 CONTINUE
           C(128)=-1.0
           C(129)=1.0
           C(130)=-1.0
           C(135)=1.0
           C(136)=-1.0
           C(137)=-1.0
           C(150)=1.0
           C(154)=1.0
           C(160)=-1.0
C          READ INPUT PARAMETERS
           READ (5,40) (J(I),I=1,14)
           READ (5,210) (C(I),I=1,7)
   210 FORMAT (7E10.3)
           WRITE (6,220) J(14)
   220 FORMAT( 1H1,20X,27HPROGRAM QUASI PROBLEM NO. =,I5)
           WRITE (6,160) (J(I),I=1,14)
           WRITE (6,170) (C(I),I=1,7)
           READ (5,221) (C(I),I=64,77)
   221 FORMAT(7A10)
   222 FORMAT(1X,7A10)
           WRITE (6,222) (C(I),I=64,77)
           NX=J(1)
           NY=J(2)
           NZ=J(3)
           NXNY=NX*NY
           NXNYNZ=NXNY*NZ
           KX=NX-1
           KY=NY-1
           KZ=NZ-1
```

```
      KXKY=KX*KY
      NN=KX*KY*KZ
      FNX=FLOAT(NX)
      FNY=FLOAT(NY)
      FNZ=FLOAT(NZ)
      NTHETA=J(7)
      NPHI=J(8)
      NT=J(5)
      NS=J(10)
      KBRN=J(11)
      NML=J(12)
      NOP=KBRN/8
      DX=C(1)
      DY=C(2)
      DZ=C(3)
      DT=C(4)
      J(41)=J(5)/J(6)
      J(101)=J(7)*J(8)
      J(102)=2*J(9)-1
      J(103)=J(1)+J(2)-1
      J(104)=NOP
      J(110)=NXNY
      J(111)=NXNYNZ
      J(112)=KX
      J(113)=KY
      J(114)=KZ
      J(115)=NN
      J(142)=KX
      J(143)=KXKY
      J(144)=NN
      J(145)=NN-KX+1
      J(146)=NN-KXKY+1
      J(147)=KXKY-KX+1
      J(148)=NN-KXKY+KY
      LX=KX-1
      LY=KY-1
      LZ=KZ-1
      J(150)=LX
      J(151)=LY
      J(152)=LZ
      J(154)=J(142)
      J(155)=J(143)
      J(157)=J(147)
      J(158)=J(146)
      J(159)=J(145)
      J(161)=KX
      J(162)=J(146)
      J(163)=J(148)
      J(165)=KX
      J(166)=J(147)
      J(167)=KXKY
      J(116)=KX*KY
      C(85)=C(85)*C(6)
      C(86)=1.0/FLOAT(2*J(9))
```

```
      C(88)=1.0/(DX*DY*DZ*1.E+6)
      C(91)=0.5*C(90)/(C(1)*C(2)*C(3)*0.75/C(87))**(0.33333)
      C(92)=C(4)
      C(96)=C(96)*C(4)
      C(99)=C(4)*C(93)/C(94)
      C(100)=C(4)/C(1)
      C(101)=C(4)/C(2)
      C(102)=C(4)/C(3)
      C(103)=C(4)*C(93)/FLOAT(J(101))
      C(106)=-0.25/C(1)
      C(107)=-0.25/C(2)
      C(108)=-0.25/C(3)
      C(113)=FNX
      C(114)=FNY
      C(115)=FNZ
      I08=J(13)
      I01=I08+1
      I02=I08+NX
      I03=I08+NXNY
      I04=I01+NX
      I05=I02+NXNY
      I06=I03+1
      I07=I06+NX
      I1=I08/NXNY
      I09=J(13)-I1*J(103)-(J(13)-I1*NXNY)/NX
      J(121)=I01
      J(122)=I02
      J(123)=I03
      J(124)=I04
      J(125)=I05
      J(126)=I06
      J(127)=I07
      J(120)=I08
      J(129)=I09
C
C          READ X-RAY DATA
C
      K=1
  230 READ (5,210) FT1(K),FT2(K),FT3(K),FMNY,FLG
      FT4(K)=2.0/(FT3(K)+FT2(K)-FT1(K))
      WRITE (6,231)
  231 FORMAT(50X,*X-RAY DATA*,//,7X,3HFT1,10X,3HFT2,10X,3HFT3,10X,3HFT4,
     $8X,11HNO. OF PTS.)
      WRITE (6,170) FT1(K),FT2(K),FT3(K),FT4(K),FMNY,FLG
      MNY=INT(FMNY)
      READ (5,210) (XIF(I,K),I=1,MNY)
      WRITE (6,232)
  232 FORMAT(50X,6HXIF(I))
      WRITE (6,170) (XIF(I,K),I=1,MNY)
      NMAX(K)=MNY
      K=K+1
      IF (FLG.GT.0.0) GO TO 230
```

```
C
C          DRAW SATELLITE
C
C          AND SETUP SURFACE NODE ARRAYS
      CALL SETUP
      NMLN=3*NML+1
      NSIDES=6*(KXKY+KX*KZ+KY*KZ)+NMLN
      J(105)=NSIDES
      DO 240 I=NMLN,NSIDES
      CN(I)=0.
  240 CONTINUE
C
C          STORE 3 SURFACE NORMALS AT EACH CORNER OF THE MESH
C
      I2=NMLN+4
      I3=NMLN+8
      DO 250 I=1,8
      K1=J(140+I)
      NORM(K1)=-(30000+NMLN)
      CN(NMLN)=C(140+I)
      CN(I2)=C(148+I)
      CN(I3)=C(156+I)
      NMLN=NMLN+9
      I2=NMLN+4
      I3=NMLN+8
  250 CONTINUE
C
C          STORE 2 SURFACE NORMALS ALONG EACH EDGE OF THE MESH
C
      I1=0
      DO 260 I=1,3
      L1=J(149+I)
      INC=J(152+I)
      DO 260 K=1,4
      I1=I1+1
      KK=J(155+I1)
      DO 260 L=2,L1
      L2=NMLN+J(134+I)
      KK=KK+INC
      NORM(KK)=-(20000+NMLN)
      CN(L2)=C(126+K)
      NMLN=NMLN+3
      L3=NMLN+J(137+I)
      CN(L3)=C(133+K)
      NMLN=NMLN+3
  260 CONTINUE
C
C          STORE 1 SURFACE NORMAL AT THE FACES OF THE MESH
C
      DO 270 I=2,LY
      DO 270 K=2,LZ
      KK=1+KX*(I-1)+KXKY*(K-1)
      NORM(KK)=NMLN
      CN(NMLN)=1.0
```

```
      NML=NML+3
      KK=KX*I+KXKY*(K-1)
      NORM(KK)=NML
      CN(NML)=-1.0
      NML=NML+3
  270 CONTINUE
      DO 280 I=2,LX
      DO 280 K=2,LZ
      KK=I+KXKY*(K-1)
      NORM(KK)=NML
      CN(NML)=1.0
      NML=NML+3
      KK=I+KXKY*K-KX
      NORM(KK)=NML
      CN(NML)=-1.0
      NML=NML+3
  280 CONTINUE
      DO 290 I=2,LX
      DO 290 K=2,LY
      KK=I+KX*(K-1)
      NORM(KK)=NML
      CN(NML)=1.0
      NML=NML+3
      KK=KK+NU-KXKY
      NORM(KK)=NML
      CN(NML)=-1.0
      NML=NML+3
  290 CONTINUE
      NSN=NS
      DO 300 I=1,NY
      DO 300 K=1,NZ
      II=1+NX*(I-1)+NXNY*(K-1)
      NSN=NSN+1
      IA(NSN)=II
      NSN=NSN+1
      IA(NSN)=II+NX-1
  300 CONTINUE
      DO 310 I=1,NX
      DO 310 K=1,NZ
      II=I+NXNY*(K-1)
      NSN=NSN+1
      IA(NSN)=II
      NSN=NSN+1
      IA(NSN)=II+NXNY-NX
  310 CONTINUE
      DO 320 I=1,NX
      DO 320 K=1,NY
      NSN=NSN+1
      II=I+NX*(K-1)
      IA(NSN)=II
      NSN=NSN+1
      IA(NSN)=II+NXNYNZ-NXNY
  320 CONTINUE
```

```
C
C          END OF SURFACE NORMALS
C          GET INJECTION ANGLES
C
      CALL TRANTP
      DO 330 I=1,NEW
      IX=XEP(I)
      IY=YEP(I)
      IZ=ZEP(I)
      K1=IX+1+NX*IY+NXNY*IZ
      DO 330 K=1,NSN
      IF (IA(K).EQ.K1) IB(1)=K
  330 CONTINUE
      KENEG=1
C
C          SET SELF-ELASTANCE COEFFICIENTS
C
      DO 340 I=1,NS
      II=IA(I)
      SII(II)=C(90)/A(T)
  340 CONTINUE
      KK=0
C
C          SET OTHER ELASTANCE COEFFICIENTS
C          AND ZERO FIELDS
C
      DO 350 IZ=1,NZ
      TIZ=FLOAT(IZ-1)*DZ
      TIZ=TIZ*TIZ
      DO 350 IY=1,NY
      TIY=FLOAT(IY-1)*DY
      TIY=TIY*TIY
      DO 350 IX=1,NX
      KK=KK+1
      QQ(KK)=0.0
      V(KK)=0.0
      IF (KK.EQ.1) GO TO 350
      TIX=FLOAT(IX-1)*DX
      TIX=TIX*TIX
      SIJ(KK)=C(90)/SQRT(TIX+TIY+TIZ)
      TYPE(KK)=1.0
  350 CONTINUE
      K=0
C
C          DELETE DUPLICATED SURFACE NORMALS
C          AND SET SELF-ELASTANCE FOR MESH BOUNDARY
C
      DO 360 I=1,NSN
      II=IA(I)
      IF (TYPE(II).EQ.0.0) GO TO 360
      K=K+1
      IA(K)=IA(I)
      TYPE(II)=0.0
      IF (I.GT.NS) SII(II)=C(91)
  360 CONTINUE
      NSN=K
      IA(K)=NSN
```

```
C
C          WRITE FIRST OUTPUT TAPE RECORD
C          PRINT PROBLEM PARAMETERS
C
      J(34)=NMLN
      WRITE (1) J,C,IA,IB,NODE
      WRITE (6,361)
  361 FORMAT(* FLOATING POINT PARAMETERS (C=S)*)
      WRITE (6,170) C
      WRITE (6,362)
  362 FORMAT(* FIXED POINT PARAMETERS (J=S)*)
      WRITE (6,160) J
      WRITE (6,363)
  363 FORMAT(* INDIRECT ADDRESSING (IB=S) FOR EMISSION NODES,*,/,
     1* I.E. CHARGE IS EMITTED FROM QQ(IA(IB(I)))*)
      WRITE (6,160) (IB(I),I=1,NEW)
      WRITE (6,364)
  364 FORMAT(* INDIRECT ADDRESSING (IA=S) FOR SURFACE NODES,*,/,
     1* I.E. SURFACE CHARGE IS REDISTRIBUTED BY SUB, LOAD FOR QQ(IA(I))*
     2)
      WRITE (6,160) (IA(I),I=1,NSN)
      WRITE (6,365)
  365 FORMAT(* =TYPE= OF EACH NODE,I.E. TYPE=0.(SURFACE NODE)*,/,
     1       *                          TYPE=1.0 (SPACE NODE)*)
      WRITE (6,170) (TYPE(I),I=1,NXNYNZ)
      WRITE (6,366)
  366 FORMAT(* =NORM= FOR EACH CELL,I.E.,*,/,
     2* NORM=0 ( NO ADJACENT SURFACES)*,/,
     1*                NORMAL COMPONENT      X-AXIS      Y-AXIS      Z-AXIS*,/
     3* NORM=1111                           CN(III)     CN(III+1)   CN(III+2)*
     A,//,
     5* NORM=-2IIII          1ST           CN(III)     CN(III+1)   CN(III+2)*
     A,/,
     7*                      2ND           CN(III+3)   CN(III+4)   CN(III+5)*
     A,//,
     9* NORM=-3IIII          1ST           CN(III)     CN(III+1)   CN(III+2)*
     A,/,
     B*                      2ND           CN(III+3)   CN(III+4)   CN(III+5)*
     A,/,
     C*                      3RD           CN(III+6)   CN(III+7)   CN(III+8)*
     D)
      WRITE (6,161) (NORM(I),I=1,NN)
      WRITE (6,367) (NODE(1,I),I=1,KBRN,NOP)
      WRITE (6,368) (NODE(2,I),I=1,KBRN,NOP)
  367 FORMAT(* NODES OF BRANCHES FOR OUTPUT CURRENTS*,//,* OUTPUT POINT*
     $,* NO. = *,4X,1H1,4X,1H2,4X,1H3,4X,1H4,4X,1H5,4X,1H6,4X,1H7,4X,1H8
     $,4X,1H9,3X,2H10,3X,2H11,3X,2H12,//,10X,*FROM NODE *,12I5)
  368 FORMAT(10X,*TO   NODE *,12I5)
C          START OF TIME LOOP
C          INCREMENT CURRENT IN TIME
  370 CALL LOAD
C          ZERO SPACE CHARGES
      DO 380 I=1,NXNYNZ
      Q(I)=0.0
  380 CONTINUE
```

```
C          CALCULATE ELECTRIC FIELDS
      I=0
      DO 390 II=1,NN
      I=I+1
      I1=I+1
      I2=I+NX
      I3=I+NXNY
      I4=I3+NX
      I5=I3+1
      I6=I2+1
      I7=I5+NX
      A1=V(I7)-V(I)
      A2=V(I4)-V(I1)
      A3=V(I5)-V(I2)
      A4=V(I6)-V(I3)
      EX(II)=C(106)*(A1-A2+A3+A4)
      EY(II)=C(107)*(A1+A2-A3+A4)
      EZ(II)=C(108)*(A1+A2+A3-A4)
      IF (MOD(II,KX).EQ.0) I=I+1
      IF (MOD(II,KXKY).EQ.0) I=I+NX
  390 CONTINUE
C          EMIT PARTICLES
      N=1
      WMIN=1.0
C          NEW=NO. EMISSION NODES
      DO 430 I=1,NEW
      FT=FTIME(C(92),I)
      IF (FT.LE.0.0) GO TO 430
      I1=INT(WMIN)
      X1=FLOAT(I1)
      X2=WMIN-X1
      I4=IEM(I)
      X3=XIF(I1,I4)
      X4=XIF(I1+1,I4)
      X5=X3-X2*(X3-X4)
      XNE=C(85)*AR(I)*X5
      XWT=C(103)*FT*XNE
      IF(ABS(C(98)).GE.ABS(XWT)) GO TO 430
      I5=IB(I)
      I5=IA(I5)
      QQ(I5)=QQ(I5)+C(96)*FT*XNE
      I2=NMAX(I4)
      X6=X5*C(86)
      I1=J(102)
      I3=1
      DO 410 K=1,I1,2
      X1=FLOAT(K)
      X2=X1*X6
  400 I2=I2-1
      IF (XIF(I2,I4).LT.X2) GO TO 400
      X3=X2-XIF(I2+1,I4)
      X4=XIF(I2,I4)-XIF(I2+1,I4)
      X7=FLOAT(I2+1)
      I2=I2+1
```

```
      X8=X7*X3/X4
C         XA=ENERGY OF PARTICLE (KEV)
      YGAM=1.0+XA*C(97)
      VV(I3)=C(95)*SQRT(1.0-1.0/(YGAM*YGAM))
      I3=I3+1
  410 CONTINUE
      I2=J(101)
      DO 420 K=1,I2
      VX(N)=VV(KENEG)*CX(I,K)
      VY(N)=VV(KENEG)*CY(I,K)
      VZ(N)=VV(KENEG)*CZ(I,K)
      XP(N)=XEP(I)
      YP(N)=YEP(I)
      ZP(N)=ZEP(I)
      WT(N)=XWT
      N=N+1
  420 CONTINUE
  430 CONTINUE
      IEMIT2=N-1
      KENEG=KENEG+1
      IF (KENEG.GT.J(9)) KENEG=1
      J(51)=IEMIT2
      IF (IEMIT2.LE.0) GO TO 440
C         STORE PARTICLES INTO LCM
      IOUT1=J(40)+1
      SMALLOUT(XP,PX(IOUT1),IEMIT2)
      SMALLOUT(YP,PY(IOUT1),IEMIT2)
      SMALLOUT(ZP,PZ(IOUT1),IEMIT2)
      SMALLOUT(VX,PVX(IOUT1),IEMIT2)
      SMALLOUT(VY,PVY(IOUT1),IEMIT2)
      SMALLOUT(VZ,PVZ(IOUT1),IEMIT2)
      SMALLOUT(WT,PWT(IOUT1),IEMIT2)
      J(40)=J(40)+IEMIT2
C         END OF EMISSION
C
C         MOVE PARTICLES
C
  440 CALL MP
      TQ=0.0
C         NSN=NO. OF SURFACE NODES
      DO 450 I=1,NXNYNZ
      TQ=TQ+Q(I)
  450 CONTINUE
      DO 460 I=1,NSN
      II=IA(I)
      Q(II)=QQ(II)+Q(II)
  460 CONTINUE
      IF (J(40).LE.0) GO TO 470
      C(98)=0.01*TQ/FLOAT(J(40))
C         END OF PARTICLE MOVEMENT
C         END OF STORAGE LOOP
```

```
C          ZERO OUT VOLTAGE
  470 SQ=0.0
      DO 480 I=1,NXNYNZ
      SQ=SQ+Q(I)
      V(I)=0.0
  480 CONTINUE
C          CALCULATE NEW VOLTAGE
      JJ=0
      DO 520 JZ=1,NZ
      DO 520 JY=1,NY
      DO 520 JX=1,NX
      JJ=JJ+1
      IF (Q(JJ).EQ.0.0) GO TO 520
      KK=0
      DO 510 IZ=1,NZ
      LZ=IABS(IZ-JZ)*NXNY+1
      DO 510 IY=1,NY
      LY=IABS(IY-JY)*NX+LZ
      DO 510 IX=1,NX
      KK=KK+1
      IF (KK.EQ.JJ) GO TO 490
      LX=IABS(IX-JX)
      TSIJ=SIJ(LX+LY)
      GO TO 500
  490 TSIJ=C(91)
      IF (TYPE(KK).EQ.0.0) TSIJ=SII(JJ)
  500 V(KK)=V(KK)+Q(JJ)*TSIJ
  510 CONTINUE
  520 CONTINUE
C          INCREMENT TIME AND CYCLE NUMBER
      C(92)=C(92)+C(4)
      J9=J(9)
      IF(J(29).EQ.1) WRITE (6,521) (VV(I),I=1,J9)
  521 FORMAT(25X,*VELOCITIES AT WHICH PARTICLES ARE EMITTED*,/,1X,
     $12E10.3,/,1H1,/,50X,*START OF TIME OUTPUT*,/)
      J(29)=J(29)+1
      J(42)=J(42)+1
      CALL SECOND (XCPYY)
      IF (J(42).GE.J(41)) GO TO 530
      IF (XCPYY.GE.(XCP1X+C(5))) GO TO 560
      IF (XCPYY.GE.XCPXX.OR.J(29).GE.J(5)) GO TO 530
      GO TO 370
C          END OF TIME LOOP
C          WRITE OUTPUT
  530 WRITE (6,550) J(29),J(40),C(92),J(51),TQ,SQ,C(98)
      WRITE (6,540) Q(IO8),Q(IO1),Q(IO2),Q(IO3),Q(IO4),Q(IO5),Q(IO6),Q(I
     $O7)
      WRITE (6,540) V(IO8),V(IO1),V(IO2),V(IO3),V(IO4),V(IO5),V(IO6),V(I
     $O7)
      AMT=C(89)*(Q(IO1)+Q(IO2)+Q(IO3)+Q(IO4)+Q(IO5)+Q(IO6)+Q(IO7)+Q(IO8)
     $)
      AVG=AMT*C(88)
```

```
C          WRITE DUMP TAPE
  560 XCPYX=XCPYY
      WRITE (2) C,J,EX,EY,EZ,QQ,V,NORM,CN,NX,NY,NZ,KXKY,NEW,KX,KY,KZ,NXN
     1Y,NXNYNZ,NN,TYPE,IA,AR,XTP,IB,IEM,XEP,ZEP,CX,CY,CZ,NMAX,SIJ,YEP,CU
     2R,D,NS,KBRN,DT,DX,DY,DZ,NSN,SUM,NODE,FRT,SII,FT1,FT2,FT3,FT4,PX,PY
     3,PZ,PVX,PVY,PVZ,PNT,A,NOP
      END FILE 2
      BACKSPACE 2
      J(199)=J(199)+1
      WRITE (6,570) J(199),C(92),J(29)
  570 FORMAT (/,5X,9HDUMP NO. ,I3,5X,9HTAKEN AT ,E10.3,10H SECONDS (,I6,
     18H CYCLES),//)
      IF (XCPYY.GE.XCPXX.OR.J(29).GE.J(5)) STOP 10
      GO TO 370
      END
      WRITE (6,540)EX(109),EY(109),EZ(109),ANT,AVG
      WRITE (6,170) (CUR(I),I=1,KBRN,NOP)
      WRITE (1) J(20),J(40),J(49),(CUR(I),I=1,KBRN),(Q(I),I=1,NXNYNZ),(V
     1(I),I=1,NXNYNZ),(EY(I),I=1,NN),(EY(I),I=1,NN),(EZ(I),I=1,NN),(QQ(I
     2),I=1,NXNYNZ)
  540 FORMAT (2X,8E15.3)
  550 FORMAT(1X,*CYCLE NO. =*,I5,* NO. PART. =*,I5,* TIME =*,E10.3,
     $        *PART./CYCLE =*,I5,* SPACE Q =*,E10.3,* TOTAL Q =*,
     AE10.3,* AVG. Q =*,E10.3)
      J(42)=0
      IF (XCPYY.GE.XCPXX.OR.J(29).GE.J(5)) GO TO 560
      GO TO 370
```

```
SUBROUTINE TRANTP

QUASI ROUTINE TO CALCULATE X,Y,Z COORDINATES OF SAMPLE POINTS
    EQUALLY PROBABLE ABOUT A SET OF EMISSION POINT NORMALS

DIRECT QUESTIONS TO ..
 EQUATIONS    - DAN HIGGINS
 PROGRAMMING - JOHN SUNDERSON, JR.

INPUTS FROM CARDS (READ FROM DEVICE IUNIT)
  ONE CARD FOR EACH EMISSION POINT (MAX=30) CONTAINING
IEMM    - INTEGER INDICATING SURFACE MATERIAL (NOT EQUAL 0)
X
Y       - LOCATION COORDINATES
Z
THETA   - DIRECTION OF SURFACE NORMAL (IN RADIANS)
PHI     - DIRECTION OF SURFACE NORMAL (IN RADIANS)
RT      - RETARDATION TIME
AREA    - AREA REPRESENTED
  FOLLOWED BY A BLANK CARD
 EACH EMISSION CARD HAS THE FOLLOWING FORMAT(I5,5E11.0,2E10.0)

INPUTS FROM COMMON BLOCK /EMMSET/
NTHETA - NUMBER OF EQUALLY PROBABLE THETAS DESIRED
NPHI   - NUMBER OF PHIS DESIRED
NOTE.....NTHETA IS FORCED TO BE LESS THAN OR EQUAL TO 6 (MIN=1)
          NPHI   IS FORCED TO BE LESS THAN OR EQUAL TO 8 (MIN=1)

OUTPUTS TO COMMON BLOCK /EMMSET/
IEM     - AN ARRAY (MAX LENGTH=30) FILLED WITH IEMMS FROM CARDS
XEP     - AN ARRAY (MAX LENGTH=30) FILLED WITH X LOCATION COORD.
YEP     - AN ARRAY (MAX LENGTH=30) FILLED WITH Y LOCATION COORD.
ZEP     - AN ARRAY (MAX LENGTH=30) FILLED WITH Z LOCATION COORD.
THEP    - AN ARRAY (MAX LENGTH=30) FILLED WITH SURFACE NORMAL DIREC
PHEP    - AN ARRAY (MAX LENGTH=30) FILLED WITH SURFACE NORMAL DIREC
AR      - AN ARRAY (MAX LENGTH=30) FILLED WITH AREA REPRESENTED
ERT     - AN ARRAY (MAX LENGTH=30) FILLED WITH RETARDATION TIME
CX
CY      - DOUBLE SUBSCRIPTED ARRAYS OF SAMPLE POINT COORDINATES
CZ          FIRST INDEX (MAX=30) - EMISSION POINT INDEX
            SECOND INDEX (MAX=48)- REPRESENTS PARTICULAR
                  PHI PRIME, THETA PRIME PAIR USED
                  ORDER...SMALLEST THETA PRIME ALL PHI PRIMES,
                          NEXT THETA PRIME ALL PHI PRIMES, ETC.
NEW     - COUNT OF EMISSION POINTS INPUT

ROUTINES USED
    FLOAT                - INTEGER TO REAL CONVERSION
    SIN                  - SINES OF ANGLES
    COS                  - COSINES OF ANGLES
    MINO                 - MINIMUM OF A SET OF INTEGERS
```

```
C          ASIN (NON ASA STANDARD) = ARCSINE OF A NUMBER
C
C
C      PROGRAM DECLARATIONS
C
       COMMON /EMMSET/ NTHETA,NPHI,NEW,IEM(30),XEP(30),YEP(30),ZEP(30),TH
      1EP(30),PHEP(30),AR(30),FRT(30),CX(30,48),CY(30,48),CZ(30,48)
C
       DIMENSION PHIP(8), THETAP(6), THETA1(7)
C
       DATA P102/1.5707963268/
       DATA TWOPI/6.2831853072/
C
C
C      PROGRAM TRANTP
C
C
C      READ DATA CARDS
C
       NEW=0
       WRITE (6,5)
     5 FORMAT(* EMISSION DATA*,/,* EMISSION  X*,10X,1HY,10X,1HZ,8X,
      $5HTHETA,7X,3HPHI,4X,6HRETARD,/,* NO.*,2X,5(3X,8HPOSITION),3X,
      $4HTIME,5X,4HAREA)
       DO 10 I=1,30
       READ     (5,110) IEM(I),XEP(I),YEP(I),ZEP(I),THEP(I),PHEP(I),FRT(I
      1),AR(I)
       WRITE (6,110) IEM(I),XEP(I),YEP(I),ZEP(I),THEP(I),PHEP(I),FRT(I),A
      1R(I)
       IF (IEM(I).EQ.0) GO TO 20
       NEW=NEW+1
    10 CONTINUE
       READ (IUNIT,110)
C
C      CALCULATE A SET OF PHI PRIMES
C
    20 NPHI=MINO(NPHI,8)
       DELPHI=TWOPI/FLOAT(NPHI)
       PHIP(1)=0.0
       DO 30 I=2,NPHI
       PHIP(I)=FLOAT(I-1)*DELPHI
    30 CONTINUE
C
C      CALCULATE A SET OF THETA PRIMES
C
C          CALCULATE A SET OF THETAIS FIRST
       NTHETA=MINO(NTHETA,6)
       DELTH=1.0/SQRT(FLOAT(NTHETA))
       THETA1(1)=0.0
       THETA1(2)=ASIN(DELTH)
       IF (NTHETA-2) 60,60,40
    40 DO 50 I=3,NTHETA
       THETA1(I)=ASIN(DELTH*SQRT(FLOAT(I-1)))
    50 CONTINUE
```

```
   60 THETA1(NTHETA+1)=PIO2
C          CALCULATE A SET OF THETA PRIMES FROM THE SET OF THETA1S
      DO 70 I=1,NTHETA
      THETAP(I)=THETA1(I)+(THETA1(I+1)-THETA1(I))*0.5
   70 CONTINUE
C
CC
C     SELECT A PARTICULAR EMISSION POINT
C
      DO 100 IEP=1,NEW
      THEPI=THEP(IEP)
      PHEPI=PHEP(IEP)
      CTCP=COS(THEPI)*COS(PHEPI)
      SPM=-SIN(PHEPI)
      STCP=SIN(THEPI)*COS(PHEPI)
      CTSP=COS(THEPI)*SIN(PHEPI)
      CP=COS(PHEPI)
      STSP=SIN(PHEPI)*SIN(THEPI)
      STM=-SIN(THEPI)
      CT=COS(THEPI)
C
CC          SELECT A PARTICULAR THETA PRIME
C
      DO 90 ITHP=1,NTHETA
      CTP=COS(THETAP(ITHP))
      STP=SIN(THETAP(ITHP))
C
CC               SELECT A PARTICULAR PHI PRIME
C
      DO 80 IPHP=1,NPHI
C
CC    CALCULATE X PRIME, Y PRIME, Z PRIME
C
      XPRIM=STP*COS(PHIP(IPHP))
      YPRIM=STP*SIN(PHIP(IPHP))
      ZPRIM=CTP
C
CC    CALCULATE X,Y,Z COORDINATES
C
      J=(ITHP-1)*NPHI+IPHP
      CX(IEP,J)=XPRIM*CTCP+YPRIM*SPM+ZPRIM*STCP
      CY(IEP,J)=XPRIM*CTSP+YPRIM*CP+ZPRIM*STSP
      CZ(IEP,J)=XPRIM*STM+ZPRIM*CT
C
CC               END OF PHI PRIME LOOP
C
   80 CONTINUE
C
CC          END OF THETA PRIME LOOP
C
   90 CONTINUE
```

```
C
C       END OF EMISSION POINT LOOP
C
  100 CONTINUE
      RETURN
C
C       FORMATS
C
  110 FORMAT(I5,7E10.3)
      END
```

```
      FUNCTION FTIME (T,I)
      COMMON C(200),J(200),XIF(150,4),NMAX(4),YV(20),IB(30),EX(1000),EY(
     11000),EZ(1000),FT1(4),FT2(4),FT3(4),FT4(4),XP(1023),YP(1023),ZP(10
     223),VX(1023),VY(1023),VZ(1023),KT(1023),FQ(8),TYPE(1331),SIJ(1331)
     3,SII(1331),Q(1331)
      COMMON /ENDSET/ NTHETA,NPHI,NEW,TEM(30),XEP(30),YEP(30),ZEP(30),TH
     1EP(30),PHEP(30),AR(30),FRT(30),CX(30,48),CY(30,48),CZ(30,48)
      COMMON /CONST/ DT,DX,DY,DZ,NT,NX,NY,NZ,KBRN,NS,NML
      YT=T-FRT(I)
      IF (YT.LE.0.0) FTIME=0.0
      I1=IEN(I)
      IF (YT.GT.0.0.A.YT.LE.FT1(I1)) FTIME=FT4(I1)*YT/FT1(I1)
      IF (YT.GT.FT1(I1).A.YT.LE.FT2(I1)) FTIME=FT4(I1)
      IF (YT.GT.FT2(I1).A.YT.LE.FT3(I1)) FTIME=FT4(I1)*(1.0-(YT-FT2(I1))
     1/(FT3(I1)-FT2(I1)))
      IF (YT.GT.FT3(I1)) FTIME=0.0
      RETURN
      END
```

```
      SUBROUTINE SETUP
C     READ DATA AND SET UP TABLES
      COMMON /TABLE/ SUM(200),NODE(2,200),D(4,200),A(200),NORM(1000),CN(
     12500)
      COMMON /COUPLE/ V(1331),QQ(1331),CUR(200),IA(1000)
      COMMON /CONST/ DT,DX,DY,DZ,NT,NX,NY,NZ,KBRN,NS,NML
      DATA FPI/0.07957747151/
C
C     READ SURFACE NODE LOCATIONS, RADII, AND COMPUTE SPATIAL
C      NODE NUMBERS
      WRITE (6,5)
    5 FORMAT(* SURFACE NODE DATA*,/,* CARD NODE*/2X* NO.  NO.  IX   IY*,
     $*   IZ    AREA*)
      DO 10 N=1,NS
      READ 130, IX,IY,IZ,AREA
      A(N)=SQRT(FPI*AREA)
      IA(N)=IX+1+NX*IY+NX*NY*IZ
      WRITE (6,140) N,IA(N),IX,IY,IZ,AREA
   10 CONTINUE
      D=IX*DX
      WRITE (6,190)
C
C          READ SURFACE NORMAL DATA
C
      N2=3*NML
      KX=NX+1
      KY=NY+1
      WRITE (6,15)
   15 FORMAT(* SURFACE NORMAL DATA*,/,5X,*POSITION*,10X,*NORMAL TO*,/,
     $*   IX    IY    IZ    X-AXIS    Y-AXIS    Z-AXIS*)
      DO 50 N=1,N2,3
      READ 20,IX,IY,IZ,CN(N),CN(N+1),CN(N+2)
      PRINT 20,IX,IY,IZ,CN(N),CN(N+1),CN(N+2)
   20 FORMAT(3I5,3E10.3)
      KK=IX+1+KX*IY+KX*KY*IZ
      NORM(KK)=N
      IF (KK.EQ.N1) 30,40
   30 N3=N3+1
      NORM(KK)=-(30000+N+3*N3)
      GO TO 50
   40 N3=0
      N1=KK
   50 CONTINUE
      WRITE (6,190)
C
C     READ BRANCH DATA AND CALCULATE CONSTANTS
      WRITE (6,55)
   55 FORMAT(* BRANCH DATA*,/,* BRN  FROM TO*,/,* NO.  CARD CARD ITYPE*,
     $5X,2HR ,11X,1HL,12X,1HC,12X,2HD1,11X,2HD2,11X,2HD3,11X,2HD4)
      DO 110 K=1,KBRN
      READ 150, NODE(1,K),NODE(2,K),ITYPE,R,AL,CC
      GO TO (60,70,80), ITYPE
```

```
C
C    RESISTIVE CIRCUIT
   60 CONTINUE
      D(1,K)=1./R
      D(2,K)=0.
      D(3,K)=0.
      D(4,K)=1.0
      GO TO 100
C
C    RL CIRCUIT
   70 CONTINUE
      TLC=0.
      RTL=R*DT/AL
      D(2,K)=EXP(-RTL)
      D(1,K)=(1.0-D(2,K))/R
      D(3,K)=0.
      D(4,K)=1.0
      IF (RTL.LT.0.8) GO TO 100
      PRINT 160, K
      PRINT 170, RTL,TLC,DT
      GO TO 100
C
C    RLC CIRCUIT
   80 CONTINUE
      D(1,K)=DT/AL
      D(3,K)=-DT/(AL*CC)
      RTL=R*DT/AL
      TLC=DT*DT/(AL*CC)
      IF (RTL.LT.0.8.AND.TLC.LT.0.8) GO TO 90
      PRINT 160, K
      PRINT 170, RTL,TLC,DT
   90 CONTINUE
      D(2,K)=1.0-0.5*(RTL+TLC)
      D(4,K)=1.0/(1.0+0.5*(RTL+TLC))
  100 CONTINUE
      WRITE (6,180) K,NODE(1,K),NODE(2,K),ITYPE,R,AL,CC,D(1,K),D(2,K),D(
     13,K),D(4,K)
  110 CONTINUE
C
C    INITIALIZE ARRAYS
      DO 120 I=1,KBRN
      CUR(I)=0.
      SUM(I)=0.
  120 CONTINUE
      RETURN
  130 FORMAT(3I5,E10.3)
  140 FORMAT (5I5,3X,E10.3)
  150 FORMAT(3I5,3E10.3)
  160 FORMAT (1H0,10HBRANCH NO.,I4)
  170 FORMAT (1H ,22H***** RT/L, T2/LC, DT=,3(3X,E10.3))
  180 FORMAT (4I5,7(3X,E10.3))
  190 FORMAT (1H0)
      END
```

```
      SUBROUTINE LCAD
C
C     SOLVE CIRCUIT EQUATIONS
      COMMON /TABLE/ SUM(200),NODE(2,200),D(4,200),A(200),NORM(1000),CN(
     12500)
      COMMON /COUPLE/ V(1331),QQ(1331),CUR(200),IA(1000)
      COMMON /CONST/ DT,DX,DY,DZ,NT,NX,NY,NZ,KBRN,NS,NML
      DO 10 K=1,KBRN
C
C     DETERMINE SURFACE NODE NUMBERS
      N1=NODE(1,K)
      N2=NODE(2,K)
C
C     DETERMINE SPATIAL NODE NUMBERS
      I1=IA(N1)
      I2=IA(N2)
C
C     COMPUTE POTENTIAL DIFFERENCE
      DV=V(I1)-V(I2)
C
C     COMPUTE NEW CURRENT
      CTMP=(D(1,K)*DV+D(2,K)*CUR(K)+D(3,K)*SUM(K))*D(4,K)
C
C     CALCULATE TRANSFERRED CHARGE AND REDISTRIBUTE IT
      DQ=0.5*DT*(CTMP+CUR(K))
      QQ(I1)=QQ(I1)-DQ
      QQ(I2)=QQ(I2)+DQ
      SUM(K)=SUM(K)+DQ
      CUR(K)=CTMP
   10 CONTINUE
      RETURN
      END
```

```
      SUBROUTINE MP
      COMMON /COUPLE/ V(1331),QQ(1331),CUR(200),IA(1000)
      COMMON /TABLE/ DUM(1600),NORM(1000),CN(2500)
      COMMON /CONST/ DT,DX,DY,DZ,NT,NX,NY,NZ,KBRN,NS,NML
      COMMON C(200),J(200),XIF(150,4),NMAX(4),VV(20),IB(30),EX(1000),EY(
     11000),EZ(1000),FT1(4),FT2(4),FT3(4),FT4(4),XP(1023),YP(1023),ZP(10
     223),VX(1023),VY(1023),VZ(1023),WT(1023),FQ(8),TYPE(1331),SIJ(1331)
     3,SII(1331),R(1331)
      LARGE PX(30000),PY(30000),PZ(30000),PVX(30000),PVY(30000),
     1PVZ(30000),PWT(30000)
C          THIS ROUTINE MOVES PARTICLES
      JIN1=1
      JIN2=MIN0(J(31),J(40))
      JOUT1=1
      IF(JIN2.EQ.0) RETURN
   10 J(37)=JIN2+JIN1-1
      JOUT=0
      J37=J(37)
      SMALLIN(XP,PX(JIN1),J37)
      SMALLIN(YP,PY(JIN1),J37)
      SMALLIN(ZP,PZ(JIN1),J37)
      SMALLIN(VX,PVX(JIN1),J37)
      SMALLIN(VY,PVY(JIN1),J37)
      SMALLIN(VZ,PVZ(JIN1),J37)
      SMALLIN(WT,PWT(JIN1),J37)
      DO 170 I=1,J37
      IF (WT(I)-C(98)) 20,170,170
   20 JOUT=JOUT+1
C          FIND NEW VELOCITIES AND POSITIONS
      IX=INT(XP(I))
      IY=INT(YP(I))
      IZ=INT(ZP(I))
      KK=IX+1+J(112)*IY+J(116)*IZ
      VX(JOUT)=VX(I)+C(99)*EX(KK)
      VY(JOUT)=VY(I)+C(99)*EY(KK)
      VZ(JOUT)=VZ(I)+C(99)*EZ(KK)
      XP(JOUT)=XP(I)+VX(JOUT)*C(100)
      YP(JOUT)=YP(I)+VY(JOUT)*C(101)
      ZP(JOUT)=ZP(I)+VZ(JOUT)*C(102)
      IX=INT(XP(JOUT))
      IY=INT(YP(JOUT))
      IZ=INT(ZP(JOUT))
      XFF=(XP(JOUT)-FLOAT(IX))
      XFT=XFF*WT(I)
      XMT=WT(I)-XFT
      XMF=1.0-XFF
      YFF=YP(JOUT)-FLOAT(IY)
      YMF=1.0-YFF
      ZFF=ZP(JOUT)-FLOAT(IZ)
      ZMF=1.0-ZFF
      KK=IX+1+J(112)*IY+J(116)*IZ
      N8=IX+1+J(1)*IY+J(110)*IZ
      N1=N8+1
```

```
      N2=N8+J(1)
      N3=N8+J(110)
      N4=N1+J(1)
      N5=N2+J(110)
      N6=N3+1
      N7=N6+J(1)
      A1=XFT*YFF
      A2=XMT*ZFF
      A3=XFT*YMF
      A4=XMT*ZMF
      FQ(1)=A3*ZMF
      FQ(2)=A4*YFF
      FQ(3)=A2*YMF
      FQ(4)=A1*ZMF
      FQ(5)=A3*ZFF
      FQ(6)=A2*YFF
      FQ(7)=A1*ZFF
      FQ(8)=A4*YMF
      Q(N1)=Q(N1)+FQ(1)
      Q(N2)=Q(N2)+FQ(2)
      Q(N3)=Q(N3)+FQ(3)
      Q(N4)=Q(N4)+FQ(4)
      Q(N5)=Q(N5)+FQ(5)
      Q(N6)=Q(N6)+FQ(6)
      Q(N7)=Q(N7)+FQ(7)
      Q(N8)=Q(N8)+FQ(8)
      IF (NORM(KK)) 30,170,40
C
C          MORE THAN ONE SURFACE
C
   30 K2=-NORM(KK)/10000
      K1=-NORM(KK)-10000*K2
      GO TO 50
C
C          ONE SURFACE
C
   40 K1=NORM(KK)
      K2=1
   50 DO 160 L=1,K2
      K3=K1+1
      K4=K1+2
      IF ((VX(JOUT)*CN(K1)+VY(JOUT)*CN(K3)+VZ(JOUT)*CN(K4)).GE.0.) GO TO
     1 150
      L1=IFIX(ABS(CN(K1))+2.*ABS(CN(K3))+4.*ABS(CN(K4)))
      GO TO (60,70,100,80,110,120),L1
   60 X1=XFF
      IF (CN(K1).LT.0.) X1=XMF
      GO TO 90
   70 X1=YFF
      IF (CN(K3).LT.0.) X1=YMF
      GO TO 90
   80 X1=ZFF
```

```
      IF (CN(K4).LT.0.) X1=ZMF
   90 IF (X1.GT.C(7)) GO TO 150
      GO TO 140
  100 X1=XFF
      X2=YFF
      IF (CN(K1).LT.0.) X1=XMF
      IF (CN(K3).LT.0.) X2=YMF
      GO TO 130
  110 X1=XFF
      X2=ZFF
      IF (CN(K1).LT.0.) X1=XMF
      IF (CN(K4).LT.0.) X2=ZMF
      GO TO 130
  120 X1=YFF
      X2=ZFF
      IF (CN(K3).LT.0.) X1=YMF
      IF (CN(K4).LT.0.) X2=ZMF
  130 X1=X1+X2
      IF (X1.GT.1.0+C(7)) GO TO 150
  140 WT(JOUT)=FQ(1)*TYPE(N1)+FQ(2)*TYPE(N2)+FQ(3)*TYPE(N3)+FQ(4)*TYPE(N
     14)+FQ(5)*TYPE(N5)+FQ(6)*TYPE(N6)+FQ(7)*TYPE(N7)+FQ(8)*TYPE(N8)
      Q(N1)=Q(N1)+FQ(1)*(1.0-TYPE(N1))
      Q(N2)=Q(N2)+FQ(2)*(1.0-TYPE(N2))
      Q(N3)=Q(N3)+FQ(3)*(1.0-TYPE(N3))
      Q(N4)=Q(N4)+FQ(4)*(1.0-TYPE(N4))
      Q(N5)=Q(N5)+FQ(5)*(1.0-TYPE(N5))
      Q(N6)=Q(N6)+FQ(6)*(1.0-TYPE(N6))
      Q(N7)=Q(N7)+FQ(7)*(1.0-TYPE(N7))
      Q(N8)=Q(N8)+FQ(8)*(1.0-TYPE(N8))
      QQ(N1)=QQ(N1)+FQ(1)*(1.0-TYPE(N1))
      QQ(N2)=QQ(N2)+FQ(2)*(1.0-TYPE(N2))
      QQ(N3)=QQ(N3)+FQ(3)*(1.0-TYPE(N3))
      QQ(N4)=QQ(N4)+FQ(4)*(1.0-TYPE(N4))
      QQ(N5)=QQ(N5)+FQ(5)*(1.0-TYPE(N5))
      QQ(N6)=QQ(N6)+FQ(6)*(1.0-TYPE(N6))
      QQ(N7)=QQ(N7)+FQ(7)*(1.0-TYPE(N7))
      QQ(N8)=QQ(N8)+FQ(8)*(1.0-TYPE(N8))
      GO TO 170
  150 K1=K1+3
  160 CONTINUE
  170 CONTINUE
      JOUT2=JOUT1+JOUT-1
      IF (JOUT.LE.0) GO TO 180
      SMALLOUT(XP,PX(JOUT1),JOUT)
      SMALLOUT(YP,PY(JOUT1),JOUT)
      SMALLOUT(ZP,PZ(JOUT1),JOUT)
      SMALLOUT(VX,PVX(JOUT1),JOUT)
      SMALLOUT(VY,PVY(JOUT1),JOUT)
      SMALLOUT(VZ,PVZ(JOUT1),JOUT)
      SMALLOUT(WT,PWT(JOUT1),JOUT)
```

REFERENCES

1. Messier, M. A., The Quasi-static Method Applied to Satellite Structural Return Current Analysis: Surface Node Analysis, MRC-R-179, March 1975.

2. Higgins, D. F., QUASI: A Hybrid Quasi-static Code for Calculating SGEMP Structural Replacement Currents - Theory and Results, MRC-R-180, March 1975.